UNIVERSITY of NICOSIA | DEPARTMENT OF ENGINEERING

A Paradigm Shift for Selectively Decarbonising China and Cyprus and Lowering Vehicle Emissions.

Mr. Evangelos Demetriou

A thesis submitted to the University of Nicosia
in accordance with the requirements of the degree of
PhD (Doctor of Philosophy) in Oil, Gas and Energy Engineering

Department of Engineering

March, 2022

Abstract

China is the world's top emitter of CO_2 with power generation being the main culprit. Cyprus on the other hand is unique because the island relies on oil-fired power generation. Similar to other countries a substantial amount of air pollutants, such as particulate matter and nitrogen oxides in Cyprus originate from transport and residential heating activities.

Extending between 2017 and 2050 a projection of the future Chinese electricity production is made. China predominantly relies on coal for its power generation and the Coal Free scenario showed that the country can abandon the use of coal by 2050. Alternatively, the Renewables scenario where all electricity is met chiefly by solar and wind energy is not feasible unless supplemented by fossil fuels. At 0.207$/kWh, the Renewables scenario yields the most expensive electricity which is twice as costly as the Coal Free case. Concerning CO_2 emissions, if China kept the energy mix of 2017 its emissions would double by 2050. Carbon sinks from the Land Use-Land Use Change and Forestry sector could help the Carbon Free and Renewables scenarios realise net-zero emissions. Lastly, the Goals scenario that reflects the national targets of China along with the Coal Free scenario fulfil China's COP21 targets.

Returning to Cyprus, different estimates were made concerning its future electricity needs, cost and other factors from 2018 until 2050. Passenger vehicle-to-grid units and desalination plants helped estimate the grid's electrical load at an hourly scale. Projections revealed that the scenario which utilises only renewables and electricity storage by 2050 will yield net-zero emissions but at a cost of 0.115€/kWh and high electricity loss (40%). The Business As Usual and the Least Cost cases that rely mostly on natural gas fail to meet the European Commission's goals, while if natural gas power plants were to utilise the Carbon Capture and Storage technology would abide with the 2°C target. Carbon tax plays a key role since at a value of 250€/tonne the Renewables scenario is more economical compared to the least cost case. Meanwhile, RESc enables full decarbonisation.

Lastly, CO, NO_x, $PM_{2.5}$ and PM_{10} air pollutants were simulated at the centre of Nicosia during a 9-month period. The levels of NO_x and PM were validated with actual measurements. Moreover, several scenarios and cases were used to obtain the emissions and deduce the mortality risks in Nicosia. Euro 6 standard and the banning of passenger

and light-duty vehicles contained NO_x-related deaths, which were calculated to be 238, by 70%. Concluding, $PM_{2.5}$ in 2030 could be meaningfully slashed by banning fireplaces.

Keywords

China, Cyprus, CO_2 levels, scenarios, 100% renewables, zero emissions, Nicosia, urban air pollution, nitrogen oxides, particulate matter, dispersion modelling, premature mortality.

Acknowledgements

First and foremost, I would like to express my sincere gratitude to my supervisor Associate Professor Constantinos Hadjistassou for his invaluable advice, continuous support and patience during my Ph.D. studies and related research. His immense knowledge and experience have encouraged me during all of the stages of my research.

Furthermore, my gratitude extends to the Ministry of Energy, Commerce, and Industry for providing significant financial support, without it my research will not be possible. Additionally, I would like to especially thank Mr. Alexis Avgoustis, Transportation Engineer, from the department of Civil Works for sharing traffic data with us. I am also grateful to Dr. Chrysanthos Savvides from the Department of Labour Inspection for supplying us with field measurements from their national air quality station network.

I also like to thank both my supervisors Dr. Marios Nestoros and Dr. Elias Yfantis for their support during my studies and their useful ideas that helped me with my research.

Finally, I would like to thank my parents, Marios and Flora, my wife, Rafaella and my brother and sister, Petros and Loukia for motivating me to continue and not to give-up my studies.

Declaration

I declare that the work in this thesis was carried out in accordance with the regulations of the University of Nicosia. It is a product of original work of my own, unless otherwise mentioned through references, notes, or any other statements.

Signed:  Date: Saturday 25th of June, 2022.

Contents

List of Tables

List of Figures

List of Appendices

Abbreviation index

°C	Degrees Celsius
BAU	Business As Usual (scenario)
BCM	Billion cubic metres
CCSc	Carbon Capture and Storage (scenario)
CFr	Coal free (scenario)
CNREC	China National Renewable Energy Centre
CO	Carbon monoxide
CO_2	Carbon dioxide
CSP	Concentrated solar power
EC	European Commission
EEA	European Environment Agency
EIA	Energy Information Administration
EU	European Union
g/GJ	Grams per Gigajoule
GDP	Gross Domestic Product
Goals	Goals (scenario)
GRAL	Graz Lagrangian Model
Gt	Gigatonnes
GW	Gigawatt (10^6 W)
IEA	International Energy Agency
IER	Integrated response function
INDCs	Intended Nationally Determined Contributions
km/hr	Kilometres per hour
kt	Kilotonnes (1,000 tonnes)
kWh	Kilowatthour (1,000 Wh)
LCOE	Levelised cost of electricity ($/kWh)
LCSc	Least Cost Scenario
LDV	Light duty vehicles
LULUCF	Land Use, Land-Use Change and Forestry
MAPE	Mean Absolute Percentage Error
MW	Megawatt (10^6 W)
MWh	Megawatthour (10^6 Wh)
NO_x	Nitrogen oxides
NREL	National Renewable Energy Laboratory (USA)
PJ	Petajoules
PM_{10}	Particulate matter with diameter less than or equal to 10 μm
$PM_{2.5}$	Particulate matter with diameter less or equal to 2.5 μm
PV	Passenger vehicles
P-V-2-G	Passenger-Vehicle-to-Grid
PWh	Petawatthour

RES	Renewable Energy Sources
RESc	Renewables scenario
TW	Terawatt (10^9 W)
TWh	Terawatthour (10^9 Wh)
UNFCCC	United Nations Framework Convention on Climate Change
WHO	World Health Organization

List of publications

Demetriou, E., Hadjistassou, C., 2021. Can China decarbonize its electricity sector? *Energy Policy* 148, 111917, https://doi.org/10.1016/j.enpol.2020.111917.

Demetriou, E., Mallouppas, G., Hadjistassou, C., 2021. Embracing carbon neutral electricity and transportation sectors in Cyprus. *Energy* 229, 120625, https://doi.org/10.1016/j.energy.2021.120625.

Demetriou, E., Hadjistassou, C., 2022. Lowering mortality risks in urban areas by containing atmospheric pollution. Environmental Research 211, 113096, https://doi.org/10.1016/j.envres.2022.113096.

1. Introduction

Carbon dioxide emissions are a key factor to contain temperature increase to 2ºC compared to the pre-industrial era. In 2019, China with a share exceeding 27.9% of carbon dioxide (CO_2) emissions was by far the world's top emitter followed by the United States with 14.5%, the European Union (EU) with 9.0% and India with 7.2% (Ritchie and Roser, 2020b) of global emissions. Remarkably, the Chinese energy sector was responsible for about 80% of the total domestic emissions (United Nations Framework Convention on Climate Change, 2015). In turn, the Chinese energy industries, which are a division of the energy sector, released about 35% of the total emissions in 2012 (United Nations Framework Convention on Climate Change, 2015). For China to attain a material reduction in its emissions, it needs to adopt bolder measures. In an effort to boost its emissions sinks, the Chinese State Forestry Administration has unveiled that, by 2050, national forests will occupy 25% of the land compared to 21.6% in 2018 (State Council the People's Republic of China, 2018). Incongruently, China's forest stock will increase from 15.1 billion cubic metres (bcm) to 26.5 bcm bringing the country a step closer to becoming carbon neutral (State Council the People's Republic of China, 2018). Meanwhile, China has set national targets (Intended Nationally Determined Contributions) until 2030 such that: a) the Chinese CO_2 emissions to plateau by 2030 or earlier, b) to boost the share of non-fossil fuels to 20% and c) to expand the domestic penetration of natural gas (China, 2015). Lastly, the president of China in September 2020 stated that, by 2060, the country will achieve carbon neutrality (Ministry of Foreign Affairs of the People's Republic of China, 2020).

The European Union (EU) the third top pollution entity in 2021, has instituted a long-term strategy toward net-zero emissions by 2050 with one milestone being to curb heat-trapping emissions by 55% until 2030. Empowered by the Green Deal (European Commission, 2019), the EU aims to arrest temperature increase to 1.5°C compared to the pre-industrial levels (European Commission, 2018). A less ambitious drop in emissions of 80–95%, by 2050, compared to 1990, could very likely be adequate to help contain the temperature rise to 2°C above the pre-industrial era (Langsdorf, 2011; European Commission, 2018). More precisely, to achieve the preceding goals, the transportation sector will need to roll out electric vehicles at an unprecedented scale and utilise biofuels. In an effort to reduce CO_2 emissions, the EU will need to accelerate the

shift to renewable energy production as well as to catalyse progress in carbon capture and storage and energy efficiency.

Cyprus, as an EU Member State, differs from other EU countries in that its electricity grid functions as an independent network in isolation. It is the only EU country that is not connected to the European power network and relies entirely on its own domestic production. Currently, the island's electricity system heavily depends on fossil fuels with over 91% of the total electricity production met from diesel and heavy fuel oil. In June 2023, natural gas is anticipated to be introduced in the Cypriot electricity sector to replace (other) oil liquid products (Psyllides, 2021) and diversify the island's energy mix. Most of the island's emissions originate from the electricity and the transportation sectors which account for 47% and 30% of the aggregate emissions, respectively. According to the latest UNFCCC report in 2019, 67% of transportation emissions are released from vehicles (Cyprus Department of Environment, 2019). In tandem with the other EU countries, Cyprus has set emission reduction goals for 2030. More explicitly, at the national level, Cyprus intends to cut its electricity, ceramics, cement and industrial emissions by 42%, by 2030, compared to the year 2005 (Cyprus Department of Environment, 2018). Collectively, emissions reductions from other sectors such as agriculture, waste and the remaining ones are envisaged to reach 24%, by 2030 (Cyprus Department of Environment, 2018).

Carbon dioxide is not the only gas considered to affect people's lives and the environment. The European Environment Agency (EEA) has emphasised that 74% and 4% of the total urban population in Europe was exposed to $PM_{2.5}$ (particulate matter with a diameter less than 2.5μm) and nitrogen oxides pollution, respectively, exceeding the annual mean World Health Organization (WHO) air quality levels (European Environment Agency, 2020a). Particulate matter and nitrogen oxides (NO_x) concentrations have been associated with premature, cardiovascular, lung cancer, and respiratory mortality risks (Cao *et al.*, 2011b; Atkinson *et al.*, 2014; Stockfelt *et al.*, 2015; Mbelambela *et al.*, 2017; European Environment Agency, 2020a; Rodrigues Teixeira *et al.*, 2020). During the last decade, in the European Union (EU), premature mortality risks related to pollutants had decreased by about 15%, but still, more than 400,000 premature deaths were attributed to air pollution (European Environment Agency, 2020a). Road transport, in 2017, in the EU, was to blame for over 16.9% and 6.3% of the total NO_x and PM emissions, correspondingly (European Environment

Agency, 2020b). Vehicles were not only accountable for tail-pipe but also for non-exhaust emissions such as tyre, brake, and road surface wear. Non-exhaust pollution was responsible for about 80% of the total vehicle emissions (European Environment Agency, 2020b). Stationary residential emissions which included fireplaces and residential boilers produced 2.1% of NO_x and 10.3% of PM pollution (European Environment Agency, 2020b).

Cyprus was one of the most polluted countries in Europe regarding nitrogen oxides as their concentration was the second-highest in the EU in 2018 (European Environment Agency, 2020b). Its NO_x emissions originated mostly from the transport sector (43%) and stationary residential heat emissions which accounted for 2.2% of the aggregate emissions (European Environment Agency, 2020b). Anthropogenic particulate matter emissions at the island, are liberated from road transport (21.5%) and stationary residential heat sources (3.2%) (European Environment Agency, 2020b). Sea salt and dust had a tremendous effect on the PM concentration as they constituted 41.6% of the total particulate matter pollution as measured in the background station of Ayia Marina, in 2017, due to the island's high proximity to the Sahara desert (Department of Labour Inspection of Cyprus, 2019).

1.1 Problem definition

The electricity sector is responsible for most of the carbon dioxide (CO_2) emissions in both China and Cyprus. Furthermore, the transportation sector in Cyprus accounts for a substantial amount of CO_2 and along with the stationary residential heat sources contribute most of the NO_x and PM emissions. Not surprisingly, most of the countries and entities, including China and the EU, have stated that in the following decades they will become carbon neutral. In order to achieve this goal, the countries should adapt their electricity production and transportation policies as well as expand their forest stock to achieve carbon neutrality.

Remarkably, the majority of the studies concentrating on electricity production in China omit to take into consideration the effect of forest stock on the country's emissions. At the same time, even though China's electricity sector has been studied by various scholars, very few have considered the possibility of a carbon-neutral electricity sector. Geographically, China consists of a total of 31 provinces with each one possessing different renewable electricity potential which is rarely considered.

Moreover, to evaluate a feasible, economic, and uninterrupted electricity supply an hourly electricity mix should be examined which is often neglected by other studies. Finally, for electricity production, a gap exists which concerns the impact of future electricity storage facilities, such as battery storage and hydrogen storage along with a significant share of renewable energy penetration.

Cyprus despite emitting insignificant emission levels which amount to 0.02% of the world's production, in 2019 (Ritchie and Roser, 2020a), it can be considered a unique case because it is the only EU member state with an isolated electricity grid. The European Commission has set ambitious goals to contain temperature increase by transforming itself into a carbon-neutral economy. Natural gas is considered by scholars as one of the fuels which can help tackle CO_2 emissions, without considering the penetration of a substantial percentage of renewables such as wind and solar, and hydropower production (Boretti and Al Zubaidy, 2021; Mohammad *et al.*, 2021). Electric passenger vehicles are regarded instrumental in diminishing the transport sector's emissions. Surprisingly, no study to the best of the found knowledge has examined the synergy between renewable energy and electric vehicles to achieve an uninterrupted power supply. To this end, it will be helpful to develop a model which will investigate whether a fully renewable energy grid could possibly integrate electric vehicles at a viable cost.

In tandem with CO_2, the transportation sector emits other pollutants such as particulate matter, nitrogen oxides, carbon monoxide, and others. Concentrations of the preceding gases above a threshold carry the risk of premature mortality. Cyprus was the second most polluted European country regarding NO_x pollution in 2018 (European Environment Agency, 2020a). Nitrogen oxides, particulate matter and carbon monoxide pollution derive mostly from road traffic and the residential heat sector. Modelling and validating pollutant concentrations through a dispersion model is a complex procedure since it requires meteorological and traffic data inputs as well as the city's topography. Owing to the inherent benefits that dispersion modelling offers, such as investigating what-if scenarios, a dispersion model incorporating road traffic and residential heat sources in Nicosia, Cyprus, is proposed here. The software used, namely, GRAL® was calibrated with NO_x, $PM_{2.5}$, PM_{10} and CO for a 9-month period during 2017 with weather data acquired from the Department of Labour Inspection and traffic related emissions from the Cyprus Department of Civil Works. Lastly, after validating the

model different scenarios can be tested to determine the best policy intended to lower the concentration of pollutants while curbing premature mortality in the city of Nicosia.

1.2 Research objectives

Numerous countries and companies have stated that in the following decades will become carbon neutral. The electricity and transport sectors were estimated to be the most polluting categories. Pollutants are also responsible for a considerable number of premature deaths. Therefore, this work aims to suggest different policies to address the problems mentioned above. More specifically, the objectives of our research are the following:

- Estimate the future electricity production and installed capacity needs, until 2050, of Cyprus and China under four different scenarios with the aid of statistical methods.
- China's energy scenarios are the Business as Usual scenario which follows the trend of 2017 until 2050 and the Goals scenario which mirrors the goals stated by China in 2030. Additionally, the Coal free scenario was formulated which assumes that no coal is utilised by 2050. Finally, the Renewables scenario has investigated whether it is possible to draw all of China's electricity from renewables and storage. All of these scenarios have been crafted with the minimum electricity cost in mind.
- For Cyprus, the Business as Usual scenario assumes that natural gas is the only fossil fuel used along with renewables and power storage while minimising emissions. Akin to the BAU case, the Least cost scenario aims to minimise power costs. The other two devised scenarios are the Renewables scenario which draws electricity only from renewables, storage and passenger-vehicle-to-grid and the Carbon Capture case where natural gas facilities are fitted with carbon capture and storage technologies.
- Develop an hourly electricity model with all electricity production sources including battery and hydrogen storage for China and passenger vehicle to grid, battery, and pumped hydro storage for Cyprus.
- Determine whether carbon neutrality is possible for the electricity and transportation sectors as well as for Land Use, Land Use Change and Forestry for Cyprus and China.

- Create a dispersion model to validate pollutant concentration of nitrogen oxides and particulate matter with diameter less than or equal to 2.5μm and smaller than or equal to 10μm and carbon monoxide, originating from road traffic and residential heat sources in the city centre of Nicosia, Cyprus.
- Test different traffic scenarios to determine which policy can lower pollutant concentration and reduce mortality risks.

1.3 Originality of thesis findings

Numerous researchers have investigated the future electricity production of China. This thesis was among the few studies which incorporated both the future electricity production and emissions along with Land Use, Land Use Change and Forestry carbon sinks. Considering China, even with the utilisation of the country's entire renewable energy potential it is deemed not possible to meet domestic energy demand. Moreover, for Cyprus, we have integrated for the first time to the electricity network vehicle to grid units, which presupposes the active cooperation between electric vehicle owners with electricity utilities. This investigation has demonstrated that a fully electric passenger vehicle and bus fleet are possible by 2050. Clearly, for Cyprus, a combination of electricity battery storage banks and vehicle-to-grid facilities are key for realising a fully renewable energy mix. Additionally, this thesis presented the first dispersion model in Cyprus, that considered different pollutants, namely, nitrogen oxides, particulate matter and carbon monoxide, which are encountered in Nicosia. Moreover, utilising the results of the dispersion model it was possible to formulate different scenarios which helped determine the mortality rates in the capital. Results have showed that if Cyprus was to ban non-Euro 6 and diesel passenger and light duty vehicles it would result in a reduction of mortality by 70% for nitrogen oxides. Lastly, regarding particulate matter, banning fireplaces is the most effective solution to save lives.

1.4 Thesis outline

This work is subdivided into five sections. In the first part, a brief description of emissions sources from countries and entities was offered, followed by their long-term goals. Since the electricity and the transport sectors are the top two most polluting in both Cyprus and China this research has focussed on emission mitigation policies.

Pertinent research efforts which form part of the literature review are presented in the second part of the thesis. Initially, statistical methods were applied to estimate electricity production. Secondly, the renewable energy potential and the percentage penetration of both China's and Cyprus' electricity grid was studied along with electricity storage facilities such as lithium batteries and hydrogen. Lastly, information was provided about the health hazards of four main pollutants, their origin in Nicosia, and briefly mentioned the scenarios and cases that will be studied. In the third part, the methodology to estimate electricity production, costs, and emissions from the power generation sector was explained. Moreover, to estimate the concentration of the pollutants at the city of Nicosia, the city's centre was simulated in the GRAL® software together with the dispersion parameters, based on the concentration of the pollutants the premature mortality is calculated. In the fourth part, all of the research findings are presented, such as the future electricity cost and emissions for China and Cyprus. Also, the impacts associated with each traffic and residential emission mitigation course of action are detailed in this section. Concluding, the last section summarises the main thesis results and outlines some future research directions.

2. Literature review

In this chapter, the history behind greenhouse gases is outlined, especially carbon dioxide, the international conventions enacted to contain them and the goals set to mitigate their consequences. Later, the thesis focuses on the costs and the pollution footprint of the electricity sector and finally on pollutant dispersion modelling. Even though the electricity sector and the emissions of China and Cyprus have been examined extensible, the impacts of future policy measures that are expected to attain carbon neutrality are not yet meticulously investigated. At first, the different methodologies used to forecast electricity production are explained. Secondly, the studies involving renewable electricity penetration and their emissions are summarised. Moreover, simulations are performed to estimate the concentration of pollutants at the city scale for Nicosia, the capital of Cyprus. Next, the health effects of pollutants and their sources in Cyprus are reviewed. Eventually, dispersion modelling is applied to the city of Nicosia.

2.1 Conferences of Parties for the environment

Protecting the environment is not a new topic as it dates back to the ancient Greeks and Romans times (Tarlock, 2009). The first environmentally affiliated international law was enacted in 1956, by the United Nations, and stated that oil discharges at sea pose a danger to the life of marine species and pollute maritime ports and sea beaches (International Law Commission, 1956). The first general assembly of the United Nations on the environment took place in Stockholm in 1972. It declared among others that natural resources and wildlife should be preserved, and non-renewable sources should be used frugally to prevent their depletion in the future. Most importantly, it mentioned that pollution discharges should not be at such volumes that they cause irreversible environmental damage (Handl, 2012). This assembly led to the creation of the United Nations Environment program.

Perhaps the most well-known international convention is that of Kyoto, Japan which was held in December 1997 and was enforced in February 2005. The Kyoto Protocol was an agreement that aimed to decrease and limit the production of greenhouse gases (GHG) from the EU15 and 37 other countries excluding China. Each entity or country pledged to comply with emissions targets for the period of 2008 until

2012 compared to 1990 levels. The EU15 and other European countries have set the most ambitious target of reducing emissions by 8% while Iceland committed to containing the rise of six greenhouse gases, including CO_2, by up to 10% (United Nations Framework Convention on Climate Change, 2021). The Paris Agreement (COP21) was an international convention, held in 2015, in Paris and aimed at combating climate change. It endeavoured to restrain world temperature increase below 2°C compared to the pre-industrial levels or even at 1.5°C by curbing emissions as soon as possible. Every State was supposed to individually determine its national contribution goals to mitigate the phenomenon of climate change. Out of the 195 states, only five have not yet signed the agreement, namely, Turkey, Iran, Iraq, Yemen, and Eritrea (United Nations Treaty Series, 2015).

China, for example, has set three main targets by 2030. Firstly it has pledged to reach peak carbon dioxide emissions, secondly to grow its non-fossil energy consumption to 20% and thirdly to boost its forest stock volume by 4.5 billion m^3 (China, 2015). It is worth mentioning that, in September 2020, Chinese President Xi Jinping has announced that China will be carbon neutral by 2060 (Ministry of Foreign Affairs of the People's Republic of China, 2020). Similarly, the European Union has set comparable goals such as limiting emissions by 55%, in 2030, in relation to 1990 and has fixed a long-term goal of diminishing carbon emissions and becoming carbon neutral by 2050 (European Commission, 2020).

2.2 Atmospheric carbon dioxide concentration and top polluting entities.

Global carbon dioxide concentration has increased dramatically surpassing the concentration of 410ppm in 2019 (Keeling and Keeling, 2021), which is 1.5 times greater compared to the year 1770 (280ppm) (Prentice *et al.*, 2001). Carbon dioxide emissions are intimately linked to a rise in temperature. During the period between 1850 until 1900, the average world temperature was 0.78°C lower compared to the average temperature in the years 2003 to 2012 (Schlömer S *et al.*, 2014). Additionally, from 1960 until 2020 carbon dioxide levels continued to rise unabated as pictured in Fig. 2.1. Reflecting this trend, according to NASA in 2018 (NASA's Goddard Institute for Space Studies, 2018) the last 17 out of 18 years were the hottest in a 136 year period. Suffice

to mention that emissions have been still surging at a rate of about 1.3% per year from 1970–2000 and at about 2.2% between 2000–2010 (Schlömer S *et al.*, 2014).

In 2019, six entities and countries, namely, China, the United States, EU28, India, Russia, and Japan accounted for 65.3% of the 36.47Gt World's CO_2 emissions (Friedlingstein *et al.*, 2020). The majority originated from China 27.9%, whereas 14.5% was from the USA, 9.0% from EU28 bloc, 7.2% from India, 4.6% from Russia and 3.0% from Japan (Friedlingstein *et al.*, 2020). In 1990, CO_2 emissions amounted to 22.7Gt with the US and the EU being the main emitters collectively producing about 40% of the aggregate emissions (Fig. 2.2).

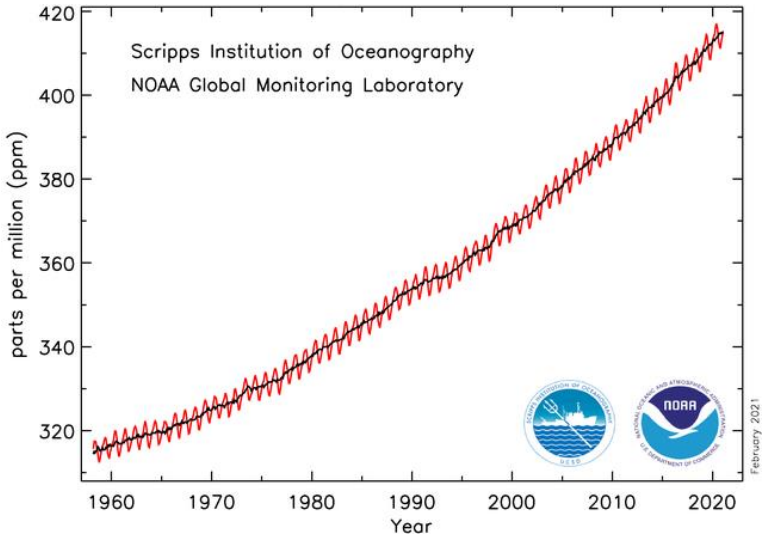

Fig. 2.1. Carbon dioxide concentration at Mauna Loa Observatory spanning from 1958 until February 2021 (Keeling and Keeling (2021)).

Carbon dioxide is either emitted or absorbed by six specific sectors (United Nations Climate Change, 2020): energy, industrial processes, agriculture, land-use, land-use change and forestry (LULUCF), waste, and other. In turn, all of these sectors have sub-divisions, for example, energy is divided into energy and manufacturing industries, transport, and other. It should be pointed out that, from all six sectors only LULUCF captures carbon emissions through forest lands. In 2016, the world's emissions sources derived: 73.2% from the energy sector, 11.2% from agriculture, 7.2% from LULUCF, 5.2% from the industry, and 3.2% from waste (Ritchie and Roser, 2020b). The top polluting sub-sector, in 2016, was power generation and the transport sector comprising 30.4% and 15.9% of the total CO_2 emissions, respectively (Ritchie,

2020). China's pollution in 2016 mostly emanated from electricity 47.3%, manufacturing 29.0%, and the construction and the transport sectors amounting to 8.5%. Cyprus' dominant sectors were the electricity and the transport sectors accounting for 48.2% and 29.6%, in 2018, correspondingly (Kythreotou and Mesimeris, 2020). The electricity sector dominates carbon dioxide pollution in China and in Cyprus along with the transport sector and hence they merit further attention.

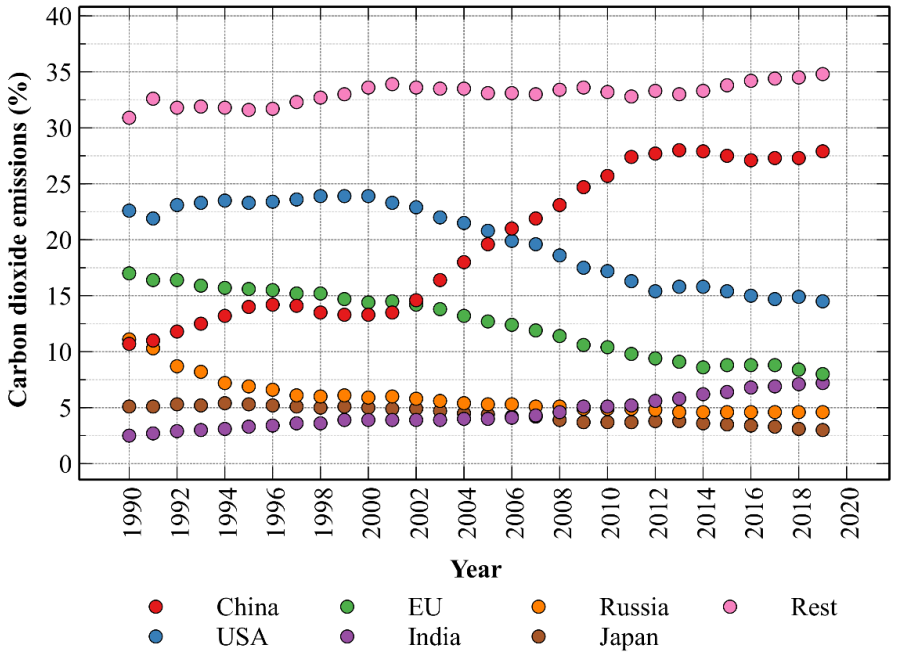

Fig. 2.2. Share of carbon dioxide emissions of the top 6 entities from 1990 to 2019. Source: Friedlingstein *et al.* (2020).

2.3 The electricity sector

2.3.1 China's electricity sector

China's electricity generation has grown rapidly during the past 15 years. In 2006, the total installed capacity was 624GW, while in 2012 it reached 1,062GW and escalated to 1,900GW in 2018 (Fig. 2.3) (China Energy Portal, 2018). This gigantic growth is attributed to two factors. Firstly, the increased electricity needs of China have almost tripled from 2,836TWh in 2006 to 6,900TWh in 2018 (Fig. 2.4). Secondly, China tried to increase its renewables share which comprised only 0.3% of the total installed capacity in 2006 and reached 19.2% in 2018 (China Energy Portal, 2018). This is most probably attributed to one of China's pledges to foster the non-fossil share

power generation to 20%. Noticeably, coal and hydropower provided almost all of the electricity production in China, 98% and 83% of the total electricity production in 2006 and 2018 respectively (China Energy Portal, 2018).

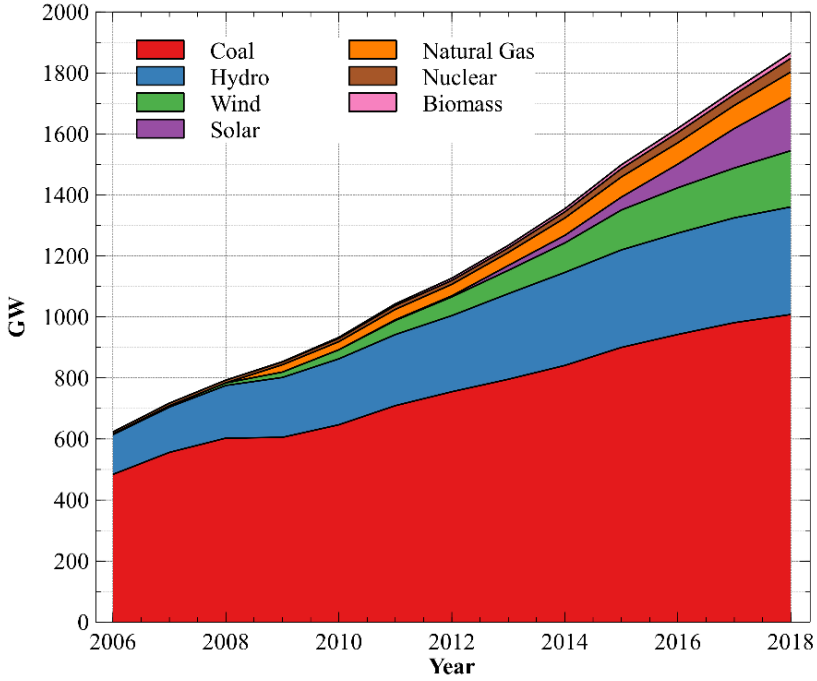

Fig. 2.3. Installed electricity capacity in China from 2006 to 2018 (GW) (China Energy Portal, 2018).

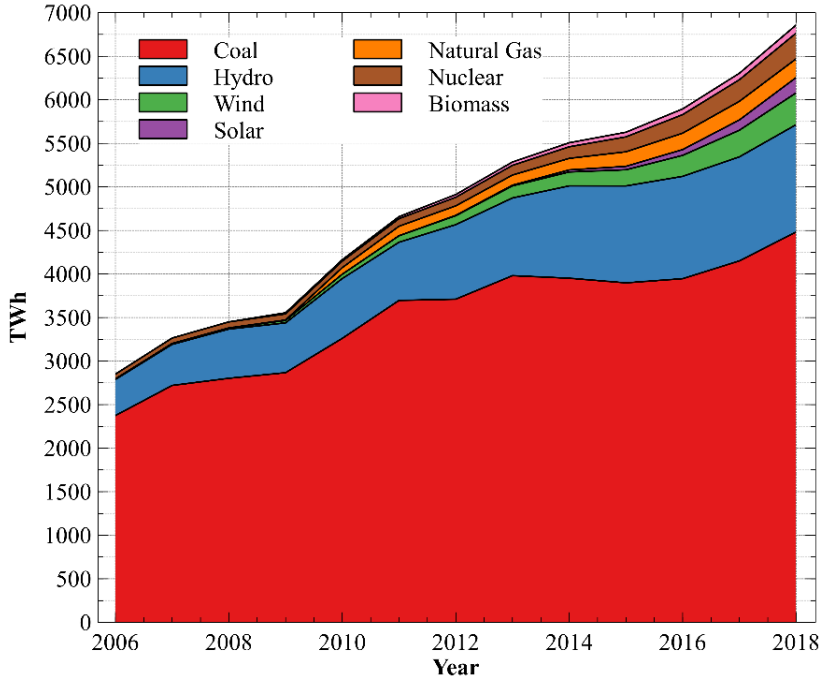

Fig. 2.4. Electricity capacity in China from 2006 to 2018 (China Energy Portal, 2018).

2.3.2 Cyprus' electricity sector

In 2009, the EU has set a long-term goal of waning carbon emissions by between 80 to 95%, by 2050, in relation to 1990 (European Commission, 2018). In July 2021, the EU endorsed a higher objective, that is, to realise carbon neutrality by 2050 (European Commission, 2021).

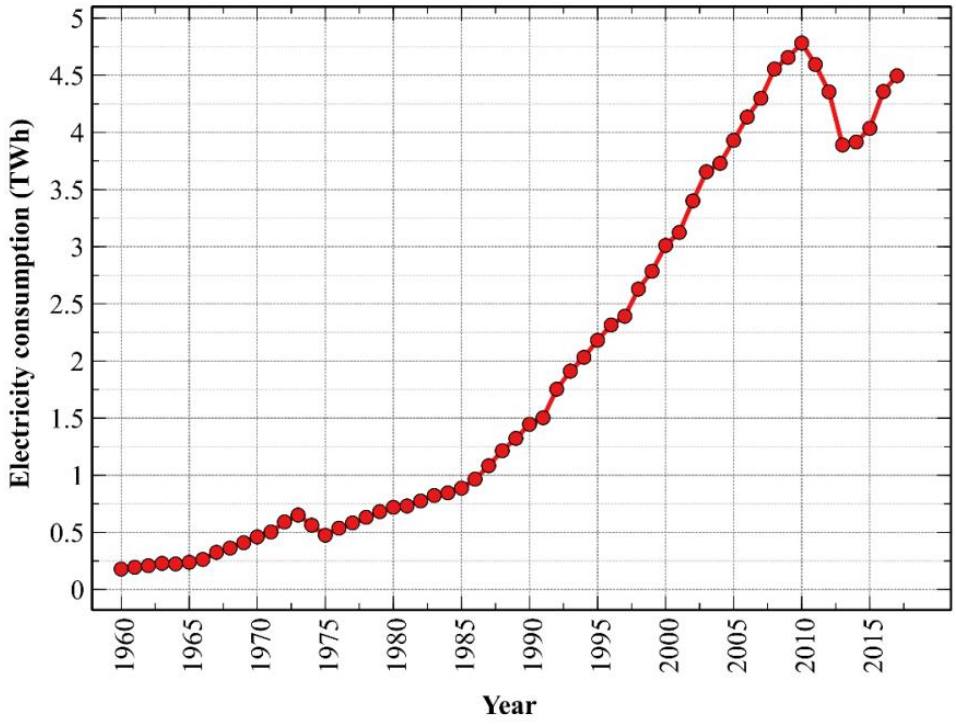

Fig. 2.5. Electricity consumption in Cyprus from 1990 to 2017 (TWh) (CYSTAT, 2018).

Cyprus is considered a distinct case regarding its electricity production. The island is isolated from all the other grids of Europe and relies mostly on heavy fuel oil and diesel just like China depends on coal for most of its power generation. Its electricity sector has grown rapidly over the last decades. Cyprus' electricity consumption was only 0.18TWh in 1960. Its electricity needs quadrupled, in 1980, to 0.72TWh. After one decade its electricity utilisation reached 1.44TWh and reached its maximum consumption, in 2010, at a value 4.78TWh (Fig. 2.5) (CYSTAT, 2018). In 2011, a powerful explosion knocked down the largest power station of Cyprus resulting in the loss of 60% of the island's installed capacity (Zachariadis and Poullikkas, 2012) triggering a significant shortfall in electricity supply in the following years (Fig. 2.5) (CYSTAT, 2018). Nevertheless, during the last ten years, Cyprus has tried to enhance

the penetration of renewables in its electricity grid. In 2011, renewables accounted for a mere 3.3% of the total electricity production whereas, in 2019, this figure had tripled reaching 9.5% with the remaining percentage fulfilled by fossil fuels (Cyprus Transmission System Operator, 2019b).

2.3.3 Forecasting electricity production in China and Cyprus

Estimating future electricity needs is fundamental to future energy policies. Through the years, many researchers have applied different methods to forecast China's electricity production. Grey modelling has been used to predict electricity generation (Wu *et al.*, 2018). Owing to their properties, Monte Carlo methods have been mainly utilised to simulate different scenarios pertaining to future electricity consumption from renewable energy sources (Santos *et al.*, 2016). In parallel, the Autoregressive Moving Average (ARMA) and the logistic method have been employed in projecting future electricity production (Bodger and Tay, 1987; de Oliveira and Cyrino Oliveira, 2018).

During the past decade, several scholars have applied different methods to forecast Cyprus' electricity production considering, also the prospect of diversifying the island's power mix. For example, an econometric model was applied to predict the future electricity consumption of different sectors in Cyprus (Zachariadis, 2010; Zachariadis and Taibi, 2015). A bottom-up approach was implemented by Taliotis *et al.* (2017) to project the future natural gas supply and its utilisation in the electricity sector. Two studies have dealt with the integration of electric passenger vehicles into the power grid of Cyprus (Heidt *et al.*, 2017; Vougiouklakis *et al.*, 2017). Heidt *et al.* (2017) estimated that, by 2050, a maximum of 15% of the total passenger cars could be electric and Vougiouklakis *et al.* (2017) predicted that less than 1% of the total electricity needs of the island will be dedicated to the transportation sector. Other investigations have analysed various scenarios in energy demand, namely, Vougiouklakis *et al.* (2017) examined three different forecasts: i) a reference scenario, ii) a realistic scenario and iii) the maximum technical potential of final energy demand. Mesimeris and co-authors (2020) examined two hypothetical cases, which considered the impact of "existing measures" and "planned policies and measures", until 2030.

Different scenarios have been suggested which attempt to forecast the future energy and electricity needs of Cyprus, until 2030. Taliotis *et al.* (2017) have reviewed

six distinct cases which focussed on energy efficiency, liquefied natural gas, energy storage and interconnectivity with the Euro-Asia Interconnector until 2030 but without factoring in electric vehicles' needs. Zachariadis and Taibi (2015) introduced four separate scenarios which dealt mainly with energy conservation.

2.3.4 Renewable energy penetration in Cyprus and China

Numerous studies have investigated future decarbonisation efforts, at the EU level (Fragkos *et al.*, 2017; Zappa *et al.*, 2019), or individual member states (Chiodi *et al.*, 2013; Fauré *et al.*, 2019; Glynn *et al.*, 2019; Sferra *et al.*, 2019) while endeavouring to limit global temperature rise by 1.5°C or 2°C. Cyprus, as an EU Member State, differs from other EU countries in that its electricity grid functions as an independent network in isolation. It is the only EU country that is not connected to the European power network and relies entirely on its own domestic production. In 2020, the island's electricity system heavily depended on fossil fuels with over 91% of the total electricity production met from diesel and heavy fuel oil. In 2023, natural gas is expected to be introduced in the electricity sector and it is anticipated to gradually displace oil products helping thus mitigate CO_2 emissions. Most of the island's emissions originate from the electricity and the transportation sectors which account for 48% and 30% of the aggregate emissions, respectively (Kythreotou and Mesimeris, 2020). According to the latest UNFCCC report, 67% of transportation emissions are released from vehicles (Cyprus Department of Environment, 2019). In tandem with the other EU countries, Cyprus has set emission reduction goals for 2030. More explicitly, at the national level, Cyprus intends to cut its electricity, ceramics, cement and industrial emissions by 42%, by 2030, compared to 2005 (Cyprus Department of Environment, 2018). Collectively, emissions reductions from other sectors such as agriculture, waste and others are envisaged to reach 24%, by 2030 (Cyprus Department of Environment, 2018).

Various other studies have examined renewable energy in China (Kahrl *et al.*, 2011; Davidson *et al.*, 2016; Zhao *et al.*, 2017b; Zhang *et al.*, 2018), emissions reductions (Liu *et al.*, 2013; Qi *et al.*, 2014; Fan *et al.*, 2019; Huang *et al.*, 2019a) and the penetration of 100% renewables in the Chinese electricity sector (Jacobson *et al.*, 2015; Clack *et al.*, 2017). Other reports feature the learning rate method which projects the future price of renewables (Junginger M. *et al.*, 2005; Joan *et al.*, 2015). Utilising

the same approach, Tu *et al.* (2019) focused on the costs of onshore wind generation in China demonstrating that grid parity can be attained prior to 2020. Yet, other investigators indicate that diseconomies of scale may emerge by ramping up RES output (Helden and Muysken, 1983; Machado *et al.*, 2016).

Reflecting the global push to decarbonise the energy sector, a plethora of studies dedicated to different regions and countries have investigated distinct options for replacing carbon intensive technologies with renewables and more environmentally benign energy alternatives. Among the jurisdictions which possess the potential to entirely generate their electricity from renewables comprise countries from the Middle East and North Africa (MENA) region (Aghahosseini *et al.*, 2020), South Africa (Oyewo *et al.*, 2019) and Jamaica (Chen *et al.*, 2020). Specifically for China, Mathews and Tan (2013) analysed the integration of renewables and fossil fuels in the context of a low-carbon energy mix without elaborating on the production of greener energy sources. Huang and co-workers (2019a) investigated the utilisation of renewables and energy storage as part of an intercity synergy framework.

A few studies have demonstrated that the adoption of microgrids can promote a high penetration of renewable energy electricity along with battery storage (Zhao *et al.*, 2012) and vehicle-to-grid applications (Liang *et al.*, 2020) considering that power production satisfies 90% of demand (He *et al.*, 2018). Meanwhile, other authors besides reviewing the renewable energy policies of China and the CO_2 footprint of coal use, have contemplated a larger share of renewables in relation to the national goals but stopped short of analysing the role of natural gas or nuclear power (Khanna *et al.*, 2016).

Other researchers (Xiao and Jiang, 2018; Yu *et al.*, 2020) have looked into a new electricity mix for China drawing on the use of nuclear power and a diminishing share of coal on a year-to-year basis. Complementing other studies, Wang *et al.* (2020) have considered a portfolio of renewable energy options in southern China with and in the absence of non-renewable energy technologies. Still, other teams have studied the input of renewables in China's energy sector at the provincial (Liang *et al.*, 2019; Cheng *et al.*, 2020; Wang *et al.*, 2020), the national (Qi *et al.*, 2014; Wu *et al.*, 2016; Zhao *et al.*, 2017b) and the regional level (Huang *et al.*, 2019b). Even more ambitious suggestions, relying entirely on renewable energy sources, such as laying a super grid corridor to electrically tie North and East China (Bogdanov and Breyer, 2016) as well as

interconnecting Europe and China (Wu and Zhang, 2018) have been proposed. Yet other reports (He *et al.*, 2016; Ding *et al.*, 2019; Zhao *et al.*, 2019; Li and Yao, 2020) have dealt with the implementation of a carbon tax as a way of minimising the utilisation of fossil fuels. Of note is the range of a carbon levy suggested in these publications which varied between 10 yuan/tonne of CO_2 (≈1.46$/tonne) and 40$/tonne of CO_2. This thesis assumed a carbon tax cost of 20$/tonne of CO_2 based on the average price of references listed above.

Several other publications have examined the contribution of renewable energy as a proportion of the aggregate power needs of China commencing from 16% (Zhao *et al.*, 2017b) to 40% (Cheng *et al.*, 2020) and spanning between 43% to 100% (Zhao *et al.*, 2017a; Liang *et al.*, 2019; Wang *et al.*, 2020). Compared to other studies, the case for meeting China's power needs entirely (100%) from renewable electricity production at an hourly resolution was made. This thesis also considered energy storage as well as power transmission and distribution costs. Furthermore, a comprehensive phase-out of coal power generation while nuclear energy serves as the main baseload supply coupled with natural gas and renewables was articulated. Two more scenarios were also formulated as part of this investigation and will be elaborated upon in the sequel.

2.3.5 Renewables potential and electricity storage nexus.

Cyprus displays a high solar power potential and a fair amount of wind energy and biomass (Alexopoulos and Hoffschmidt, 2010; Kythreotou *et al.*, 2012; Mesimeris *et al.*, 2020). The island's solar prospects are remarkably high ranging from 1,570kWh/kWp in the mountainous regions and 1,789kWh/kWp near seashore areas (Fig. 2.7). Moreover, its wind potential is concentrated mostly in the western territories of the island (Fig. 2.6). Meanwhile, China has an enormous potential for renewables and hydro (Table 2.1) but has not yet been fully exploited due to various reasons. One of them is their capital costs. Adding considerable capacity of renewables will be accompanied by substantial investments. Wind farms whether constructed inland, nearshore, or offshore manifest at variably different costs. Likewise, the electricity costs of solar power plants may differ appreciably as influenced by their distance from consumers. Solar parks in remote locations, for example, display higher installation (Hernandez *et al.*, 2015; Bukhary *et al.*, 2018) and transmission lines' costs compared to

those stationed within close proximity to consumers (Green, 2000; Mills *et al.*, 2011; International Energy Agency, 2012; Gorman *et al.*, 2019). Moreover, a more significant reason is the excess generation of electricity production during midday which results in substantial power losses (Klinge Jacobsen and Schröder, 2012; Golden and Paulos, 2015). Renewable electricity curtailment can be overhauled with the aid of various storage facilities such as batteries, hydrogen, pumped hydro and vehicle-to-grid technologies (Li *et al.*, 2015; Liu *et al.*, 2018).

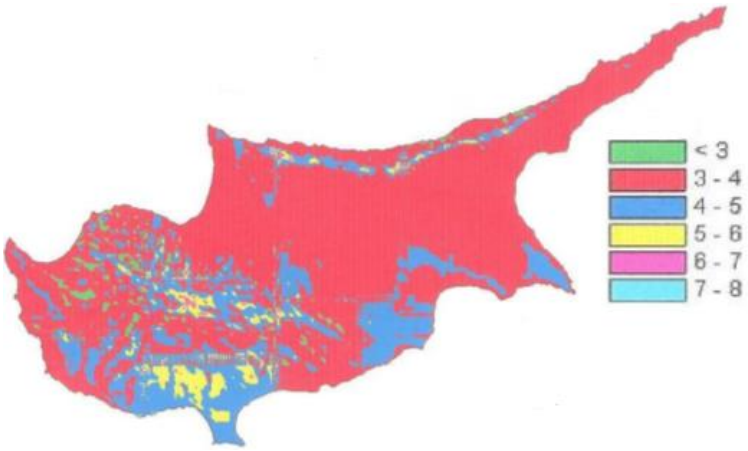

Fig. 2.6. Annual average wind speed (m/s), at a 10m height from the ground, in Cyprus. Adapted from Koroneos *et al.* (2005) and Ercan *et al.* (2013).

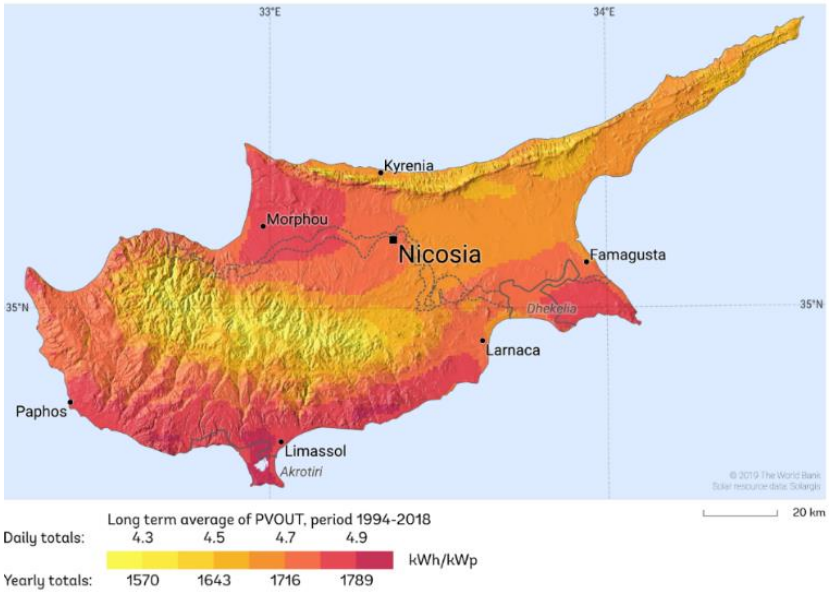

Fig. 2.7. Average solar photovoltaic potential in Cyprus during 1994–2018. Adapted from The World Bank (2019).

Table 2.1: Power generation potential of renewables and hydroelectric units.

Technology	Potential Capacity (GW)	Source
Solar	4,700	(He and Kammen, 2016)
Wind	3,900–4,500	(International Energy Agency, 2012; Yang *et al.*, 2017)
Offshore wind	600	(Yang *et al.*, 2017)
Hydro	800	(World Energy Council 2016)

2.3.6 Electricity storage technologies

Electricity storage is essential to sustain and support renewable energy production through services such as energy shifting, curtailment reduction and congestion relief. In this section, four different storage technologies beginning with pumped hydro followed by batteries and hydrogen and, eventually, vehicle-to-grid integration were analysed.

Pumped hydro currently constitutes the lion's share of energy storage where 93% of all the electricity facilities are tied to it (China Energy Storage Alliance, 2020). It uses two water reservoirs at different heights. Pumped hydro serves two specific functions. If electricity is needed by the grid, then water is allowed to flow down through a turbine to the lower reservoir. When electricity is abundant and cheap some of it is used to pump a portion of the water back to the main reservoir (Morabito and Hendrick, 2019) (Fig. 2.8). Hydroelectric power has a high efficiency spanning between 70 to 80% (Rehman *et al.*, 2015) and it is mostly suitable for peak shaving purposes.

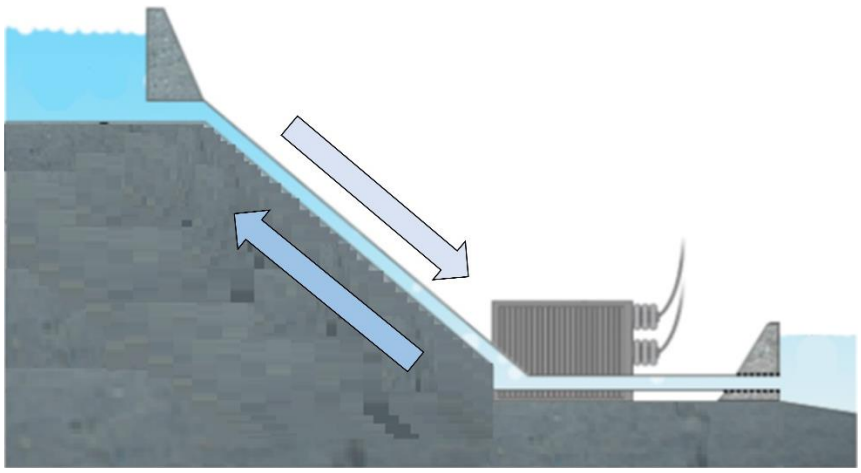

Fig. 2.8. Schematic of the pumped hydro process. After Egbo (2017).

As mentioned above pumped hydro is the most common storage method, the second is electrochemical technology storage with 5.2% of the world's storage facilities, of which 88% derives from lithium-ion batteries (China Energy Storage Alliance, 2020). Lithium-ion batteries are preferred over other battery technologies for their longer lifetime, their extended number of cycles, their efficient charging and inherently lower energy losses. Currently, their main disadvantage is their high capital costs (Vetter and Lux, 2016).

A battery system is usually comprised of solar panels or wind turbines and inverters. The energy produced at first flows through an inverter and can either be used by households, stored in battery banks or sold back to the grid (Fig. 2.9) (Vetter and Lux, 2016). Solar batteries have a lifespan of about 10 years (Lazard, 2017). Battery energy efficiency, defined as the released energy over the energy stored, is approximately 80% (Lazard, 2017) and is used mainly for peak shaving applications during the grid's high demand.

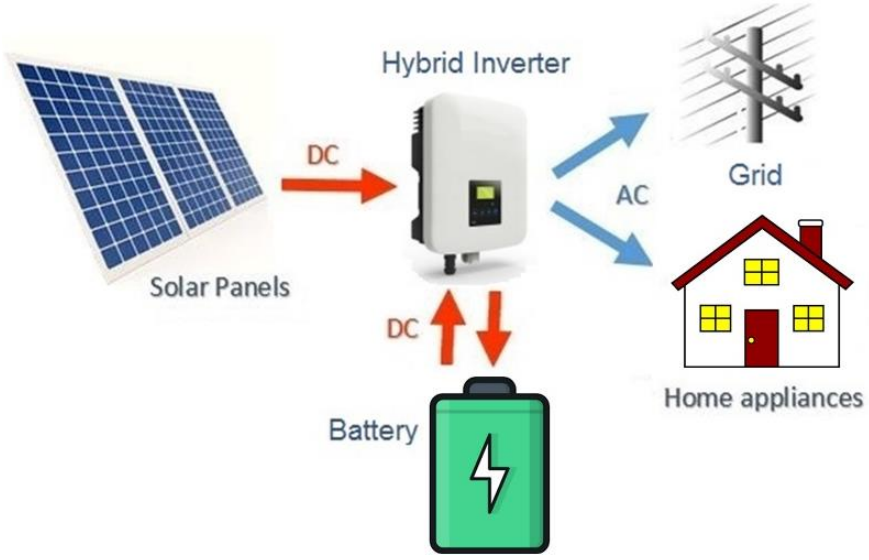

Fig. 2.9. The process of electricity battery storage.

Vehicle-to-grid (V2G) is a new concept that was emerged during the past decade. It features the same characteristics as lithium-ion batteries as it operates as a small movable battery with the ability to charge and discharge its energy into the grid. Concurrently, the concept offers an opportunity to optimise vehicle charging and discharging (Fig. 2.10) (Zaghib *et al.*, 2015). In order to be more efficient and economical, the owners of these vehicles can charge them during off-peak hours and

return their power back to the grid during peak hours motivated by financial gains. Charging and discharging of vehicles can be regulated by the transmission operator based on the grid needs through mobile or internet connections (Deivanayagam, 2017).

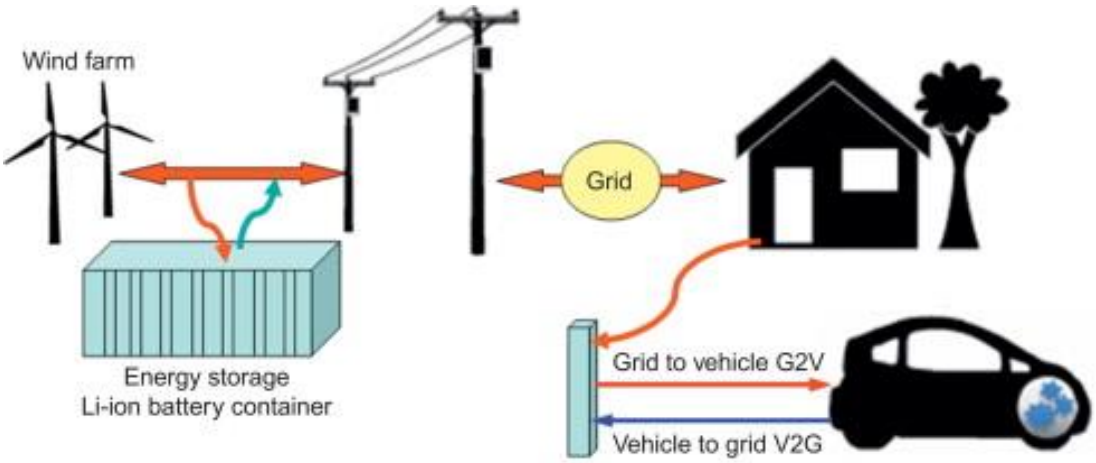

Fig. 2.10. The concept of vehicle to grid. After Zaghib *et al.* (2015).

Hydrogen storage utilises four main components: (1) an electrolyser, (2) a compressor, (3) a hydrogen tank and (3) fuel cells (Penev *et al.*, 2019) (Fig. 2.11).

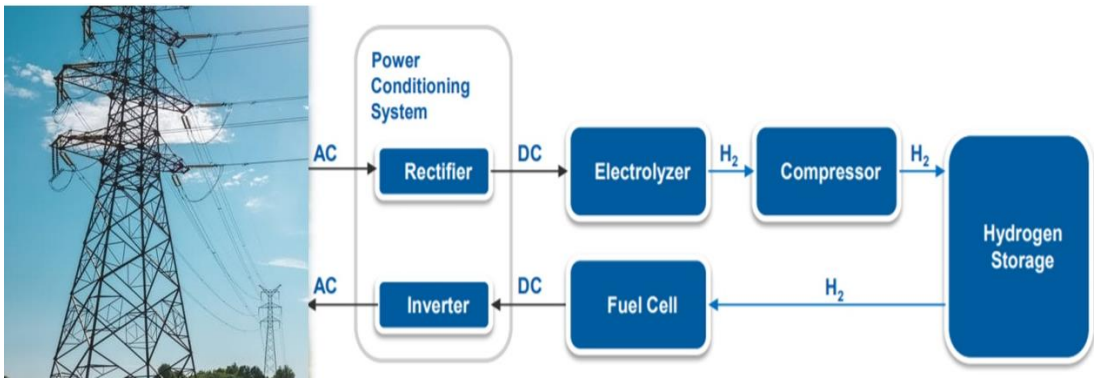

Fig. 2.11. Electrical and chemical aspects of hydrogen production, storage and conversion.

Beginning, the electrolyser water is split into hydrogen and oxygen and following a compression procedure the gas is stored in a tank with the use of electricity. All of the energy stored in the tank is converted into electricity with the aid of the fuel cell and an electrical inverter device. The main advantage of storing hydrogen is that it has insignificant leakage and higher energy density rendering it crucial for long-term

storage compared to batteries that are only used for short periods of time (Zhang *et al.*, 2017). Its main drawback is its low efficiency of 40% which is less than half of that of other storage technologies (Penev *et al.*, 2019). Lastly, hydrogen storage is minuscule compared to other technologies as its share of storage, in 2019, was about 0.01% worldwide (Penev *et al.*, 2019).

Every one of these technologies was examined in terms of its contribution in supporting the future carbon-free scenarios in conjunction with renewables and electricity storage. Specifically, for China the integration of lithium-ion batteries and hydrogen and for Cyprus vehicle-to-grid, pumped hydro and battery storage were considered.

2.3.7 Future electricity production scenarios

Four different scenarios have been formulated. First, the "Business As Usual" (BAU) scenario retains the current installed percentage capacity for each of the power generation technologies projecting them to the year 2050. Second, the "goals" scenario (Goals) considers the national target policies (China National Renewable Energy Centre, 2018) based on the integration of the non-renewable sources, and in particular coal. Next, the "renewables" scenario (RESc) assumes that, by 2050, all of the power generation potential of renewables and hydropower will be exploited. Moreover, this case examines whether the installed capacity can adequately meet the electricity demand complemented by battery storage. Last, the "coal free" (CFr) scenario derives from the goals scenario (Goals) but with the extensive use of nuclear power and natural gas for peak shaving purposes with the intent of phasing out coal by 2050. For each of these scenarios, the hourly electricity production was estimated during 30-day summer and winter periods. Motivated by the need to lower aggregate CO_2 emissions, other projections presented in this study investigated the potential of emissions sinks by considering Land Use, Land-Use Change and Forestry (LULUCF) sources.

Similarly, this investigation projects Cyprus' electricity production until year 2050. During the time horizon spanning to the year 2050, four different scenarios have been formulated. Firstly, the "Business As Usual" (BAU) case considers that, by 2050, Cyprus will draw all of its fossil fuel power generation from combined cycle natural gas power plants which feature efficiencies of ≈60% (Mechleri *et al.*, 2017; Soltani *et al.*,

2017; Mesimeris *et al.*, 2020), while minimising the electricity sector's emissions. Secondly, the "Least Cost" Scenario (LCSc) is a variant of the BAU case with the major distinction being that the LCSc aims to minimise electricity costs. Thirdly, the Carbon Capture and Storage scenario (CCSc) was developed on the condition that, by 2050, all of the natural gas power plants will be fitted with carbon capture. Lastly, the "Renewables" scenario (RESc) presupposes that, by 2050, the power generation will be derived solely from renewables, particularly, solar, wind, biomass and hydroelectricity.

2.4 Atmospheric pollutants

2.4.1 Health impacts

Carbon dioxide is not the only gas considered to be harmful to people and the environment. Other gases have been determined to have more deleterious effects. Nitrogen oxides (NO_x) have been connected to serious health and environmental issues. Nitrogen oxides coupled with sulphur dioxide can foster acid rain which when falls on trees can harm them. Other detrimental effects comprise a reduction in the population of birds, frogs and fish due to the inability of eggs to hatch under such an acidic environment (Menz and Seip, 2004; Grennfelt *et al.*, 2020). Furthermore, NO_x particles permeating in the human lungs can induce short-term respiratory complications such as inflammation and smaller lung function leading to reduced oxygen circulation (Boningari and Smirniotis, 2016). Other common issues encompass bronchitis, emphysema and heart dysfunctions as well as elevated premature mortality losses (Cao *et al.*, 2011b).

Carbon monoxide can become very toxic beginning if its concentration surpasses 1500 ppm. When inhaled it can lead to hypoxia meaning that the volume of oxygen transported to body organs and the tissue is reduced triggering heart or brain problems. At unusually high levels in excess of 40,000 ppm O_2 can lead to death in two minutes (Raub *et al.*, 2000). Particulate matter is also considered to be one of the most dangerous gases. It has been tied to hospital admissions due to respiratory problems (Zhang *et al.*, 2020b), cardiovascular (Ebisu *et al.*, 2019) and other pulmonary diseases including asthma (Grineski *et al.*, 2015). In fact, particulate matter pollution has been

linked to premature mortality, lung cancer, cardiovascular and respiratory disease (Chowdhury and Dey, 2016; Du *et al.*, 2016; Shu *et al.*, 2016).

Alarmingly, air pollution in 2015 was the cause of 4,200,000 deaths, where the majority of 1,108,000 and 1,090,000, occurred in China and India, respectively (Cohen *et al.*, 2017). According to the European Energy Agency, in 2018, in Europe alone, more than 400,000 people have prematurely lost their lives due to outdoor air pollution (European Environment Agency, 2020a). Concluding, to alleviate the consequences of these pollutants a roadmap must be adopted which endeavours to minimise emissions emanating from anthropogenic sources and actions.

2.4.2 Pollution mitigation policies

A plethora of studies have investigated traffic policies intended to slash vehicle emissions (Xia *et al.*, 2015; Tobollik *et al.*, 2016; Tischer *et al.*, 2019; Host *et al.*, 2020; Maesano *et al.*, 2020; Sousa Santos *et al.*, 2020; Tang *et al.*, 2020; Tezel-Oguz *et al.*, 2020). A few scholars have attempted to evaluate the impact of combustion-generated pollutants in Thessaloniki, Greece (Sarigiannis *et al.*, 2015) and in Beijing-Tianjin-Hebei region, in China (Liu *et al.*, 2019b).

A handful of studies have focussed on atmospheric pollution in Cyprus. Petsas *et al.* (2020) counted particulate matter concentration in various areas in the city of Limassol. Middleton *et al.* (2008) have pointed to a surge in cardiovascular and respiratory morbidity risk in Cyprus together with a rise in atmospheric PM_{10}. Another investigation by Tsangari *et al.* (2016) established that cardiovascular and respiratory admissions escalated with rainy days and cold and cloudy weather. Branching to marine transportation, Viana *et al.* (2020) estimated that the utilisation of cleaner fuels in conjunction with more environmentally minded shipboard operations, in 8 Mediterranean cities, can potentially lower the mortality rate from shipping traffic by 15%. Finally, Achilleos *et al.* (2014) besides classifying PM_{10} sources in dust storms and urban sources have indicated that traffic policies between 1993 and 2008 have led to a precipitous drop in PM_{10} concentration.

2.4.3 Origins of atmospheric pollutants in Cyprus

Integrating both actual measurements and theoretical findings, this thesis

examines road and residential heat-related emissions at the centre of Nicosia, the capital of Cyprus. In contrast to other European countries, the island of Cyprus presents certain peculiarities. With a concentration of 23.5μg/m^3, in 2018 (European Environment Agency, 2020a), Cyprus ranked second highest regarding its level of nitrogen oxides in Europe. Transport related NO_x emissions made-up 43% of the contaminants whereas stationary residential heat emissions were responsible for 2.2% of the aggregate concentration (European Environment Agency, 2020b). Anthropogenic particulate matter emissions on the island originated predominantly from road transportation (21.5%) and residential heat sources (3.2%) (European Environment Agency, 2020b). Meanwhile, sea salt and dust exerted a sizeable effect on the PM concentration as they constituted 41.6% of the background particles, in 2017, due to the island's close proximity to the Sahara desert (Department of Labour Inspection of Cyprus, 2019).

2.4.4 Modelling

Dispersion models are used to investigate the transport of a pollutant in the atmosphere (Krausmann, 2017). In order to simulate and trail the particles at a specific time period, the site topography along with the meteorological condition are essential (Krausmann, 2017). The movement of pollutants can be estimated by two different methodologies, namely, the Lagrangian and the Eulerian. The Lagrangian approach follows the trajectory of individual fluid particles over time in space based on the airflow (Li *et al.*, 2006). On the other hand, the Eulerian approach considers the concentration of particles as well as their spreading as a continuum (Saidi *et al.*, 2014). Among the two of them, the Lagrangian method has a higher computational time than the Eulerian approach which may experience numerical diffusion, but it is preferred when dry and wet deposition chemistry is needed (Li *et al.*, 2006).

At a city level, this study formulated a Graz Lagrangian (GRAL) microscale model which was used to investigate the effects of traffic and residential combustion pollutants (Oettl, 2020). Geographically, GRAL models were applied for case studies in Europe (Ketzel *et al.*, 2007; Oettl, 2014; Fabbi *et al.*, 2019) and Asia (Ling *et al.*, 2020; Zhang *et al.*, 2020a). Among else, the dispersion models have considered NO_x (Oettl *et al.*, 2003; Veratti *et al.*, 2020), particulate matter (Sturm *et al.*, 2007; Kurz *et al.*, 2014) and carbon monoxide (CO) concentration (Rafiei and Sturm, 2018). Furthermore, other

studies have analysed dispersion models and real data at the street (Ježek *et al.*, 2018; Santiago *et al.*, 2020) or the city level (Fallah-Shorshani *et al.*, 2017; Milando and Batterman, 2018; Fabbi *et al.*, 2019; Fu *et al.*, 2020).

Effectively, this thesis has developed the modelling framework for tracing four distinct pollutants, namely, 1) $PM_{2.5}$, 2) PM_{10}, 3) NO_x and 4) CO in the city centre of Nicosia, Cyprus. Theoretical results were calibrated with real traffic and residential emissions measurements, from the Department of Civil Works and the Department of Labour Inspection of Cyprus, spanning between January 1st, 2017, and September 30th, 2017. After reconciling the numerical findings of the four pollutants with actual data from an air quality station, attention shifted to 9 other scenarios which focused on $PM_{2.5}$ and NO_x emissions. Primarily, these scenarios have probed a change in road vehicle speed, the penetration of electric passenger vehicles, the mandatory use of only Euro 6 standard vehicles, and the prohibition of diesel passenger vehicles (PV) and light duty vehicles (LDV). By 2030, most of the vehicles in Cyprus will conform to Euro 6 standards. Separate cases were designed to complement Euro 6 standards by either banning fireplaces or diesel PVs and LDVs or examining the prospect of an 80% electric passenger vehicle penetration with a ±20% change in traffic flows.

3 Methodology

Chapter three describes all of the modelling methods. It was divided into two segments, that is, 1) the electricity and 2) the traffic and residential heat sectors. Initially, all of the methodologies used to forecast the electricity sector's production are presented. Secondly, the levelised cost of electricity (LCOE) and carbon dioxide emissions were estimated from each power plant such as coal, natural gas, wind, solar and others based on assumptions and calculations. Thirdly, the hourly electricity production methodology for both Cyprus and China is expressed herein. Next, all the parameters utilised to calculate the pollutants at the centre of Nicosia, the capital of Cyprus are defined. Finally, numerous scenarios regarding vehicular and fireplace policies were proposed aiming to estimate the reduction of premature mortality.

3.1 Forecasting the electricity sector power demand and generation

This section forecasts the electricity sector's electricity production and utilisation for both Cyprus and China, where the methodology displays similarities and differences. To begin with, an uninterrupted 24/7 electricity supply should be ensured. An effort was made to keep the levels of carbon dioxide emissions along with electricity costs to a minimum. Initially, a future projection of the Chinese and Cypriot installed capacity and electricity production from various power generation technologies was conducted stretching to 2050 by investigating four different scenarios. Dispatched hourly power generation is governed by different priorities, where baseload technologies such as nuclear (in the case of China) assume precedence over renewables. Subsequently, fossil fuel generation follows and finally, if warranted, electric storage capacity meets the remaining power system needs. Primarily concerned with minimising the cost and the emissions of future electricity production, the proposed electricity scenarios featured an excess amount of power generation instead of relying on more costly storage facilities. Worth mentioning the future vehicle fleet of Cyprus was projected until 2050. Next, for China solely the foreseeable future fuel and capital costs were estimated while for Cyprus these were assumed. Moreover, regarding China, two future scenarios were devised based on the future emissions of each power plant. Lastly, the hourly electricity production profile which considers production and needs from power plants along with

storage facilities for China and desalination plants, vehicle charging and PV2G needs for Cyprus was revealed.

3.1.1 Logistic growth method

To predict the future Chinese electricity production and the Cypriot vehicle fleet, a logistic growth behaviour was adopted based on one main assumption. At such, the curve asymptotically follows an upper limit with a sigmoidal (S) shape growth. Interestingly, the logistic method has been applied in several fields ranging from technology (Fisher and Pry, 1971), biology (Walford, 1946) and economics (Griliches, 1957). Similarly, this method has also been employed in a variety of case studies in the electricity sector (Bodger P. S. and Tay, 1986; Mohamed and Bodger, 2005). The historical data used to forecast electricity production span between 1990 and 2018 (International Energy Agency, 2017; China Energy Portal, 2018). To this end, the following equation was used to determine electricity production (f_t), in kWh, at year t:

$$f_t = F / (1 + e^{a_o + a_1 t}) \quad (1)$$

where F refers to the asymptotic value (maximum electricity production and vehicle fleet) while α_o & α_1 are constants.

3.1.2 Multiple linear regression model

To forecast the future needs of each sub-sector of interest, a multiple linear regression model based on the variations in certain parameters, such as, the country's population and the GDP was adopted. This method was previously applied in different countries including Cyprus (Zachariadis, 2010; Dilaver and Hunt, 2011; Zachariadis and Taibi, 2015). Seeking to minimise the margin of error, the preceding model was implemented in the sectors of agriculture, industry and commercial activities. More precisely, a presupposition was made factoring in the growth in GDP and changes in population based on the birth and mortality rates and the arrival of immigrants (Table B1 and Table B2).

For the industrial sector, the parameters which defined the future electricity needs, comprised variations in ceramic and clinker production together with the GDP and population changes, as described in the sequel. Clinker production was assumed to increase linearly, until 2029, only to reach its peak production of 2,000 kilotonnes (kt)

in the year 2030. Ceramic production was intimately linked to the number of households under construction as reflected by a correlation coefficient of 0.87 (Demetriou *et al.*, 2021). Another sector, namely, that of the agriculture embraced four distinct parameters which influenced its future electricity needs. Cattle and swine population (Fig. B2) were estimated from the Holt-Winters method (Ferbar Tratar *et al.*, 2016), together with changes in the GDP and the human population. Finally, the commercial's sector future electricity requirements are derived from the number of tourists (Fig. B1), the count of hot and cold days per year which ranged between 95 to 135 (Eurostat, 2020) along with the GDP and the island's population. The island's future electricity needs were estimated from the following equation:

$$\ln(y_{1,t}) = a_1 + a_2 \ln(b_{1,t}) + a_3 \ln(b_{2,t}) + ... + a_n \ln(b_{n-1,t}) \quad (2)$$

where t is the year, parameter y denotes the electricity needs of a particular sector, $\alpha_{1,...,}\alpha_n$ are constants and $b_{1,...,}b_{n-1}$ are pertinent parameters, such as the GDP, the population and others, used to determine the future electricity needs of each sector.

Interestingly, the residential sector is the second most energy demanding after the commercial division accounting for over 35% of the total power needs (Electricity Authority of Cyprus, 2020). Thus, electricity consumption of the residential sector was calculated as a multiple of the number of households, the size or area of each household and its electricity consumption per unit area. Table 3.1 lists all of the relevant assumptions. Desalination units consumed about 4% of the country's overall electricity consumption as estimated from the 2019 yearly fresh water desalination output (Water Development Department of Cyprus, 2019; Electricity Authority of Cyprus, 2020). Their consumption intensity was about 4.5 kWh per cubic metre of potable water (Schenkeveld *et al.*, 2004) which also comprised the power needs to deliver the water to its destination. According to the Water Development Department of Cyprus (2019), the minimum yearly water production was 65.6 million cubic metres in 2019. As far as seawater desalination is concerned, two separate scenarios were formulated. The first assumed that the desalination units' power consumption will remain unaltered until year 2050. Alternatively, the second scenario presumed that, desalination plants will satisfy at least 80% of all future tourists' and domestic water demand. Preceding water needs were obtained from an average water consumption of 180 litres per person, per day, for

Cypriot citizens and 410 litres per tourist, per day, (Iacovides, 2007) with an average of 8 days of overnight stay.

Currently, street lighting accounts for less than 2% of the overall electricity consumption in Cyprus (Electricity Authority of Cyprus, 2020). Primarily, a forecast of the road driveways' mileage was obtained through the logistic method. To estimate the island's future street lighting energy needs, the yearly road infrastructure length was either multiplied by the consumption factor of 6.85kWh/km, as it is today, or by a coefficient that is linearly reduced by 40%, until 2050, due to the higher penetration of less energy demanding LED street lamps (Demetriou *et al.*, 2021).

Table 3.1: Household parameters (Demetriou *et al.*, 2021).

Parameters	Years (2018–2029)	Years (2030–2040)	Years (2041–2050)
New household, max. size (assumed) (m^2)	190	180	160
New household, min. size (assume) (m^2)	180	160	140
Persons per home (linearly reduced)	2.9 (2018)	2.6 (2035)	2.3 (2050)
Power consumption, max. size (assumed) (kWh/m^2)	35.5	35.5	35.5
Power consumption, min. size (assumed) (kWh/m^2) (linearly adjusted)	35.2 (2020)	31.9 (2030)	32.0 (2050)

3.1.3 Levelised cost of electricity

The costs of each technology were determined from the levelised cost of electricity (LCOE). Total expenses were calculated by summing up the cost components emanating from the capital, fuel, operational and maintenance and decommissioning aspects, as stated by Carlsson *et al.* (2014) and Budinis *et al.* (2018). Collectively, the LCOE (€/kWh) for China was obtained from:

$$LCOE = [(a \times I + OM) / E] + FC + TD + EmC \quad (3)$$

as for Cyprus, the following equation was applied to determine the LCOE:

$$LCOE = [(a \times I + OM) / E] + VOM + FC + EmC + CCap + CharC \quad (4)$$

where a is the capital recovery factor, I are the total capital costs and OM are the operational and maintenance costs calculated on a monetary (€) basis. Additionally, E is

the energy produced in kWh, *VOM* are the variable operational and maintenance costs and *FC* are the fuel costs. Acronym, *EmC* refers to the emissions cost component, *TD* are the transmission and distribution costs, *CCap* are the carbon capture, transport and storage costs and *CharC* are attributed to the charging costs, estimated in €/kWh. The capital recovery factor (*a*) was derived from:

$$a = r/[1-(1+r)^{-L_T}] \quad (5)$$

where r is the interest rate and L_T is the project lifetime. Fuel costs (*FC*) were determined as a product of the fuel price and the produced electricity, divided by the conversion efficiency. Electricity production derives from the multiplication of the power generation project duration, the capacity factor and the installed capacity. For battery storage, *I* was estimated from two factors. Initially, by dividing the total battery storage with its cost per kWh. Secondly, by obtaining the ratio of the overall installed capacity and the power costs per kW. Battery storage capital costs were finally divided by the amount of produced electricity as well as their power generation efficiency.

Referring to the transportation sector, the bus electricity costs were estimated by dividing the charger costs by the total energy charged and, finally, adding the charging costs. In closing, for the passenger-vehicle-to-grid an extra term was added to bus electricity costs, that of battery costs divided by its efficiency and number of charging cycles. Table 3.2, Table 3.3 and Table 3.5 list the parameters used in the preceding calculations for each of the power generation technology of interest for Cyprus and Table 3.6, Table 3.4 and Table 3.7 for China.

Table 3.2: Battery storage data for lithium-ion batteries in Cyprus.

Parameter	Lithium-Ion	Source
Capital costs (€/installed kW)	285	(Mongird *et al.*, 2019)
Capital costs (€/installed kWh)	306	(Mongird *et al.*, 2019)
Lifetime (years)	20 (lifecycle: 10 years)	(Lazard, 2017)
O & M (€/installed kWh)	2.44–3.06	(Lazard, 2017)
Average yearly capacity (%)	91	(Sarasketa-Zabala *et al.*, 2015)
Efficiency (%)	86	(Lazard, 2017)
Cycles per year	350	(Lazard, 2017)

Lithium-ion batteries and hydrogen storage projection costs have been examined by an array of researchers (Zakeri and Syri, 2015; Murray *et al.*, 2018; Cole and Frazier, 2019; Gorre *et al.*, 2019; Schmidt *et al.*, 2019). This study adopted lithium-ion batteries after Cole and Frazier (2019), projecting that by 2050 their costs will amount to 156$/kWh. Hydrogen storage cost predictions, based on Schmidt *et al.* (2019), are explained in Table A15. Table 3.4 and Table 3.7 summarised the anticipated capital costs of batteries and hydrogen storage. Thanks to its properties, the learning rate method was used to calculate the renewable energy capital costs (Junginger M. *et al.*, 2005; Kim *et al.*, 2012). Two central ideas govern its formulation. Initially, what matters, is the experience gained from the application of the particular technology over time. Secondly, as one might expect, the first prototype of each technology is almost invariably the most expensive, but the cost of subsequent units drops as a function of production volume over time and product optimisation.

Table 3.3: Electric vehicle data for Cyprus.

Parameter	Car	Bus
Battery costs (€/installed kWh)	230[(a)]	180[(b)]
Battery capacity (kWh) (assumed)	40[(a)]	350[(b)]
Average kilometres per day (km) (assumed)	50	200
Charger costs current (assumed fixed) (€)	800[(c)]	25,000[(c)]
Charge capacity (kW)	7[(c)]	50[(c)]
Autonomy (km)	250[(a)]	200[(b)]
Lifecycles (assumed)	2,000	3,000

Data sources: a: Li *et al.* (2020), b: Hooftman *et al.* (2018), c: Nicholas (2019).

Table 3.4: Battery storage data for China.

Type of battery	Lithium-ion	Source
Capital costs ($/installed kWh)	385–419	(Lazard, 2017)
Lifetime (years)	20 (replaced in 10 years)	(Lazard, 2017)
O & M* ($/installed kWh)	2.44–3.06	(Lazard, 2017)
Average yearly capacity (%)	91	(Sarasketa-Zabala *et al.*, 2015)
Dis/Charging efficiency (%)	86	(Lazard, 2017)
Cycles per year	350	(Lazard, 2017)

*Refers to operation and maintenance.

Table 3.5: Input particulars for the various power generation technologies, in 2050, for Cyprus.

Energy source	Capital costs (€/kW)	Operation and Maintenance (%)	Variable maintenance cost (€/kWh)	Fuel price (average, assumed)	Lifetime (Years)	Conversion efficiency (%)	Average CO_2 emissions factor ($grCO_2/kWh$)	Average capacity factor (%)	Minimum utilisation factor (assumed)	Maximum utilisation factor (assumed)	Carbon capture cost (€/t of CO_2)
Natural gas	900[a]	2[c]	2[c]	5€/MMBtu	40[c]	60[i, l]	350	–	30	90	–
Wind	1,100[b]	2[b]	–	–	25[b]	–	–	17[g]	–	–	–
Solar	520[b]	2[b]	–	–	25[b]	–	–	18[g]	–	–	–
Biomass	2,500[b]	2.2[b]	8[b]	0.05€/kWh[e]	30[b]	–	–	60[g]	–	–	–
Pumped hydro	754–1,185[f]	7.36–10.98€/year[e]	–	–	30[e]	77[e]	–	10–30[e]	–	–	–
Concentrated solar power	4,500[d]	4[b]	3.1[b]	–	30[b]	–	–	40[h]	–	–	–
CCS natural gas	1,800[f]	2.5[c]	4[c]	5€/MMBtu	40[c]	45[j, k, m]	40[k]	–	30	90	60–112[c, f]

Data sources: a: Cloete and Hirth (2020), b: Carlsson *et al.* (2014), c: Budinis *et al.* (2018), d: Lilliestam and Pitz-Paal (2018), e: Poullikkas (2013), f: Rubin *et al.* (2015), g: Cyprus Transmission System Operator (2019b), h: National Renewable Energy Laboratory (2019), i: Mesimeris *et al.* (2020), j: Daggash *et al.* (2019), k: Daggash *et al.* (2019), l: Soltani *et al.* (2017), m: Pérez Sánchez *et al.* (2019).

Table 3.6: Input particulars for the various power generation technologies for China.

Energy source	Capital costs ($/kW)	Operation and Maintenance ($/kW)	Fuel price	Transmission and Distribution [k, l] ($/kWh)	Lifetime (Years)	Years to build	Conversion efficiency, η (%)	Average CO_2 emissions factor[h] ($grCO_2/kWh$)	Lowest CO_2 emissions factor[b] ($grCO_2/kWh$)	Capacity factor[j] (%)
Coal	813[a]	30.3[a]	94.7 $/tonne[e]	–	40[a, b]	4[a]–5[b]	33–48[b]	1,230	740	54
Natural gas	627[a]	24.2[a]	5.3 $/MMBtu[d]	–	30[a, b]	2[a]–4[b]	41–60[b]	856	410	31
Nuclear	1,807–2,615[a]	52.12[a]	0.0039 $/kW[i]	–	60[b]–80[a]	7[a]–9[b]	33–34[b]	17	3.7	81
Onshore wind	1,260[c]	22.2[a]	–	0.01–0.05	25[a, b]	1[a]–1.5[b]	–	46	7	20
Offshore wind	3,012[m]	22.2[a]	–	0.01–0.05	25[a, b]	1[a]–1.5[b]	–	46	7	20
Solar	1,100[c]	24.5[a]	–	0.05–0.11	25[a, b]	1[a]	–	76	18	10
Hydro	598–1,630[c]	48.2[a]	–	–	50[b]–60[a]	5[b]	–	13	4.2	37
Biomass	1,300[f]	20[f]	0.05 $/kWh[g]	–	30[a]	2[a]	–	97	45	60

Data sources: a: Nuclear Energy Agency *et al.* (2015), b: Krey *et al.* (2014), c: IRENA (2017), d: Energy Information Administration (2017b), e: BP (2018), f: Zhibin and Xiaoning (2016), g: IRENA (2012), h: Yang *et al.* (2017), i: World Nuclear Association (2019), j: China Energy Portal (2018), k: Lin and Wu (2017), l: Mills *et al.* (2012), m: International Renewable Energy Agency (2019).

Table 3.7: Hydrogen storage data for China.

Type of storage	Hydrogen	Source
Charging costs ($/kW)	942	(Penev *et al.*, 2019)
Storage costs ($/kWh)	35	(Penev *et al.*, 2019)
Discharging costs ($/kW)	574	(Penev *et al.*, 2019)
Lifetime (years)	30	(Penev *et al.*, 2019)
O & M ($/kW/year)	30	(Zakeri and Syri, 2015)
Overall efficiency (%)	40	(Schmidt *et al.*, 2019)
Cycles per year	1,460	(Schmidt *et al.*, 2019)

3.1.4 Forecasting China's fuel costs

The costs of natural gas and coal in China often fluctuate depending on market conditions. During the lifetime of natural gas and coal power plants, fuel costs are the most significant expenses far outweighing other expenditures such as capital investments. As a way of forecasting the future fuel price of natural gas and coal in China, the Autoregressive Moving Average (ARMA) method was adopted, as outlined in the sequel. Regarding Cyprus, a specific fuel price cost was assumed as reflected in Table 3.6. Other studies (García-Martos *et al.*, 2013; Elyakova *et al.*, 2017) have implemented these methods to predict the future prices of fuels and electricity. Statistically, ARMA is formulated on the current and past disturbances (Pukkila *et al.*, 1990) as expressed by:

$$y_t = a_1 y_{t-1} + a_2 y_{t-2} + \ldots + a_p y_{t-p} + \beta_1 \varepsilon_{t-1} + \beta_2 \varepsilon_{t-2} + \ldots + \beta_p \varepsilon_{t-q} + \varepsilon_t \quad (6)$$

where y_t is the realisation of the dependent variable, $y_{t-1}, y_{t-2}, \ldots, y_{t-p}$ accounts for the lagged dependent variables and $\alpha_1, \alpha_2, \ldots, \alpha_p$ are the autoregressive parameters of the model. The number of lagged values (p) of t represents the order of the process and $\varepsilon_{t-1}, \varepsilon_{t-2}, \ldots, \varepsilon_{t-p}$ refer to the realisation of the lagged disturbances.

3.1.5 China's carbon dioxide emissions and carbon sinks

Projections pertaining to the future CO_2 emissions from the electricity sector of China, between 2016 and 2050 emanate from two different scenarios. The first scenario rested on the assumption that the emissions factors of each power generation technology (Table 3.6) would remain invariant during the preceding period. This implied that no

technological improvements would occur reflecting a conservative approach. Relaxing this assumption, in the second scenario, the emissions factor of each electricity generation technology experiences a linear decay, until 2040 and thereafter stabilises to a magnitude reflecting the lowest CO_2 emissions factor (Table 3.6) (Demetriou and Hadjistassou, 2021). Evidently, this behaviour springs from technological improvements which manifest in the form of lower average emissions factors relative to the prevailing values.

Emission sinks constitute yet another effective way of mitigating the effects of China's CO_2 emissions. Drawing on their potential to lower national emissions, China has identified forest stocks as one of the most promising measures it could adopt. Therefore, it was deemed helpful to forecast the potential emissions sinks of China's LULUCF until the year 2050. When data obey a linear projection and/or there is seasonality in the figures, the Holt-Winters method is preferred. This method is based on two smoothing equations, that is, the level and the trend, as illustrated in Ferbar *et al.* (2016). These projections were obtained from Holt-Winters and the logistic method while utilising input from Zeng *et al.* (2015). Subsequently, the negative emissions of China from LULUCF were determined from the IPPC equations (Penman *et al.*, 2003), as stated in Forsell *et al.* (2016). For the record, the values of the wood density, the biomass expansion factor and root-shoot ratio were taken to be 0.43, 1.36 and 0.37, respectively. To put emissions into perspective, the estimated carbon stock emissions from this study were compared with the goals set by China's State Forestry Administration (2014).

3.1.6 Natural gas as a transition fuel in China and Cyprus

Natural gas is frequently touted as a transition fuel for high- to low-carbon intensive economies. Due to its high reliance on coal, the Chinese power generation sector was chosen as a test case. Similarly, Cyprus' electricity system depends heavily on diesel and heavy fuel oil. In June 2023, natural gas is anticipated to be introduced in the Cyprus electricity sector to replace (other) oil products (Psyllides, 2021). Viewed from the Chinese perspective, gas imports raise security of supply concerns (Kong *et al.*, 2019) and, hence, piped gas volumes are kept in check. Supplementing domestic consumption, out of the 240bcm utilised by China, in 2017, 92bcm were imported either as piped gas or as LNG from Qatar, Australia, Turkmenistan, Uzbekistan and other

sources (BP, 2018). According to official Chinese statistics, in 2016, electricity production in China "absorbed" 40.7bcm of natural gas which equates into about 20% of the overall gas consumption (National Bureau of Statistics of China, 2018). In total, a mere 3.1% of the aggregate electricity production originated from natural gas power generation (China Energy Portal, 2018). Given the power needs of each electricity mix scenario, in units of kWh, it is possible to deduce the volume of natural gas, in billion cubic meters (bcm), needed to realise the corresponding energy production.

Currently, combined-cycle gas turbines boast an efficiency slightly above 60%. This figure is expected to reach 65% within the next decade (International Energy Agency, 2018). For the record, open-cycle gas turbines feature an efficiency of 42% (International Energy Agency, 2018). Adopting a conservative approach, it was assumed that natural gas generation units would keep an average efficiency of 60% by the year 2050. Calculations are based on IEA (2011) quotes, such that, 1bcm of Russian gas contains 38.2 petajoules (PJ) of energy which yields 10.6TWh of electricity. One bcm of Qatar gas encompasses 41.4PJ which translates into 11.5TWh of power (International Energy Agency, 2011).

3.1.7 Future energy mix of China

As stated before, the future electricity mix of China was obtained from 4 scenarios, namely, (1) the Business As Usual, (2) the Goals, (3) the Coal Free and (4) the Renewables. All other scenarios, except for the BAU, predict their energy mix which consists of renewables as well as hydro and biomass through the application of the logistic method. The BAU scenario assumes the same percentage of electricity production as of 2017, ensuring the potential capacity of renewables and hydroelectric power (Table 3.6) is not exceeded by 2050. An estimate of the potential of each renewable energy generation technology is listed in Table 3.8 which comprises the hydro power potential as well. Solar and wind potential for each Chinese province are listed in Table A1.

Hydroelectric power is not considered a RES technology if its installed capacity exceeds 10MW (World Commission on Dams, 2000). This is justified on the grounds that large hydroelectric dams are accompanied by social and ecological impacts. According to the World Commission of Dams, until 2000, 40–80 million people have evacuated their homes to make space for building dams (World Commission on Dams,

2000). In addition, at least 20% of fresh water fish species are believed to have become extinct, endangered or threatened due to construction works related to hydro dams (World Commission on Dams, 2000). Interfering with water patterns, dams may change the distribution and rate of water flow (World Commission on Dams, 2000).

Table 3.8: Stated policies for renewables, hydro and nuclear energy for years 2030, 2035, and 2050.

Power generation technology	Stated policies for 2035 (GW)	Stated policies for 2050 (GW)	Source
Solar	1,486	2,157	(China National Renewable Energy Centre, 2018)
Wind	1,162	2,062	(China National Renewable Energy Centre, 2018)
Hydro	454	532	(China National Renewable Energy Centre, 2018)
Nuclear	$200^{(\text{in } 2030)\,*}$	400–500	(World Nuclear Association, 2019)

*World Nuclear Association stated policies pertain to years 2030 and 2050.

3.1.8 Future energy mix of Cyprus

Concerning Cyprus, four distinct scenarios were considered to year 2050 grounded on different approaches which draw mostly from European Commission goals aimed at containing global temperature increase to a minimum. Together, the first and second scenarios rely on the intention that by 2050 Cyprus' electricity production will no longer depend on oil but will shift towards natural gas without carbon capture. In particular, the Least Cost scenario (LCSc) aims to minimise cost while the Business As Usual (BAU) scenario intends to reduce emissions.

The third scenario, dubbed Carbon Capture and Storage (CCSc), reveals a fundamental difference compared to the BAU and the LCSc cases. Its main distinction being that natural gas combined cycle power generation units will employ carbon capture and storage. This scenario examines and calculates if the carbon and capture technology will be technologically and financially fit to minimise emissions by at least 80%, in 2050, compared to 1990. Such a goal was aligned with the European Commission targets set in 2009 which aim to minimise emissions between 80 to 95%, by 2050 (European Commission, 2018).

Taken as the most environmentally benign the fourth case, that is, the

Renewables Scenario (RESc) aims to attain carbon neutrality by limiting the temperature increase to 1.5°C, by year 2050 compared to the pre-industrial levels, as recommended by the European Commission in December 2019 (European Commission, 2019). This ambitious scenario presupposes that, by 2050, electricity production will emanate entirely from renewables as well as pumped hydro and battery storage and the uptake of passenger-vehicle-to-grid technologies. At the outset, the goal of the RESc is to minimise the electricity costs while sustaining a power grid that manages to meet power demand at all times.

3.1.9 Hourly electricity production

This sub-section is one of the main pillars of this research. It is divided into two parts: one dedicated to China and the other to Cyprus. Herein, the hourly electricity production from all power sources which include renewables, natural gas, and storage facilities such as batteries, hydrogen, and pumped hydro was estimated. China and Cyprus exhibit one main distinction as far as future energy needs are concerned. That pertains to the integration of passenger vehicle-to-grid technology for the Cypriot electricity grid which is determined from the pertinent equations which calculate the hourly electricity production on the island. Hourly power generation rests on different priorities. Baseload production from technologies such as nuclear energy (in the case of China) and biomass are introduced first on the grid complemented next by renewables. If demand is not met, fossil fuel generation is integrated into the grid and finally, if necessary, storage facilities meet the remaining power system needs. The system is cost sensitive meaning that the proposed electricity scenarios may produce an excess amount of power generation central to minimising electricity costs.

3.1.9.1 China

In order to forecast the future electricity production from renewables there is a need to consider the capacity factors during the winter and summer periods, as listed in Table 3.9. According to the National Bureau of Statistics of China and the National Energy Administration of China, the maximum electricity output of the country manifests during the winter and summer seasons (National Bureau of Statistics of China, 2019). More specifically, peak electricity demand manifests in August and the second highest during December. For this reason, only the winter and summer seasons

were considered during which the maximum demand materialised. To simplify things, it was assumed that monthly electricity production amounted to 10% of the yearly electricity generation for either the winter or the summer months.

Moreover, nuclear energy, biomass and hydropower production were used as baseload power generation technologies. Their electricity production derived from the installed capacity and their capacity factor. Solar power production (P_{solar}) is obtained from the National Renewable Energy Laboratory (NREL) PVWatts calculator (National Renewable Energy Laboratory, 2019) for each of China's provinces. It is calculated from the product of the capacity factor (*cf*) and the installed capacity of each province while factoring in energy losses. The percentage difference between the actual solar power production and PVWatts is assumed to be 14% which can be attributed to system losses.

Table 3.9: Average capacity factors of renewables and hydroelectricity for all Chinese provinces.

Power plant	Winter (%)	Summer (%)	Source
Solar	8.5	12.5	(National Bureau of Statistics of China, 2018; National Energy Administration, 2019a; National Renewable Energy Laboratory, 2019)
Wind	26	20	(National Bureau of Statistics of China, 2018; National Bureau of Statistics of China, 2019)
Hydro	28	53	(National Bureau of Statistics of China, 2019)

Wind demonstrates substantial variability and its magnitude differs on a daily (Kang, 2007) and hourly (Zhou *et al.*, 2006) basis. China's hourly wind speed was extrapolated from data published by NASA (Global Modeling Assimilation Office, 2015) for each province. Drawing on the Maximum Likelihood Method, Weibull's distribution was utilised to produce the wind speed profiles (Mohsin and Rao, 2018; Mahmood *et al.*, 2020):

$$f(u) = \frac{k}{c}\left(\frac{v}{c}\right)^{k-1} \cdot \exp\left[-\left(\frac{v}{c}\right)^{k}\right] \tag{7}$$

$$k = \left[\frac{\sum_{i=1}^{n} v_i^k \ln(v_i)}{\sum_{i=1}^{n} v_i^k} - \frac{\sum_{i=1}^{n} \ln(v_i)}{n} \right]^{-1} \tag{8}$$

$$c = \left[\frac{1}{n} \sum_{i=1}^{n} v_i^k \right]^{\frac{1}{k}} \tag{9}$$

where k and c are the shape and scale parameters of the Weibull distribution, respectively. Term $f(u)$ denotes the probability density function, letter v is the wind speed and n is the number of observations. These wind speed profiles are an integral element of wind power generation. Moreover, to generate an hourly distribution of the wind energy capacity factor, a quadratic model was considered (Diyoke, 2019), as defined by:

$$x(t) = \frac{v^k - v_{in}^k}{v_r^k - v_{in}^k} \tag{10}$$

here $x(t)$ is the capacity factor at hour t. Term k is the shape scale of Weibull's distribution, and v is the wind speed. Terms v_{in} and v_r are the cut-in and the rated velocities which differ for each turbine unit (The Wind Power, 2020). Natural gas production $\left(P_{ng_{i,j}} \right)$ was derived from the capacity factor (*cf*) and a sinusoidal equation that follows a normal distribution $N_j\ (\mu, \sigma^2)$ and varies as a function of the day (j) and hour (i):

$$P_{ng_{i,j}} = \left[I_{ng} \cdot cf \,/\, 720 \right] \cdot \left[N_j(1, 0.15) + \left(\sin(3\pi/2 + 2\pi(t-1)/24) \right) \cdot N_j(0.2, 0.05) \right] \tag{11}$$

where $N_j\ (\mu, \sigma^2) > 0$.

In the renewables scenario (RESc), battery power and hydrogen (storage) production were obtained from the following equations:

$$P_{stored_{i,j}} = \min \left[P_{stored_{i-1,j}} + \left(\mathrm{P}_{\mathrm{total_{i,j}}} - \mathrm{P_{i,j}} \right), \mathrm{P}_{\mathrm{stored_{max}}} \right] \tag{12}$$

$$\left(P_{stored_{\max}} - P_{total_{i,j}} + \mathrm{P_{i,j}} \right) > 0 \tag{13}$$

here the storage capacity, at time i, is denoted by $P_{stored_{i,j}}$. Term $P_{stored_{\max}}$ is the maximum

battery or hydrogen storage, $P_{i,j}$ are the hourly electricity needs and $P_{total_{i,j}}$ is the overall power production excluding storage. Whatsmore, the peak shaving capacity $\left(P_{Peak}\right)$ was obtained from:

$$P_{Peak} = \max(P_{total_{i,j}} - \mathrm{P_{i,j}}) \quad (14)$$

3.1.9.2 Cyprus

With the purpose of estimating Cyprus' future electricity production from renewables, it was deemed necessary to consider the hourly electricity production of each source. More details pertaining to the Cypriot electricity production system can be gleaned from Fig. 3.1.

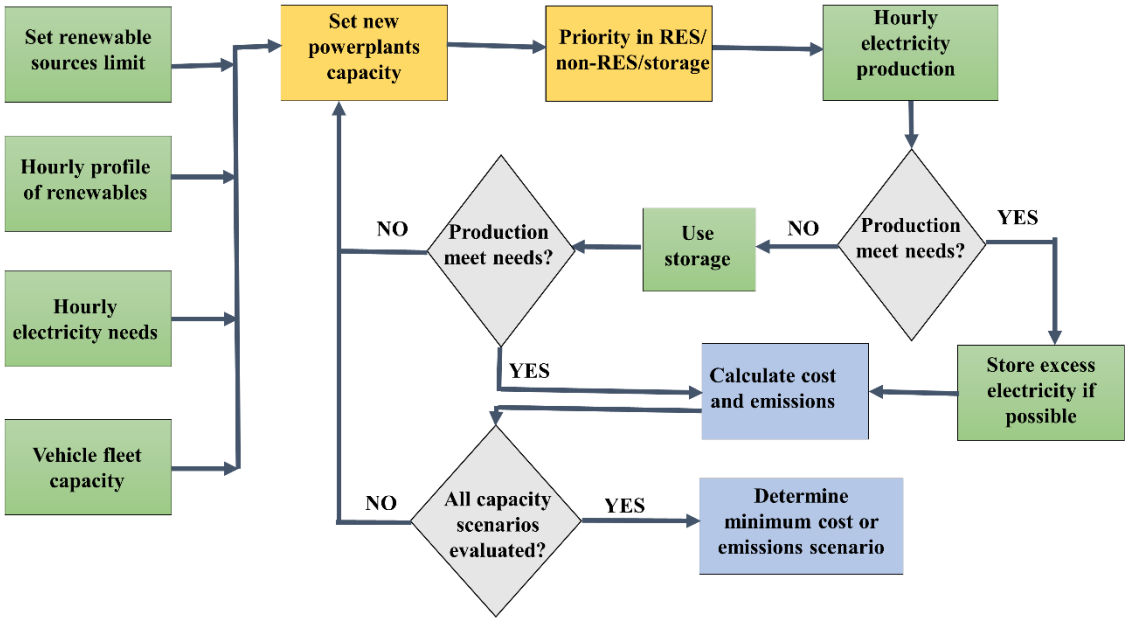

Fig. 3.1: Flowchart of the electricity model of Cyprus. Lime-green boxes denote the inputs to the integrated model, yellow-coloured boxes refer to the analytical/computational engine and the grey rhombi indicate what if loops. Steel-blue rectangles denote Cyprus' electricity model results. Simulations were implemented in Matlab® software.

The model follows a multiple what-if analysis based on different power plants and storage capacities with increments of 50MW. Each scenario has evaluated the condition of whether hourly power production meets demand at all times based on the

profile of renewables and fossil fuels. If electricity demand is not satisfied by the storage facilities such as batteries subsequently passenger vehicles-to-grid and pumped hydro are utilised. Operationally, a case is considered a failure if the island's energy needs are not covered for even an hour and, therefore, the next power generation scenario is utilised. If a simulation can successful meet demand both its electricity cost and emissions levels along with its installed capacity are stored by the code script. When the Matlab® runs conclude, the minimum emissions or cost scenario for each case is chosen.

Starting, biomass was determined as a baseload source and remained at such throughout the year. Secondly, concentrated solar power (CSP) production at the village of Alassa, in Limassol, was acquired from the typical meteorological year with the help of the PVGIS photovoltaic energy tool (EU Science Hub, 2018). Its data was integrated to the System Advisor Model— a software released by the National Renewable Energy Laboratory (NREL) to determine its hourly electricity production (National Renewable Energy Laboratory, 2019). Lastly, solar power production on an hourly resolution was obtained from the solar photovoltaic calculator PVGIS (EU Science Hub, 2018) with system losses amounting to 14%.

The hourly wind capacity factors were extrapolated from data obtained from the Cyprus Transmission System Operator (TSO) for a ten-year period stretching between 2008 to 2018 (Cyprus Transmission System Operator, 2018). To develop a random wind capacity factor profile, an ARMA(1,0) model was applied on an hour-by-hour temporal resolution for each month drawing from a three-parameter Pearson distribution (Vogel and McMartin, 1991). Likewise, to generate an hourly distribution of the wind energy capacity factor, a cyclostationary process was utilised (Tsoukalas *et al.*, 2018), as defined by:

$$x(t) = \left[\frac{\left(1-\rho_1(t)^2 \times s_x(t)\right)}{\left(1-\rho_1(t-1)^2 \times s_x(t-1)\right)} \times \rho_1(t) \right] \times x(t-1) + \varepsilon(t) \tag{15}$$

where *x(t)* and *x(t−1)* are the capacity factors at hour *t* and *t−1*, respectively. Term $\varepsilon(t)$, is the white noise emanating from the three-parameter Pearson distribution. Parameters $\rho_1(t)$ and $\rho_1(t-1)$ refer to the autocorrelation factors at hour *t* and *t−1*,

correspondingly. Finally, terms $s_x(t)$ and $s_x(t-1)$ are the standard deviations of the wind capacity factor at hour *t* and *t−1,* respectively.

Natural gas hourly electricity production can differ by 10% compared to the previous hour while realising a maximum 90% and a minimum 30% of the total installed capacity, correspondingly. The overall electricity hourly production profiles were inferred from European Union data, for Cyprus, for year 2018 (ENTSO-E transparency platform, 2019). In addition, passenger vehicle charging and PV2G were calculated from the following equations (Demetriou *et al.*, 2021):

$$p\_veh\_ch(t) = \min[7 \times pveh \times (1 - pvehgo(t) - 0.8), prod(t) - needs(t)] \quad (16)$$

$$p\_v2g(t) = \min[7 \times pveh \times (1 - pvehgo(t) - 0.8), needs(t) - prod(t)] \times 0.9 \quad (17)$$

$$p\_v2g(t) = \max(PV2G(t), pveh\_inst(t) - pveh_{\max} \times 0.2) \quad (18)$$

$$pveh\_inst(t) = pveh\_inst(t-1) + [p\_veh\_ch(t) - 0.2 \times pvehgo(t) \times pveh - p\_v2g(t)] \quad (19)$$

where *p_veh_ch(t)* is the energy available for charging an electric vehicle at time *t*, *pveh_inst(t)* is the amount of electricity stored by a passenger vehicle battery bank at time *t*, *pvehgo(t)* is the percentage of the passenger cars being driven, at time *t*, at major road arteries (Department of Public Works, 2018), for year 2018. Term *prod(t)* is the electricity produced from power plants at time *t*, *needs(t)* are the power needs at time *t* and *pveh* is the total amount of passenger vehicles. Term *p_v2g(t)* is the quantity of electricity made available to the electricity grid from vehicles. For bus charging, it was assumed that no charging occurs during daytime but only for the time window between 22:00 to 05:00. Battery storage was calculated from the following equations:

$$B_{stored}(t) = \min\left[B_{stored}(t) + \min\left(B_{capacity}, prod(t) - needs(t) - p\_veh\_ch(t)\right), B_{stored_{\max}}\right] \quad (20)$$

$$B_{stored}(t) = (B_{stored}(t-1) - B_{capacity}) \cdot 0.9 \quad (21)$$

here the storage capacity, at time *t*, is denoted by $B_{stored}(t)$. Term $B_{stored_{\max}}$ is the maximum battery storage and $B_{capacity}$ is the installed capacity of battery storage. Any excess energy production can be used to power desalination units or for pumped hydro purposes. Thereafter, an amount of remaining surplus power generation will lead to certain electricity sources being cut off the grid considering that this is more cost competitive compared to boosting electricity storage capacity.

3.2 Nicosia's city dispersion model.

Nicosia's topography, traffic flow data from the city's major road arteries and meteorological readings from the city centre were factored into the dispersion model. Ultimately, the preceding findings helped infer the health impacts for each case (Fig. 3.2).

Convective equations were utilised to estimate the hourly emissions rate concomitant to the traffic and vehicle fleet. By considering an extensive array of urban emissions sources, the GRAL (Graz Lagrangian Model) (Oettl, 2020) model was able to compute the prevalence of pollution particles. Subsequently, the model's results were validated with actual measurements of $PM_{2.5}$, PM_{10}, CO and NO_x particles obtained from a national air quality station. Reflecting a wide spectrum of possibilities, the 9 scenarios which were analysed with the aid of the model exemplified novel policies for tackling urban emissions. Broadening the scope of the investigation, 8 more cases were appraised under varying traffic conditions.

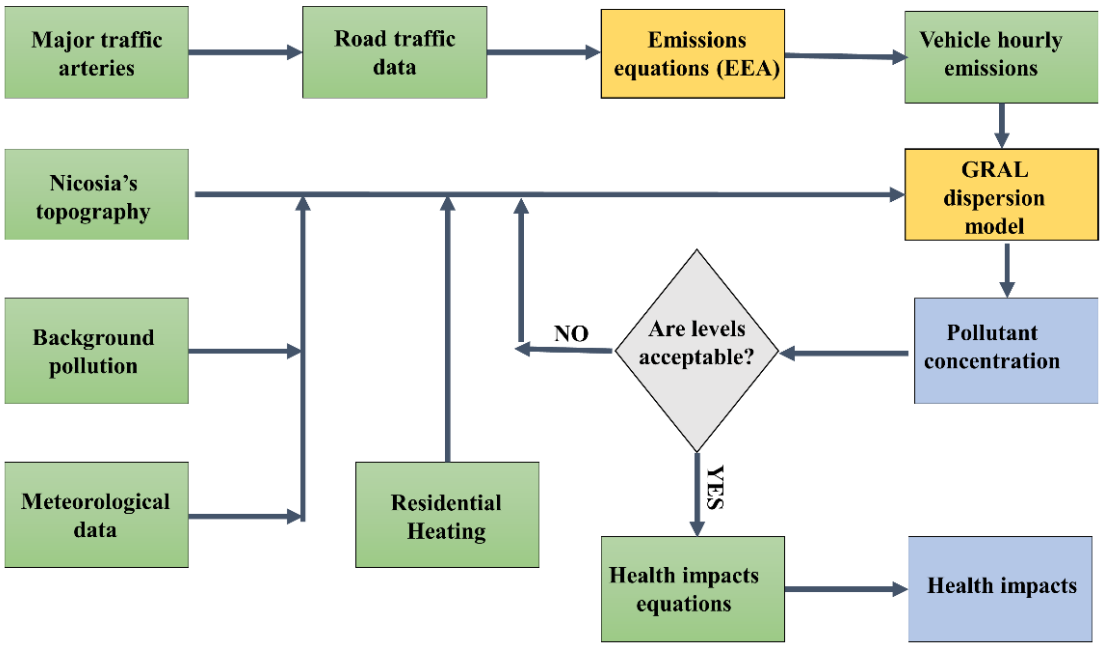

Fig. 3.2: Flowchart of the emissions dispersion model capturing the population health effects. Lime-green boxes denote the inputs to the integrated model, yellow-coloured boxes refer to the analytical/computational engine while the grey rhombus checks whether the concentration of pollutants are within acceptable limits or not. Steel-blue rectangles denote Nicosia's model results. Acronym EEA refers to the emissions methodology of the European Environment Agency (2019b).

3.2.1 Nicosia's centre model and spatial details

This section details the construction of the Nicosia city dispersion model which incorporates real road traffic and pollution observations obtained from measurement stations courtesy of the Republic of Cyprus' Department of Civil Works and the Department of Labour Inspection, correspondingly (Fig. 3.3). Two air quality stations were used to validate the model. The first one is located in the Nicosia city centre, at Strovolou Avenue, where the model's values were evaluated. Located some 40 km away from the city centre, the measurements of the second station situated at Ayia Marina Xyliatou (Department of Labour Inspection of Cyprus, 2021) served as background pollution thresholds.

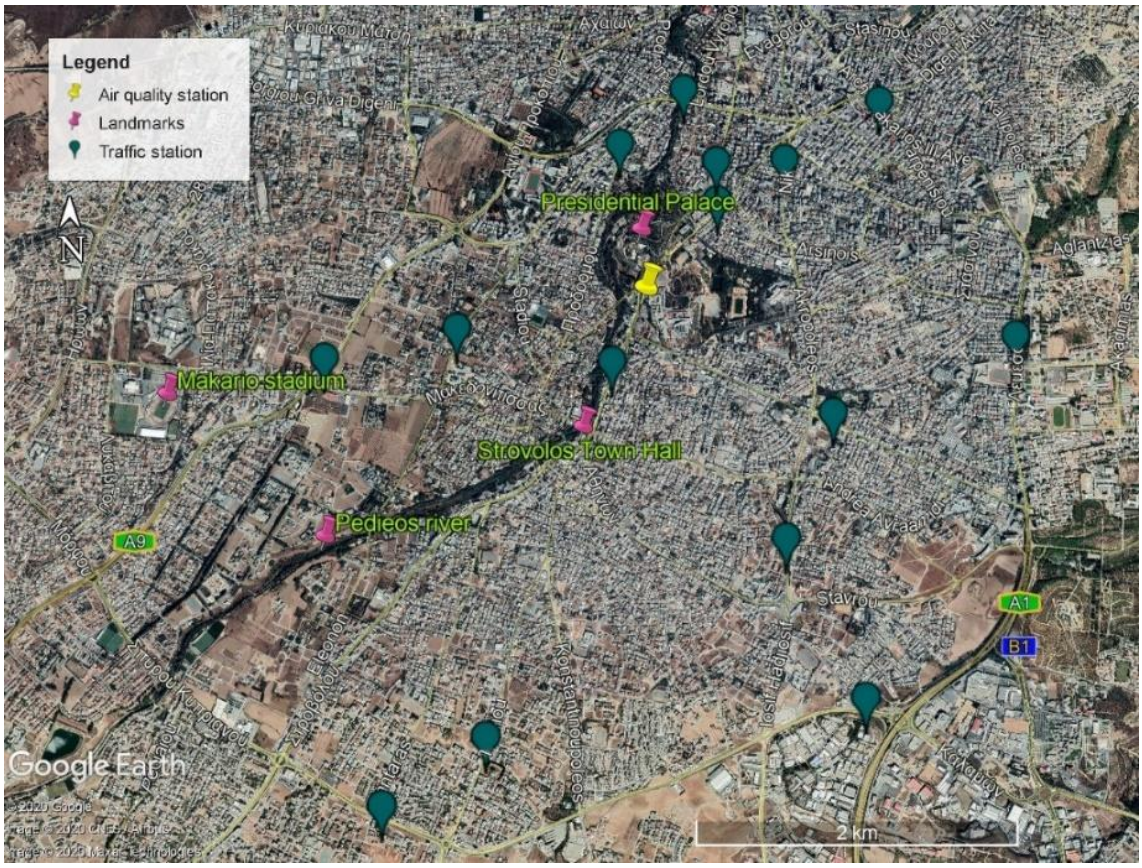

Fig. 3.3. Nicosia's map depicting the air quality station (yellow pin) and the traffic counting stations (deep green parachutes).

Air quality stations in parallel with logging the concentration of pollutants have also monitored wind speed and wind direction. In conjunction with solar irradiation data, the preceding parameters, retrieved from the European Commission (EU Science Hub, 2018), were utilised to estimate the stability class of each hour— as defined by

Pasquill (1961). Traffic counting devices were physically positioned at areas with high traffic activity. These systems registered each vehicle's speed as well as the time of the day at which the vehicle passed from that particular road location. Furthermore, vehicles were categorised into 6 distinct classes, namely, 1) motorcycles, 2) cars and vans, 3) cars and vans with trailers, 4) trucks, 5) articulated trucks and 6) buses.

Compared to other EU member states, diesel-powered passenger vehicles in Cyprus made-up just 15.9% of the overall vehicle fleet. Hence, Cyprus ranked 26th out of the 28 EU countries in terms of diesel car ownership in 2017 (European Environment Agency, 2019a). Moreover, each vehicle type was categorised according to the fuel its engine consumed (B.2) (CYSTAT, 2020b). Remarkably, more than two out of three (or >66%) vehicles in Cyprus, in 2017, were older than 10 years whereas about 18% of them were older than 20 years old (B.2). Ultimately, compared to other European nations, Cyprus has the oldest diesel passenger vehicles (PV) with an average age of 11.11 years while the EU average was 6.47 years. Similarly, Cyprus PVs were the fifth oldest in the EU (European Environment Agency, 2016).

According to the latest official Cyprus census, two-thirds of Cyprus' inhabitants live in cities (CYSTAT, 2013). Nicosia, the capital of Cyprus, in 2017, hosted 38.9% of the island's population. Of these, 73% of the city's residents or about 250 thousand dwellers resided at the capital's centre (CYSTAT, 2013; CYSTAT, 2020a). Geomorphologically, Nicosia is a rather flat basin and for this reason, only topographic features such as buildings, forests and parks have been incorporated into the model (Fig. 3.4). The air quality station's wind speed magnitudes obtained from the Cyprus Department of Labour Inspection station located at Strovolou Avenue (Fig. 3.4), indicated that more than 77% of the wind measurements were less than 2m/s. Whatsmore, 65% of the hourly wind magnitude was smaller than 1.5m/s.

Constituting the focal point of this study, a zone measuring 4,900m by 5,200m, with a horizontal spatial and temporal resolution of 15m and an hourly rate for each pollutant, was considered at the city's centre. A total of 21 line sources and 1,218 point sources were embedded in the dispersion model. Line sources originated from the major traffic arteries of Nicosia and point sources were randomly selected to denote households that emitted heat-related emissions. In each simulation, a total of 700 particles were released per second. Separately, the concentration of each pollutant was

measured at two different height levels of 1.5m, which is within the breathing zone, and at 3m where the station is situated. Background concentrations originated from readings obtained at Ayia Marina Xyliatou— a remote station located some 40km from Nicosia's centre — reflecting about a quarter (¼) of the total $PM_{2.5}$ pollution in Nicosia.

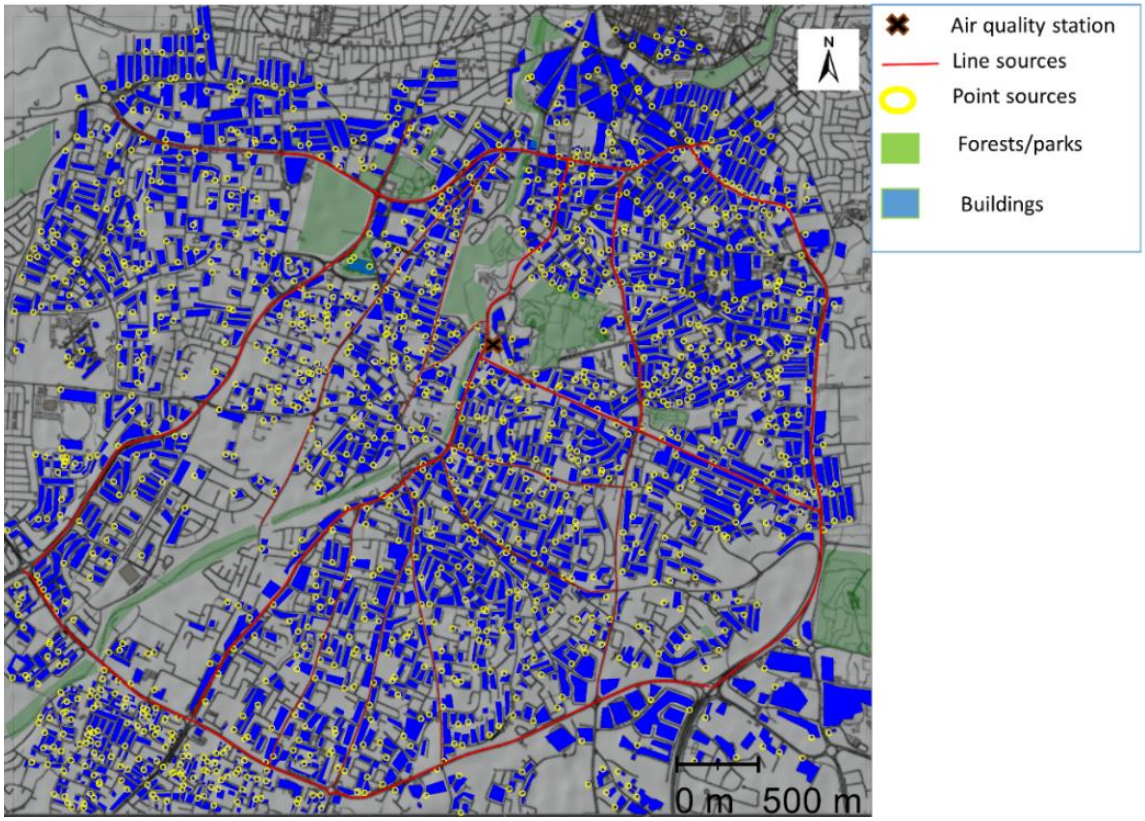

Fig. 3.4. Nicosia's integrated GRAL model depicting the air quality station denoted by a cross, forests/parks assigned in green and line and point sources shaded as red and yellow.

Central to this investigation was the utilisation of a GRAL dispersion model which rests on a Lagrangian particle tracking formulation. Foremost, the basic principle was to track the trajectory of pollution particles based on the changes in wind speed (Oettl, 2020). Each particle's position was determined from the following equation (Oettl, 2020):

$$p_{i,t} = p_{i,t-1} + \Delta t \times \left(\bar{u}_i + u_i^{'}\right) \tag{22}$$

where $p_{i,t}$ is the spatial location of a particle at time *t*, Δt is the time increment, $\bar{u}_i$ is the mean velocity of the particle and u_i' is the variable particle velocity induced from turbulent movement (Oettl, 2020). Vertical dispersion was estimated based on the following equations (Oettl, 2020):

$$dw = a(w,z) \times dt + [C_0 \times \varepsilon(z)]^{0.5} \times dW \quad (23)$$

$$dz(t) = w(t) \times dt \quad (24)$$

$$dt(z) = 0.01 \times \frac{2 \times \sigma_w^2}{C_0 \times \varepsilon(z)} \quad (25)$$

$$a(w,z) = a(z) \times w^2 + \beta(z) \times w + \gamma(z) \quad (26)$$

where *z* is the height of the simulation considering the pertinent particles, *dw* is the vertical velocity step of each particle, C_0 is a universal constant set at 4, $\varepsilon(z)$ refers to the dissipation of turbulent kinetic energy which indicates the strength of the turbulence, *dW* is a random number with an average of zero and a variance of *dt*. Additionally, *dt* follows the normal probability density function where c_w is the variance of the vertical velocity and *w* the vertical velocity. Parameters α, β, *and* γ are determined with the method of moments which is explained in the manual of GRAL (Oettl, 2020). The horizontal dispersion of particles was calculated as follows (Oettl, 2020):

$$R(\tau) = \frac{1}{e^{p\tau}} \times \cos(q\tau) \quad (27)$$

$$m = \frac{8.5}{(\bar{u}+1)^2} \quad (28)$$

$$T = \frac{m \times (200m + 350)}{2\pi(m^2+1)} \quad (29)$$

$$q = \frac{m}{(m^2+1) \times T} \quad (30)$$

$$p = \frac{C_0 \times \varepsilon}{2 \times \sigma_u^2} \quad (31)$$

where $R(\tau)$ is an autocorrelation function with time lag τ. Parameter *p* is the basic time for developing turbulence and *q* is related to an oscillatory behaviour because of meandering which occurs mainly during low wind speeds under 2.0m/s (Oettl, 2020).

Term $\bar{u}$ is the wind speed and σ_u the wind speed variance. Horizontal dispersion then is calculated with stochastic differential equations described fully in GRAL's manual (Oettl, 2020). The GRAL dispersion software was developed to simulate low wind speed condition of less than 1.5m/s at the Alpine basins. It can be employed in complex (Oettl, 2015; Ling *et al.*, 2020) and flat terrains (Oettl and Uhrner, 2011; Berchet *et al.*, 2017). Moreover, it is suitable for spatial domains starting from 50m up to 100 km (Oettl, 2020) making it applicable at the street (Oettl *et al.*, 2001; Oettl *et al.*, 2018) and the city level (Almbauer *et al.*, 2000; Kurz *et al.*, 2014). GRAL has the capability of introducing both line and point sources. Finally, the concentration of each pollutant (c) at each spatial point (x, y) of the domain was determined from:

$$c_t(x,y) = c_{b,t} + \sum_{1}^{l} c_{L,t}(x,y) + \sum_{1}^{p} c_{P,t}(x,y) \quad (32)$$

where t denoted time, l and p were the numbers of line and point sources, correspondingly. Parameters $c_{L,\,t}$ and $c_{P,\,t}$ were the line and point concentration outputs of the model and $c_{b,\,t}$ was the background concentration measured at a remote site.

Overall, the model considered the main 21 roads of Nicosia. Hourly records pertaining to the automobile category, the vehicle speed, and the number of vehicles crossing each traffic and air quality stations (Fig. 3.3), courtesy of the Cyprus Department of Civil Works, covered the period from January 1st, until September 31st, 2017. Making use of the preceding details while taking into account the composition of the vehicle fleet age in Cyprus (B.2), the pollutant hourly exhaust and non-exhaust emissions were computed in accordance with the equations featured in Ntziachristos and Samaras (2019) and Ntziachristos and Samaras (2019) (B.3). Because electric vehicles are fitted with their own battery bank are heavier compared to equivalent diesel or petrol vehicles. Beddows and Harrison (2021) and Timmers and Achten (2016) have estimated these additional non-exhaust emissions due to the extra vehicle weight. Similarly, this study used the preceding attributes to determine the electric passenger vehicle emissions.

Domestic and residential fireplaces and central heating units were treated as point sources in the simulation. Statistically, 7.3% of the households in Cyprus used a fireplace to keep residents warm during the winter as well as for domestic hot water, while 29.2% of the homes were fitted with a central heating unit (CYSTAT, 2011). Cypriot households, on average, consumed ($Consumption_f$) 355 litres of heating oil and

233 kg of wood biomass (CYSTAT, 2011) per year. The emissions factors (EF_f) of both central heating units and fireplaces were obtained from Kuenen and Trozzi (2019). Monthly heating degree days (HDD_j) is an index that describes the energy requirements of each house (Eurostat, 2020), and the hourly emission rate ($Heat\_em_{j,\,f}$) for each pollutant were determined from the following equations, respectively:

$$HDD_j = \frac{\sum_{i=1}^{n}(18°C - T_i)}{\sum_{j=1}^{12}\sum_{i=1}^{n}(18°C - T_{i,\,j})} \quad for\ T \le 15°C \tag{33}$$

$$Heat\_em_{j,\,f} = EF_f \times HC \times HDD_j \times Consumption_f \tag{34}$$

where parameters *j*, *i* and *f* were the month, the day of the month and the type of heating utilised (e.g., fireplace or boiler), respectively. *HC* represented the hourly consumption percentage rate based on the daily temperature which derived from Bundesverband der deutschen Gas- und Wasserwirtschaft (2006) (Table B7). Lastly, T_i and $T_{i,\,j}$ was the monthly and the daily average air temperature, respectively, as measured at the Athalassa's weather station from the Cyprus Department of Meteorology located in Nicosia's centre.

3.2.2 Validation of the measured pollutants.

To lend credibility to the findings of this study, the dispersion model results were validated with actual traffic and emissions data. This validation exercise comprised the comparisons between modelling and real measurements for carbon monoxide (CO), nitrogen oxides (NO_x), particulate matter with a diameter equal to or less than 10 μm (PM_{10}) and those particles whose diameter amounted to or was less than 2.5 μm ($PM_{2.5}$). Initially, the model's values were compared with measurements on an hourly and a daily resolution. Eventually, several statistical tests were performed to analyse the dispersion model's concentration values. Essentially, the typical statistical parameters encompassed the fractional mean bias (*FB*), the normalised mean-square error (*NMSE*), the normalised absolute difference (*NAD*), and the correlation coefficient (*R*). Complementing the statistical analysis, the other deduced parameter was the *FAC2* which took into account the pool of the modelled data within the range of interest, that is, $0.5 \le (C_M/C_O) \le 2$. Here, C_O and C_M refer to the observed and the modelled concentration, respectively. All statistical metrics are expressed as:

$$FB = \frac{\overline{(C_O - C_M)}}{\overline{C_O} + \overline{C_M}} \tag{35}$$

$$NMSE = \frac{\overline{(C_O - C_M)^2}}{\overline{C_O} \times \overline{C_M}} \tag{36}$$

$$NAD = \frac{\left|\overline{C_O - C_M}\right|}{\overline{C_O} + \overline{C_M}} \tag{37}$$

$$R = \frac{\overline{(C_M - \overline{C_M}) \times (C_O - \overline{C_O})}}{\sigma_{C_O} \times \sigma_{C_M}} \tag{38}$$

where the overbar symbol signified the average value and σ_c the standard deviation. Hanna and Chang (2012) have suggested the following acceptance criteria for each of these values as they pertain to urban settings:

$$|FB| \leq 0.67,\ NMSE \leq 6,\ FAC2 \geq 0.3,\ NAD \leq 0.5 \tag{39}$$

while the perfect values for *FB, NMSE* and *NAD* amount to 0 and for *FAC2* and the *R* factors this figure equates to 1.

3.2.3 Air pollution scenarios and cases

A total of 9 scenarios and 8 cases associated with NO_x and $PM_{2.5}$ emissions were formulated as presented in Table 3.11 and Table *3.12*. Carbon monoxide was not examined in this research since its mean concentration in Nicosia was about 500 μg/m^3, which is well below the threshold limit of 10,000 μg/m^3 (Department of Labour Inspection of Cyprus, 2019) recommended by the World Health Organization (World Health Organization, 2000). Furthermore, pollution mitigation policies were taken into consideration through the different scenarios which covered changes in the vehicle speed limit, banning diesel passenger vehicles (PV) and forbidding light duty vehicles (LDV). Moreover, the possibility of allowing only Euro 6 standard vehicles in the city area was examined along with the penetration of electric passenger vehicles. In parallel, the investigation examined the possibility of permitting only Euro 6 standard vehicles, as defined in Table 3.10, in urban city areas along with a progressively increasing penetration of electric passenger vehicles which made-up 80% of the vehicle fleet.

Further broadening the scope of the study, another four individual cases concerning the characteristics of vehicles as well as domestic emissions were formulated, as shown in Table 3.11. Collectively, these cases extended until the year

2030 which is deemed a milestone as all vehicles by then will need to adhere to Euro 6 standards (Demetriou and Hadjistassou, 2022). Two other adjustments examined a drop of 20% in traffic flow compared to 2017 figures. Inherently, these cases capture the impacts on traffic-related emissions in the context of various policies such as the universal roll-out of electric automobiles, banning diesel passenger and light duty vehicles and prohibiting the use of fireplaces while all vehicles abide to Euro 6 standards (Table 3.12).

Table 3.10: Emissions levels of the light-duty Euro 6 vehicle emission standard as defined in the New European Driving Cycle (NEDC) (European Parliament, 2007).

Exhaust substance	Diesel (g/km)	Petrol (g/km)
CO	1.0	0.5
NO_X	0.06	0.08
PM	0.005	0.005

Table 3.11: Scenarios considering various speed limits, penetration of electric automobiles and restrictions to vehicle use.

Scenario	Scenario Name	Description
1	30 km/hr speed limit	Vehicle speed limit of 30 km/hr.
2	50 km/hr speed limit	Vehicle speed limit of 50 km/hr.
3	Ban diesel PV	Ban diesel-powered passenger vehicles.
4	Ban diesel PV & LDV	Ban diesel passenger and light duty vehicles.
5	Euro 6	All vehicles comply with Euro 6 standards.
6	20% Electric PV	20% of older passenger vehicles are replaced by electric automobiles.
7	50% Electric PV	50% of older passenger vehicles are replaced by electric cars.
8	80% Electric PV	80% of older passenger vehicles are replaced by electric vehicles.
9	Euro 6 and ban diesel PV & LDV	Combination of scenarios 5 & 6; vehicles abide to Euro 6 and diesel PV & LDV are banned.

Table 3.12: Various cases examining changes in road traffic flows, a bigger share of electric vehicles and the banning of PVs and LDVs.

Cases	Case Name
1	Euro 6 and 20% increase in traffic rate.
2	Euro 6, ban fireplaces and 20% boost in traffic flow.
3	Euro 6, 80% electric vehicles and 20% rise in traffic flow.
4	Euro 6, ban diesel PV & LDV plus 20% growth traffic flow.
5	Euro 6 and a drop of 20% in traffic flow.
6	Euro 6, ban fireplaces and 20% reduction in traffic flow.
7	Euro 6, 80% electric vehicles & 20% cut in traffic flow.
8	Euro 6, ban diesel PV & LDV plus 20% drop in traffic flow.

3.2.4 Human health impacts

Several scenarios formulated on different traffic flows, various combinations of vehicle fleet and control measures of domestic emissions have directly influenced the concentration of $PM_{2.5}$ and NO_x particles. In turn, changes in pollution levels squarely impinge upon the relative risks of non-accidental premature, cardiovascular, and respiratory mortality in Nicosia. Official statistics regarding the morbidity rates related to the preceding causes, during 2017, were obtained from the Cyprus Statistic Department (CYSTAT, 2019b). Several studies have estimated the risk coefficients of a 10 $\mu g/m^3$ change of each of the two pollutants. Stockfelt *et al.* (2015) allude that the premature mortality risk implicated from NO_x is 1.03 [1.01, 1.05] with a confidence interval (CI) of 95%. On the other hand, the team of Cao *et al.* (2011b) has predicted a lower mortality risk of 1.015 [1.004, 1.025] with a CI of 95%.

Besides premature mortality, the publication from Cao *et al.* (2011b) cite a relative risk from cardiovascular causes for both NO_x and $PM_{2.5}$ of 1.023 [1.006, 1.041] and 1.028 [1.009, 1.046], respectively. Concerning the premature non-accidental - relative mortality for $PM_{2.5}$, two studies have demonstrated substantial variability. Notably, the European Environment Agency (2020a) assumes a risk coefficient of 1.062 [1.04, 1.083] while Atkinson *et al.* (2014), drawing on several cohort studies, have estimated the risk ratio for Europe to be 1.0123 [1.0045, 1.0256]. Lastly, the cardiovascular and respiratory mortality risk coefficients for $PM_{2.5}$ amounted to 1.0226 [1.0123, 1.0329] and 1.0381 [1.0057, 1.0716] (Atkinson *et al.*, 2014), correspondingly. Herein, to calculate the disease-specific mortality (MOR_i), an integrated exposure-

response (IER) function, is utilised by many studies (Burnett *et al.*, 2014; Wang *et al.*, 2018; Sahu *et al.*, 2020; Wang *et al.*, 2021), was adopted:

$$RR_i = \exp(\beta_i \times (C_{sc})) \tag{40}$$

$$MOR_i = BMOR_i \times POP_i \times \left(\frac{RR_i - 1}{RR_i} \right) \tag{41}$$

where C_{sc} is the concentration of the pollutant for each scenario and β_i is the risk coefficient increase per 10 μg/m^3. Abbreviation POP_i refers to the population cluster of Nicosia's older than 30 years old inhabitants which includes 153,048 individuals (CYSTAT, 2020a). Acronym *BMOR* is the baseline mortality and *MOR* the mortality while subscript *i* attributes to the death cause. In 2017, Cyprus' non accidental mortality rate was 5,841 (CYSTAT, 2019b). In the same year Cardiovascular and respiratory disease resulted in 2,001 and 597 deaths, in Cyprus, correspondingly (CYSTAT, 2019b).

4 Results and discussion

This chapter is dedicated to the research results and the discussion. It is divided into two parts: a) the electricity sector of Cyprus and China and b) the pollution dispersion model of the capital of Cyprus, that is, Nicosia. Considering, the electricity sectors of China and Cyprus, a total of four scenarios for each country are detailed here. In the beginning, a projection of the Chinese and the Cypriot electricity production needs was performed. Subsequently, the study estimated the future vehicle ownership, in Cyprus, spanning until 2050 and the percentage of electric cars and buses as a proportion of the road vehicle fleet. Next, the installed capacity and electricity production of each of the power generation technologies, such as renewables, fossil fuels and storage units, was estimated. Serving as a snapshot, an hourly electricity production mix was obtained for two specific weeks during the summer and the winter periods, correspondingly. After that, for the Chinese electricity sector, the foreseeable future fuel and renewables capital costs based on the logistic and the ARMA methods were deduced. Eventually, each scenario's costs and its emissions were obtained.

Concerning the dispersion model of the capital of Cyprus, at first, the concentration values of four pollutants, namely, CO, NO_x, $PM_{2.5}$ and PM_{10} were validated with hourly measurements from an air quality station situated in Nicosia, Cyprus, during a 9-month period extending from January 2017 until September 2017. Thereafter, with the aid of relevant statistical parameters, the performance of the model on a daily and hourly basis for all four pollutants was evaluated. Overall, 9 scenarios and 8 distinct traffic cases for NO_x and $PM_{2.5}$ were simulated. Lastly, based on the concentrations derived from each scenario/case a health impact assessment was established by an IER function and was used to estimate the premature risk mortality.

4.1 Future electricity production of China and Cyprus

Undoubtedly, future power needs constitute one of the most crucial parameters for a country's near-term planning. In obtaining this projection for China, data from the Chinese Energy Portal (2018), comprising the time period from 1990 to 2018, were used. Worth highlighting that the methodology adopted in this paper predicts a higher total electricity production compared to the International Energy Agency (IEA) and the Energy Information Administration (EIA) projections, spanning until 2040. Conversely,

the approach forecasts a smaller trend in power generation in relation to a Chinese National Renewable Energy Centre (CNREC) study published in 2018 (China Energy Portal, 2018; China National Renewable Energy Centre, 2018). Ostensibly, the logistic method adopted here estimates China's electricity needs will reach 11.3PWh, 12.1PWh and 13.1PWh in years 2035, 2040 and 2050, respectively (Fig. 4.1) (Demetriou and Hadjistassou, 2021).

Furthermore, future electricity production in Cyprus was considered until 2050. Firstly, a projection for the power generation requirements, for agriculture and the commercial and industrial sectors was derived. As briefly mentioned in sub-section 3.1.9.2, estimations pertaining to the electricity needs extending until 2050 were determined from different parameters, such as the GDP and the population (Table B1 and Table B2) among others. The objective for each one of the parameters was to minimise the mean absolute percentage error (MAPE) as illustrated in Table 4.1.

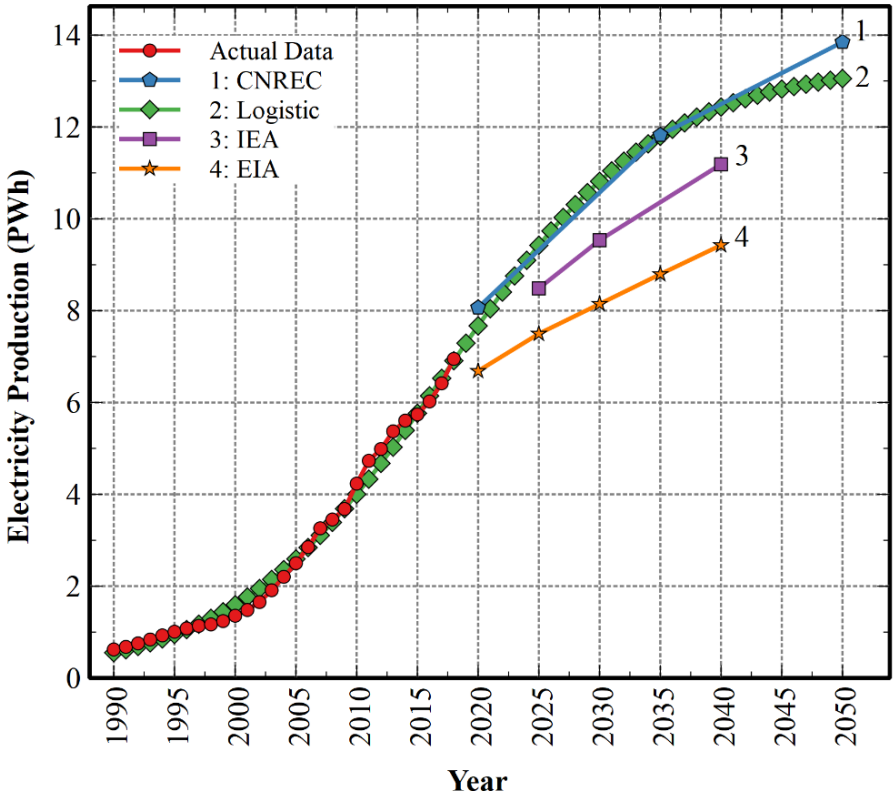

Fig. 4.1. Forecast of electricity generation of China using the logistic method. Plot also displays the IEA (2018), the EIA (2017a) and the CNREC (2018) projections.

Electricity consumption of the lighting and residential sectors was thoroughly explained earlier in section 3.1.2. In accord with previous studies, such as those of

Taliotis *et al.* (2017) and Zachariadis and Taibi (2015), the methodology in this thesis predicted lower total electricity production compared to the Cyprus Transmission System Operator (2019a). The future electricity consumption of these sectors was estimated to reach 5.89–6.17TWh, 6.31–6.90TWh and 6.41–7.34TWh in years 2030, 2040 and 2050, correspondingly, as shown in Fig. 4.2.

Table 4.1: Constant parameters for agriculture, the commercial and the industrial sectors of Cyprus used to obtain the Mean Absolute Percentage Error (MAPE).

Parameter	Agriculture	Commercial	Industry
a_1	6.826	−0.881	10.019
GDP	0.965	0.843	0.155
Human population	−0.728	−0.149	0.007
Swine and cattle population	−0.092	–	–
Clinker production	–	–	0.009
Ceramic production	–	–	0.088
Tourism	–	0.084	–
Hot and cold days	–	0.279	–
MAPE (%)	3.86	5.72	2.48

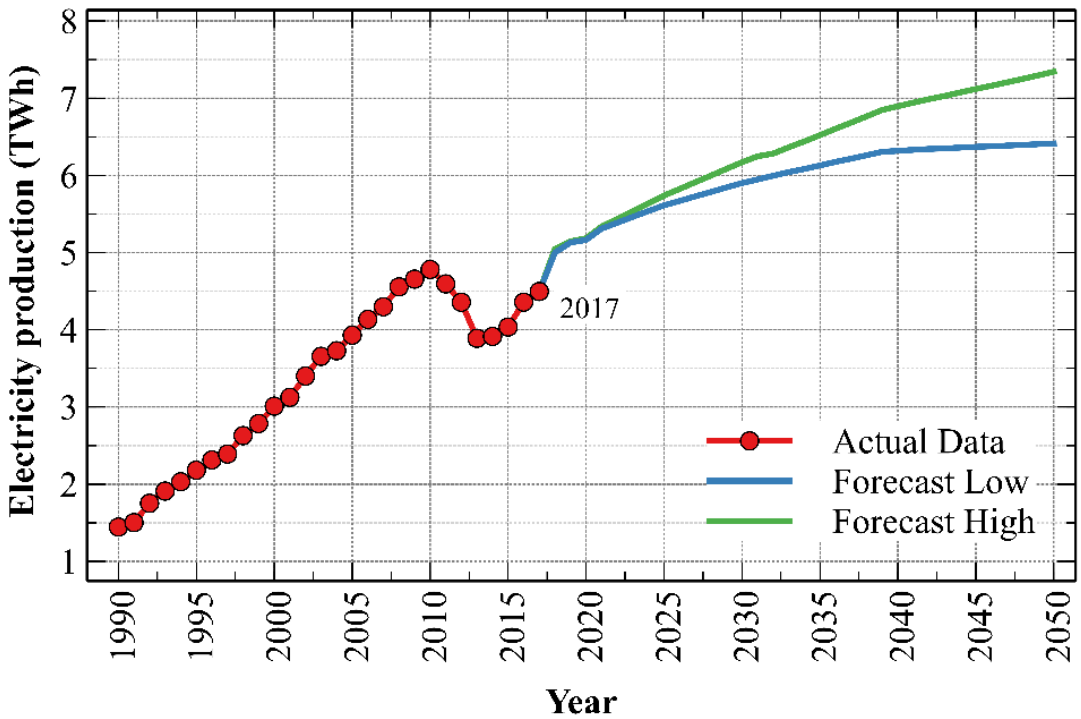

Fig. 4.2. Forecast of electricity consumption of the five main sectors comprising agriculture, commercial, industrial, lighting, and residential including the desalination units but excluding the transport needs, spanning from 2018 until 2050 for Cyprus.

4.2 Cyprus future vehicle fleet

Two different approaches were adopted which aimed to forecast the future car fleet size of Cyprus. For the first scenario, it was assumed that the car fleet ownership per capita will remain unaltered until 2050. For the second scenario, the logistic method was implemented. Compared to actual data, spanning from 1990 to 2017 (CYSTAT, 2019c), this method registered a mean absolute percentage error of 4.4%. The second scenario has estimated the future vehicle ownership rate to increase from 705 to 725 and 756 cars per 1,000 citizens by the year 2030, 2040 and 2050, respectively, as shown in Fig. 4.3. Concerning the aggregate bus fleet size, it has remained constant, during the last three years, to 3,000 vehicles (CYSTAT, 2019c). For our study, the bus fleet is expected to grow by 1,000 vehicles reaching 4,000 buses by 2050 (Demetriou *et al.*, 2021).

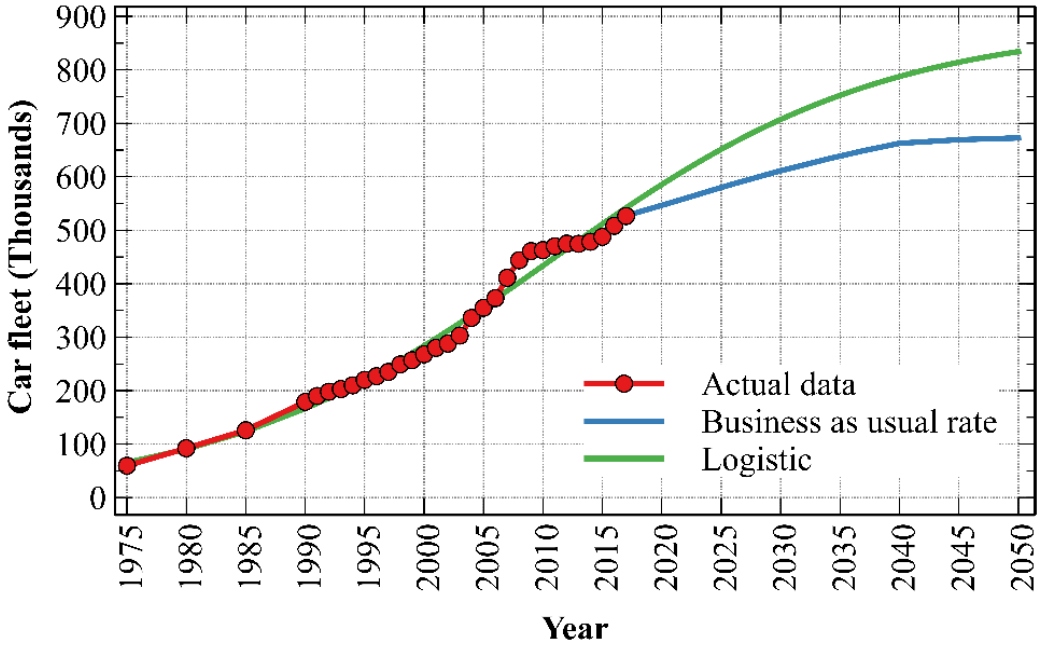

Fig. 4.3. Cyprus car fleet between 1975 and 2050. Plot displays actual vehicle fleet size until 2017. Business As Usual projections assume the same per capita vehicle ownership as in 2017. The logistic growth method estimates a sigmoidal growth in vehicle fleet.

4.3 Future electricity installed capacity and production up to 2050

In this section, the future installed capacity and production of Cyprus and China separately were plotted. Two different methodologies were applied to estimate the

future electricity needs of China and Cyprus and for that reason, they are described in two distinct sub-sections. Primarily, the Chinese electricity sector's installed capacity and production are considered, from 2025 until 2050, for each power generation technology. For all four scenarios, the technologies comprised natural gas, coal, wind, solar, batteries and hydrogen (Demetriou *et al.*, 2021). Next, for Cyprus, the study spans until year 2050, showing not only the installed capacity but also the production of each power generation mode at the particular areas where the electricity in Cyprus is utilised.

4.3.1 China

4.3.1.1 Future installed capacity

Mid-term projections of the installed power generation capacity of China were based on the electricity capacity factors. Thus, between the years 2025 and 2050, forecasts sketched the future installed electricity capacity for each scenario and power generation technology. As a point of reference, during 2017, the total installed capacity of China amounted to 1.81 terawatts (TW) (China Energy Portal, 2018). Projecting the installed capacity to 2050, the BAU scenario will require 3.78TW, the Goals scenario 6.59TW, the CFr scenario 6.31TW and the RESc case 11.33TW excluding electricity storage (Fig. 4.4).

As far as the RESc scenario is concerned, it is worth emphasising some major points. Integral to the RESc is the extraordinary capacity of battery and hydrogen gas storage. Meeting its electricity demand China will need a battery storage of 2,900,000MWh and a hydrogen storage volume equivalent to 12,000,000MWh (Demetriou and Hadjistassou, 2021), by 2050, compared to 10,740MWh in 2018 (China Energy Storage Alliance, 2019). Comparatively, the world's battery storage capacity in 2018 was just 17,000MWh (Bloomberg New Energy Finance, 2019). To put things into perspective, China will require about 150 times the world's battery storage capacity, in the year 2018, to meet its energy needs in 2050 (China Energy Storage Alliance, 2019). Because 93% of the total battery storage banks feature lithium-ion units (China Energy Storage Alliance, 2019), it was assumed that the battery storage capacity of China will consist of lithium-ion cells.

Remarkably, the installed capacity of coal power generation will shrink only by 37% to 748,000MW from 1,024,000MW, in 2017 (Fig. 4.4). The respective coal capacity for the rest scenarios is as follows: the BAU at 2,446,000MW, the Goals at

682,000MW and negligible for the CFr. Biomass is expected to make-up less than 1% of the total share in all four scenarios. Results are further elaborated upon in the next section. Strikingly enough, the RESc scenario seems unable to produce enough electricity even when supported by battery storage (Demetriou and Hadjistassou, 2021). Therefore, part of the electricity demand is invariably met by fossil fuels.

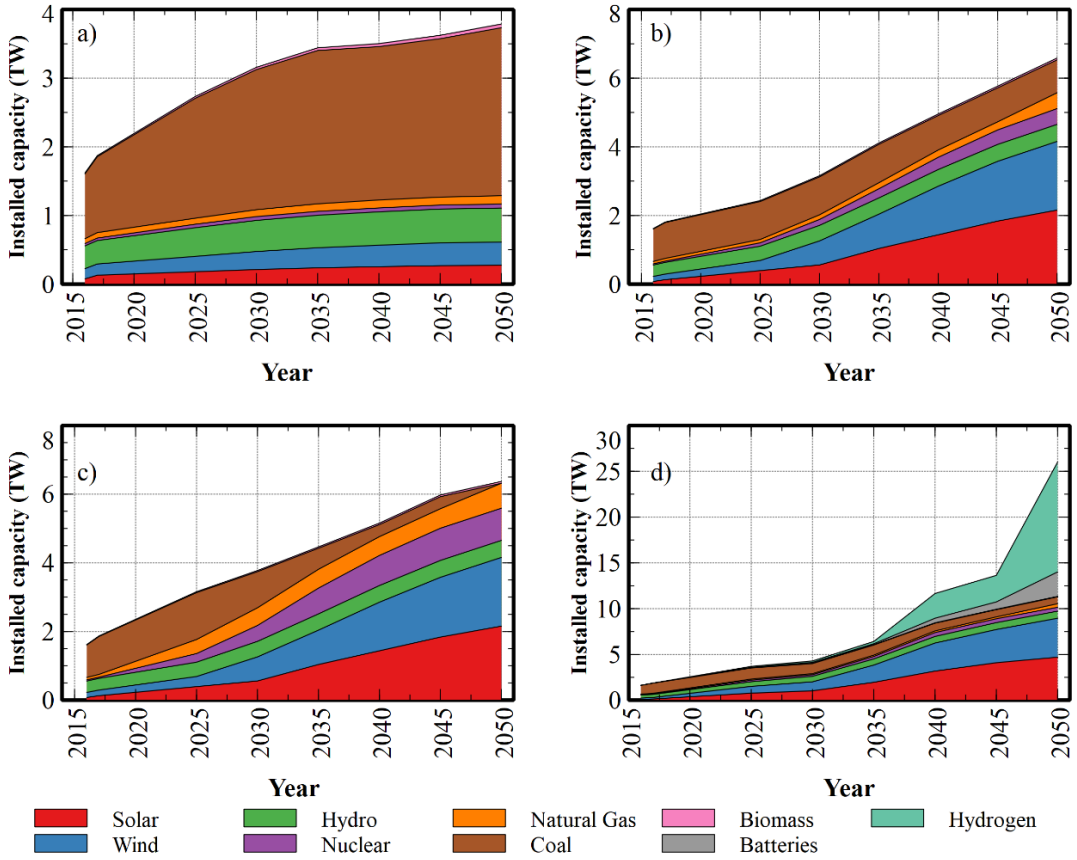

Fig. 4.4. Installed electricity generation capacity between 2016 and 2050. Plot a) depicts the Business As Usual, b) the Goals, c) the coal free and d) the renewables scenarios.

4.3.1.2 Future electricity production

The yearly electricity production for each of the four scenarios, on a five-year time window, is calculated in the current sub-section and presented in Fig. 4.5. These results demonstrate that in the Business As Usual scenario, coal continues to play an increasingly dominant role in the foreseeable future. In the Renewables' scenario, there is a significant increase in the amount of electricity production from renewables, as expected. The "Coal Free" and Goals scenarios share about the same production of renewables and hydro-power. Their main distinction though is that the power generation

contribution of fossil fuels in the Goals scenario outstrips the share emanating from the CFr scenario. Like the majority of the world's nations, China has pledged to fulfil a number of ambitions until 2030 according to its Intended Nationally Determined Contributions (INDCs) submitted in Paris in 2015 (Wu *et al.*, 2018).

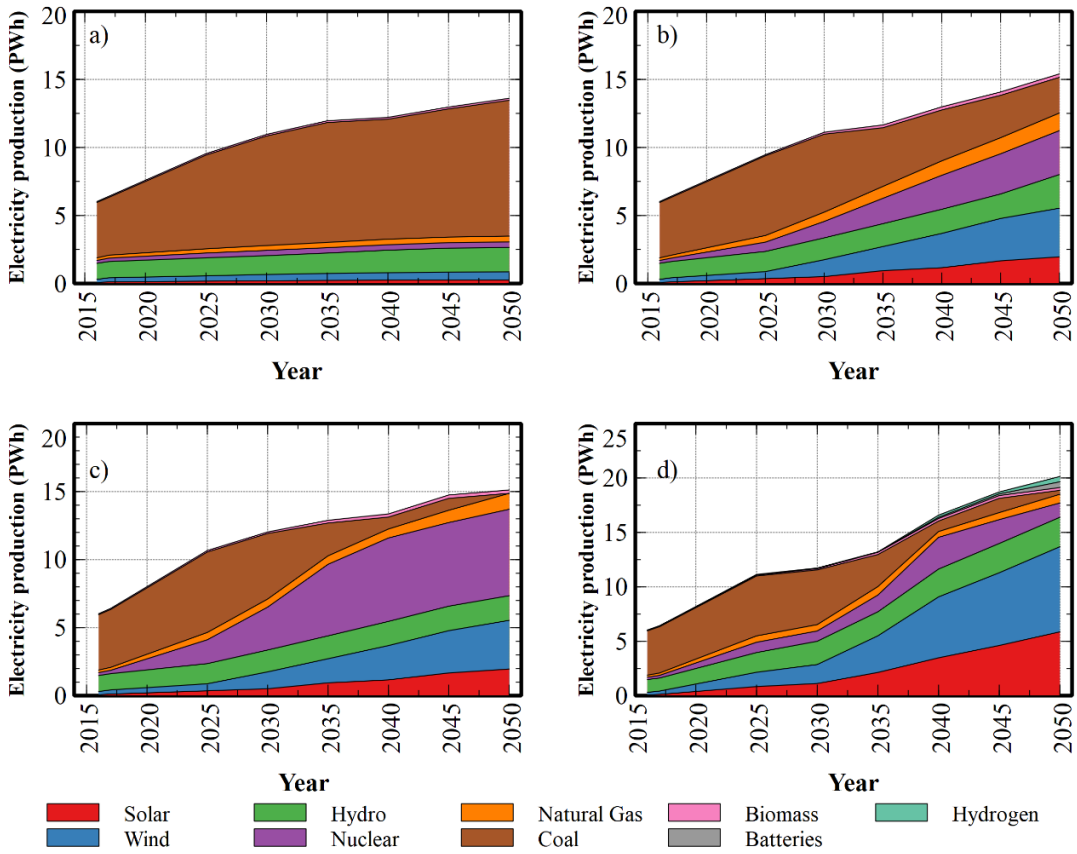

Fig. 4.5. China's projected electricity production from 2018 to 2050 for: a) Business As Usual, b) Goals, c) Coal Free and d) Renewable's scenarios, respectively. Years 2016 and 2017 constitute actual data (China Energy Portal, 2018).

Concerning non-fossil fuel technologies, the country vowed to expand their share to at least 20% of the total power utilisation. At the same time, China promised to increase natural gas consumption. Suffice to mention that the BAU scenario is not poised to boost natural gas use but instead it will increase coal consumption. In particular, coal's share is expected to surge by 1.8 times, in 2030, and by twofold, in 2050, compared to 2017. Meanwhile, the percentage of RES and hydro collectively will shrink from 25% to 20%, compared to 2017. Even though natural gas consumption will experience an increase, it is not expected to surpass the 3.3% threshold. The rest scenarios comply with or marginally meet all of the goals set.

Within a twenty-year time horizon, the share of renewables and hydro in the Renewables (RESc), the Goals and the Coal Free (CFr) scenarios will surge from 36%, 30% and 28%, in 2030, to 81%, 46% and 48%, in 2050, respectively. Formulated on the assumptions described in subsection 3.1.6, the Goals scenario will utilise 203bcm, the CFr scenario 184bcm, the RESc scenario 125bcm and the BAU scenario 68bcm of natural gas in 2050. The preceding values compare well with BP projections such that, in 2040, the Chinese electricity sector will require 150bcm of gas (BP, 2019). By 2050, CNPC estimates that this figure will rise to 205bcm (CNPC Economics and Technology Research Institute, 2018).

Thus, even by the most optimistic calculus, natural gas is not expected to make-up a sizeable proportion of coal power generation. Instead, as illustrated in Fig. 4.5, natural gas is deemed to meet at best 8.4% of the Goals scenario needs, 7.7% of the CFr scenario, 4.0% of the RESc and 3.3% of the BAU scenarios. Therefore, the preceding cases refute the claim that natural gas can either act as a transition fuel or constitute a dominant fuel in China's future electricity mix (Demetriou and Hadjistassou, 2021).

4.3.2 Cyprus

4.3.2.1 Future installed capacity of electricity in 2050

Projections of the installed power generation capacity of Cyprus were driven by the need to either minimise emissions or costs. Serving as a point of reference, during 2018 the total fossil fuel installed electricity production capacity amounted to 1,478MW and the total RES installed capacity, including biomass, was 289.9MW (Cyprus Transmission System Operator, 2019b). Predicting installed electricity capacity, to 2050, the LCSc scenario will require 1,100MW and both the BAU and the CCS 900MW each and, finally, the RESc will run free of any natural gas installed capacity. Notably, the renewables capacity for each scenario was estimated to be 1,920MW for the LCSc, 3,120MW for the BAU, 3,920MW for the CCSc scenario and 11,920MW for the RESc case. Lastly, the battery storage capacity was deduced to be 400MW (800MWhr) for the BAU and the CCSc and 1,400MW (5,600MWhr) for the RESc. Remarkably, the LCSc scenario is not supplemented by battery storage. Moreover, the RESc employs 530MW of pumped hydro as already suggested by another study (Poullikkas, 2013).

As far as the RESc scenario is concerned, it is worth highlighting a few major points. What stands out is the extraordinary battery storage of 5,600MWh that Cyprus will need to install, by 2050 (Demetriou *et al.*, 2021). To put things into perspective, during 2019, the EU battery capacity consisted of 3,400MWh (EASE and Delta-EE, 2020) while across the world total battery storage, in 2018, was 17,000MWh (Bloomberg New Energy Finance, 2019). Alongside, battery storage banks could support a diverse array of services in decarbonisation efforts. Some of them could comprise energy shifting, congestion relief, curtailing demand, and investment deferral. In line with other battery projects, Cyprus' battery storage banks will be lithium-ion due to the fact that currently 93% of the battery storage capacity elsewhere is based on this technology (China Energy Storage Alliance, 2019). Beyond that, grid-connected renewable energy is expected to grow 40-fold for the island state to fulfil its energy needs, by 2050.

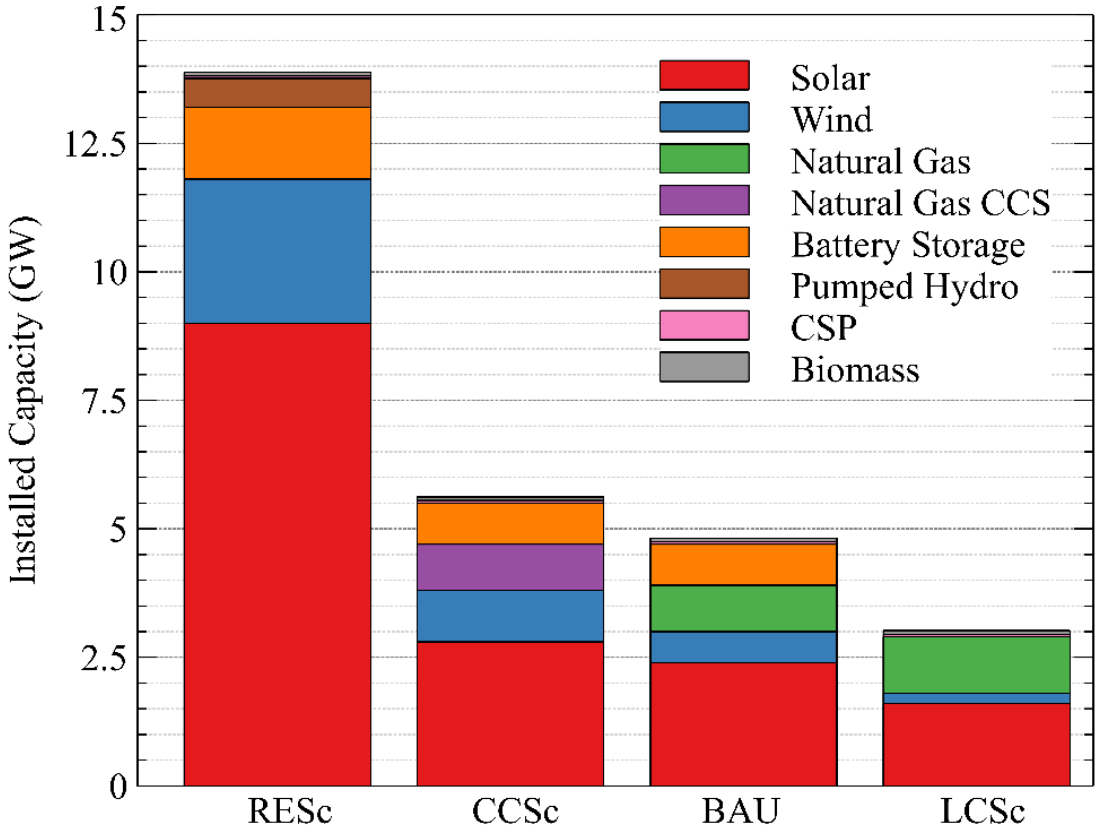

Fig. 4.6. Cyprus' installed electricity generation capacity for 2050. Bar labelled as RESc refers to the Renewables scenario, CCSc is the Carbon Capture & Storage, BAU is the Business As Usual, and, finally, LCSc is the Least Cost scenario.

Due to the inherent issues, it was deemed logical to explore various ways for minimising the non-renewable energy share of all four scenarios. Conscientiously, the installed capacity of fossil fuels power generation will shrink by 25% for the LCSc case and 39% for the BAU and the CCSc scenarios. Ultimately, the RESc will not run free of conventional fuels. Biomass is expected to reach 70MW and CSP, at 50MW, with an 8-hour a day storage that could be utilised in all scenarios. Finally, for the RESc, a pumped hydro capacity of 530MW (Poullikkas, 2013) could be implemented. Installed capacity for each of these scenarios is summarised in Fig. 4.6.

4.3.2.2 Total electricity production of Cyprus by 2050

This subsection will detail the electricity production for each of the four scenarios of interest. Power generation entails all of the different power production options including PV2G. For the Least Cost scenario, most of the power production relies on natural gas with a share of 64.2% and solar power which accounts for 25.9% of the overall needs. Other power sectors including the PV2G technology, each will yield less than 3.7% of the aggregate production. Next, the Business As Usual scenario bears many similarities with the Least Cost case. Though their main difference is that for the LCSc, natural gas production makes-up 64.2% of the electricity generation compared to 47.4% for the BAU.

Reverting to the Carbon Capture and Storage scenario, natural gas coupled with carbon capture comprises the majority of electricity production which refers to 41.5% while solar energy amounts to 38.6% and wind accounts for 13%. Of interest is the renewables scenario which is unique in many respects. Firstly, solar energy generates two thirds of the total electricity production. Ranked as the second biggest power source, wind meets 19.5% of the overall electricity needs. Pumped hydro and PV2G are expected to satisfy 5.9% and 3.3% of the total production, correspondingly. This happens because there is a need to store energy either in battery banks or to pump water back to hydroelectric reservoirs. A portion of the energy could be used to meet Cyprus' water needs by powering desalination units. Examining each scenario individually, the LCSc could generate 9.80TWh, the BAU 10.76TWh, and the CCSc 11.53TWh. Finally, the RESc at 21.47TWh, as illustrated in Fig. 4.7, produces twice as much electricity when compared to other scenarios.

Meticulously reviewing each scenario, the economy's sectors where electricity

production is utilised were examined. More precisely, the electricity consumption from the five main sectors, which comprise agriculture, commercial, industrial, lighting, and residential needs was analysed. On top of that, desalination units, automobile and bus charging, pumped hydro storage and battery storage were considered. An important parameter in this study was the excess energy production. With 9.1%, the Least Cost scenario presented the lowest amount of unutilised electricity followed by the CCSc case with 15.3% and, finally, the BAU whose excess electricity made-up 22.2%. Owing to its remarkably high variable renewable energy production, the RESc case losses mount to 39.5% (Demetriou *et al.*, 2021).

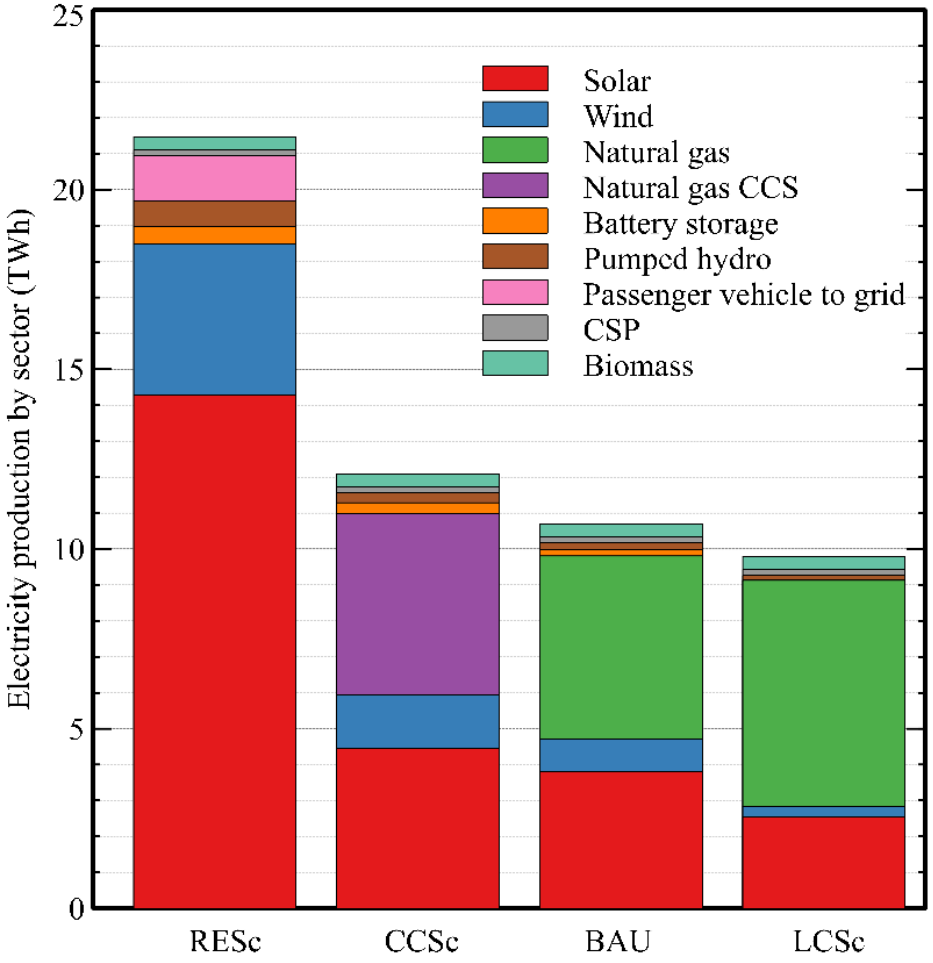

Fig. 4.7. Projected electricity production for Cyprus in year 2050. Acronym RESc is the Renewables scenario, CCSc is the Carbon Capture & Storage, BAU stands for Business As Usual and LCSc is the Least Cost scenario.

At the consumption side, the main sources of demand originate from five sectors, that is, agriculture, commercial, industrial, lighting, and residential, which

jointly account for 6.67TWh. Car charging follows with a consumption ranging between 1.26TWh and 3.15TWh while the RESc pumped hydro storage reaches 1.64TWh, as illustrated in Fig. 4.8. If Cyprus were to draw all of its electricity generation from renewable energy sources, it is striking to note that the excess energy loss is disproportionally high compared to other scenarios by at least a factor of 2.5. Even with the integration of pumped hydro storage and battery charging, the excess amount of electricity loss remains high owing to the storage capacity which is insufficient to utilise the produced energy. If the storage capabilities were to be expanded, it would have contributed to a significantly higher electricity cost. In turn, this development fails to meet the objective of minimising the price of electricity for instance in the least cost scenario. Distinctively, the BAU and the Carbon Capture and Storage scenarios do not reveal large discrepancies among them. Due to its higher reliance on renewables, the BAU scenario is characterised by a higher excess power production in relation to the LCSc.

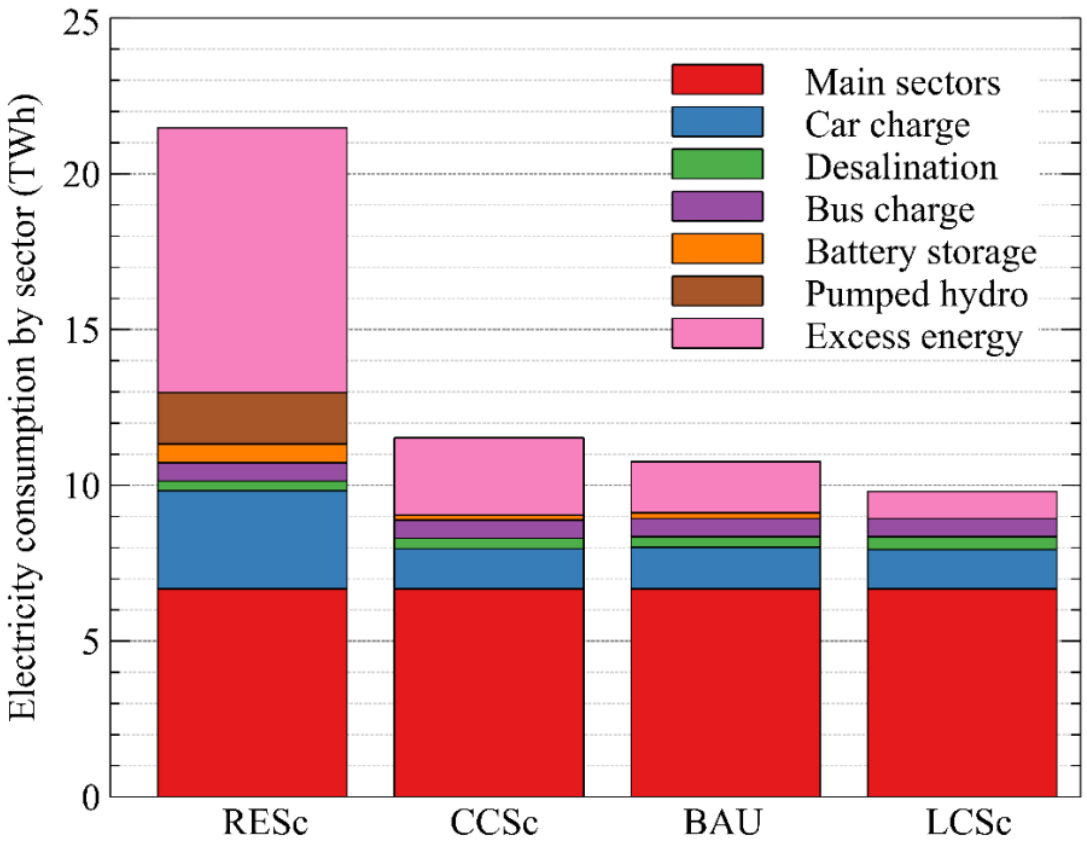

Fig. 4.8. Cyprus' electricity consumption in 2050. RESc bar depicts the Renewables, CCSs stands for the Carbon Capture & Storage, BAU is the Business As Usual and LCSc for the Least Cost scenarios.

4.4 Hourly electricity production in 2050

4.4.1 China

The hourly electricity mix for the year 2050 was obtained from the calculations summarised in §3.1.9.1. Regarding the Chinese electricity sector and the estimation of its hourly production, a 30-day hourly electricity production mix for all the scenarios applied during the summer and winter periods was obtained. Noticeable spikes manifest in all of the scenarios (Fig. 4.9 and Fig. 4.10), except in the BAU case where coal plays a dominant role while the least amount of excess electricity production is found. Additionally, the Goals and CFr scenarios meet demand principally on RES and hydro production. Of note is the RESc scenario which demonstrates that only during the summer period (Fig. 4.9), renewable energy sources, and battery and hydrogen storage can collectively meet electricity production (Demetriou and Hadjistassou, 2021).

In contrast, the winter season paints a different picture regarding the required installed capacity. First, there are fewer surges in power generation and, hence, less electricity losses. Second, the RESc scenario drawing on RES, hydro and batteries does not suffice to fulfil all of the electricity demand. At best, the RESc scenario can satisfy 55% of the total power demand during wintertime. Concomitantly, natural gas, nuclear, coal or their combinations need to supplement power generation, as depicted in Fig. 4.10. Even though at a first glance the CFr and the Goals scenarios seem similar, in fact, they exhibit a stark distinction. Simply stated, in the CFr the dominant power generation source is nuclear energy, whereas in the Goals scenario coal meets a sizeable proportion of the electricity demand.

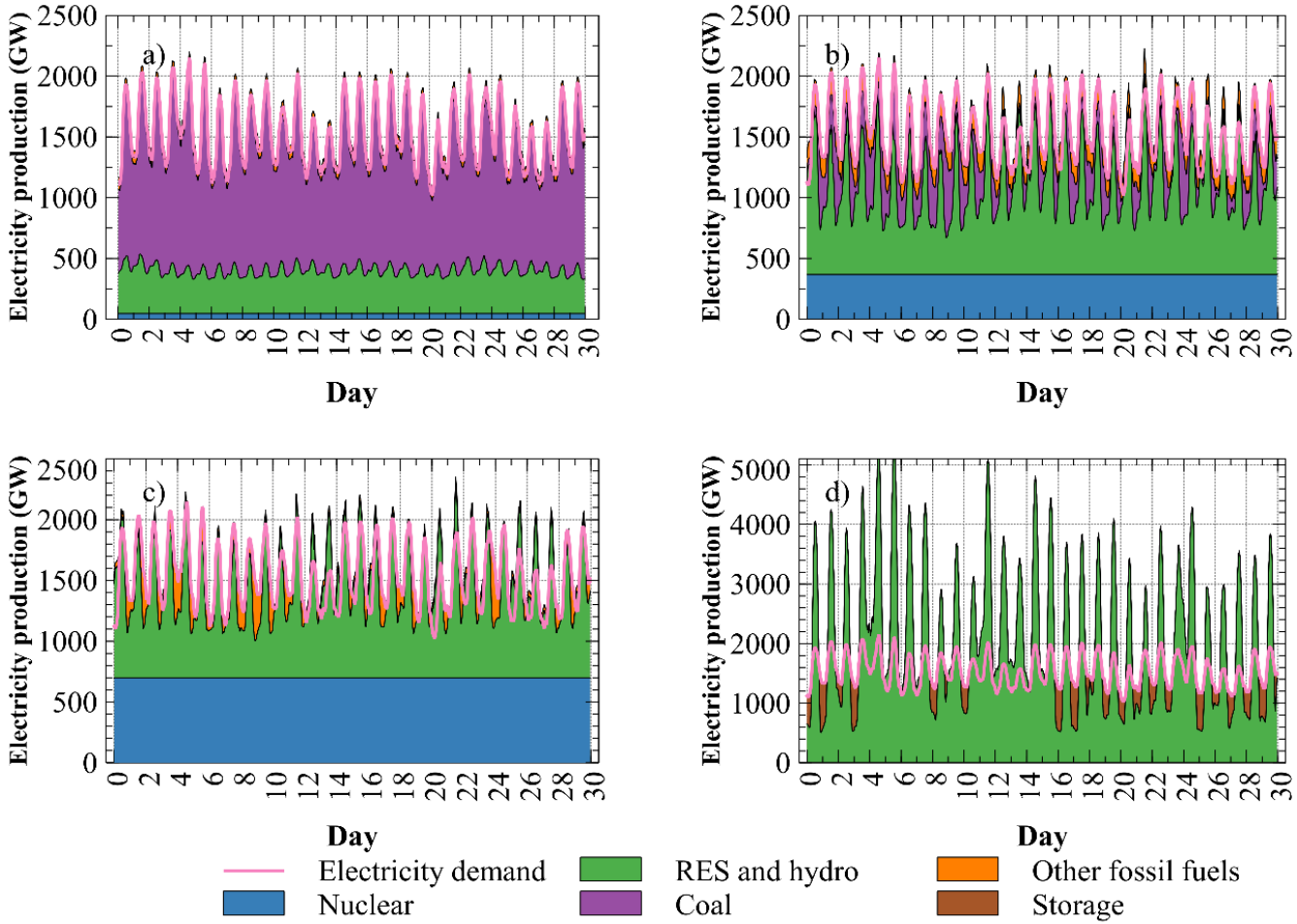

Fig. 4.9. China's summer hourly electricity production for a 30-day period, in year 2050, for all power generation technologies. Plot a) refers to the Business As Usual, b) the Goals, c) the Coal Free and d) the RES scenario, respectively.

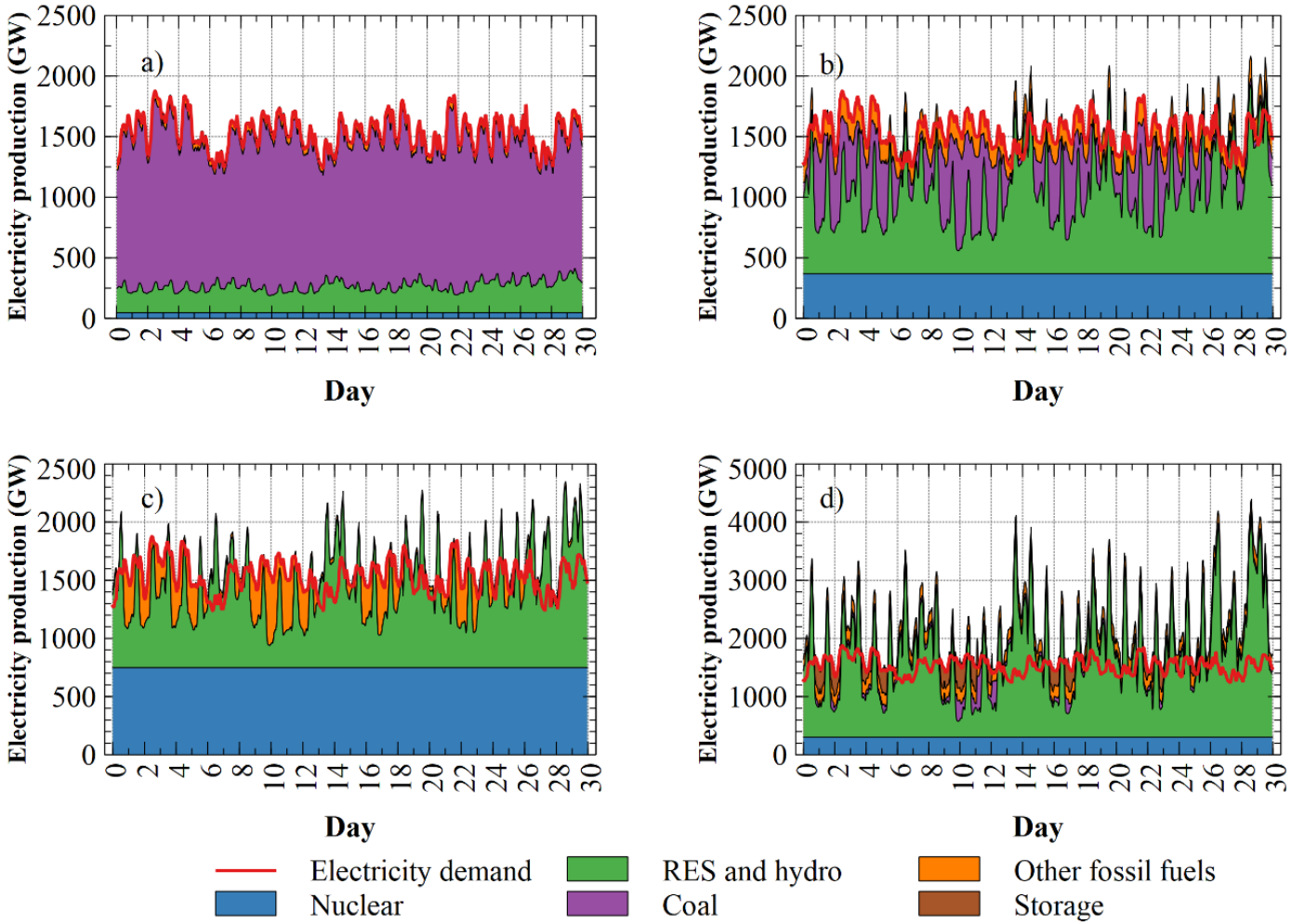

Fig. 4.10. Winter hourly electricity production spanning a 30-day period, in year 2050, for all power generation technologies for China. Plot a) refers to the Business As Usual, b) alludes to Goals, c) is coal free and d) is the renewables scenario, correspondingly.

4.4.2 Cyprus

Based on the methodology outlined in subsection 3.1.9.2, a weekly hourly electricity profile concerning electricity consumption and production was depicted in Fig. 4.11, Fig. 4.12, Fig. 4.13 and Fig. 4.14. More specifically, results pertain to a typical week during January and July based on the estimated values for 2050. Starting, this subsection presents four figures which help illustrate the similarities and distinctions between the CCSc and the RESc scenarios during winter and summer seasons. Referring to Fig. 4.11, Fig. 4.12, Fig. 4.13 and Fig. 4.14, they display the hourly electricity production for each powerplant in conjunction with the power used for vehicle and bus charging, pumped hydro, battery storage and desalination.

Initially, the focal point was the winter period during which daytime power production spikes manifest (Fig. 4.11 and Fig. 4.12). Considering the RESc, hourly electricity generation peaks range between 4,000–7,000MWh in contrast with the CCSc where maximum production spans from 1,800 to 2,500MWh. Clearly, the RESc case demonstrates sizeable spikes due to the high penetration of variable renewable energy production. It is also interesting to note that battery storage, vehicular power discharge to the grid and hydropower are utilised mostly during night-time in the absence of solar power production. Additionally, during periods of high solar power generation, the RESc case cannot absorb all of the electricity produced and this results into electricity losses of up to 5,000MWh. Irrefutably, the RESc scenario is capable of meeting electricity needs anytime during the winter season, as displayed in Fig. 4.12.

Noticeably, the summer season displays certain peculiarities in comparison to the winter period. For instance, hourly spikes are more pronounced in relation to wintertime, with the main dissimilarity being that they attain about the same peak value during that 7-day period. Together, the summer and the winter periods of the RESc scenarios were characterised by considerable hourly power losses. During the summer period, the RESc and the CCSc could have produced an excess amount of electricity of 70% and 40%, respectively (Fig. 4.15, Fig. 4.16). Whatsmore, as anticipated electricity needs in contrast to the winter period, appear inflated by 18% for the RESc and by 25% for the CCSc (Fig. 4.13 and Fig. 4.14). The decrease in electricity production for batteries and vehicles is less than 5%. Apparently, vehicle and battery charging needs do not exhibit marked differences between summer and winter seasons.

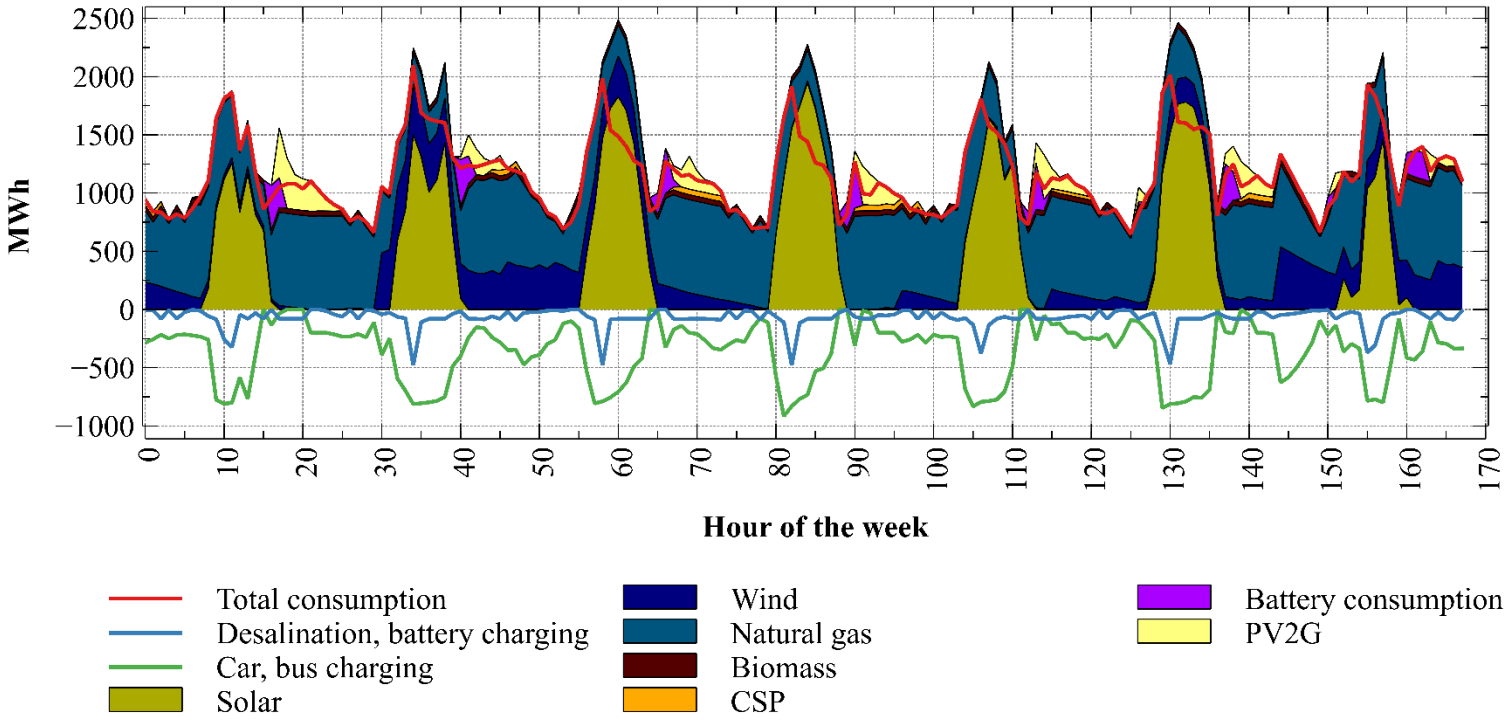

Fig. 4.11. Winter hourly electricity production and consumption, for a one-week period, during January 2050 for the Carbon Capture & Storage scenario for Cyprus.

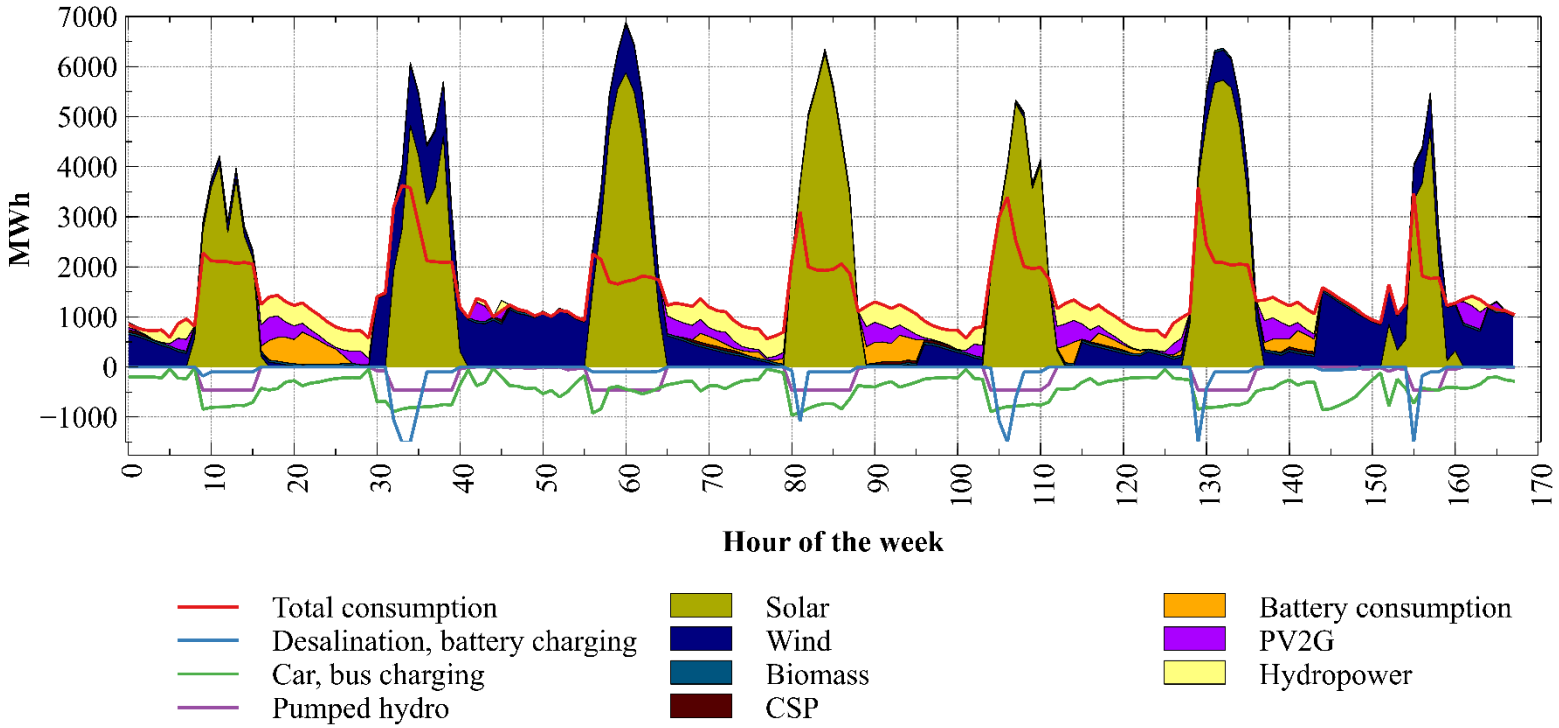

Fig. 4.12. Cyprus winter hourly electricity production and consumption, for a one-week period, during January 2050 for the Renewables scenario.

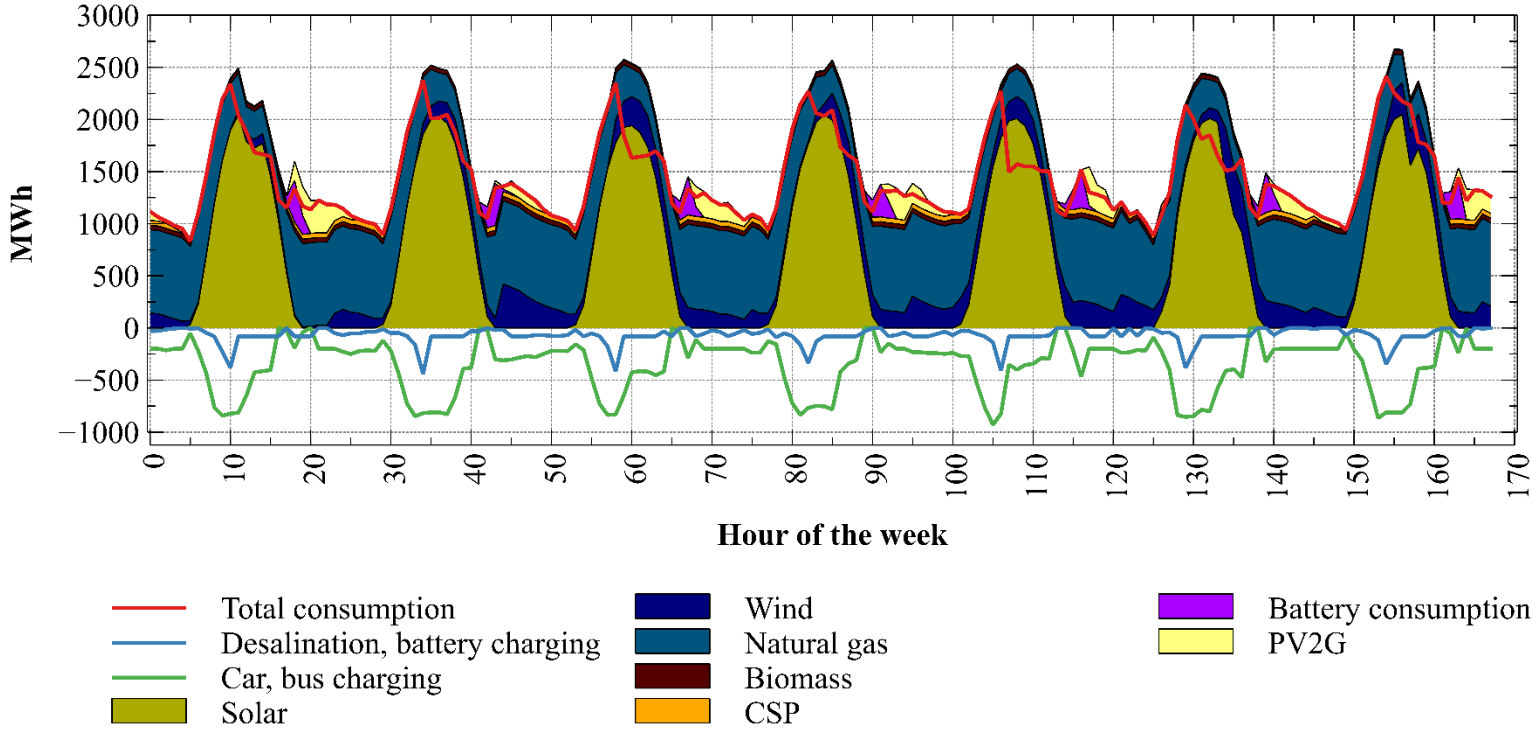

Fig. 4.13. Summer hourly electricity production and consumption, for a typical week, during July 2050, for the Carbon Capture & Storage scenario, for Cyprus.

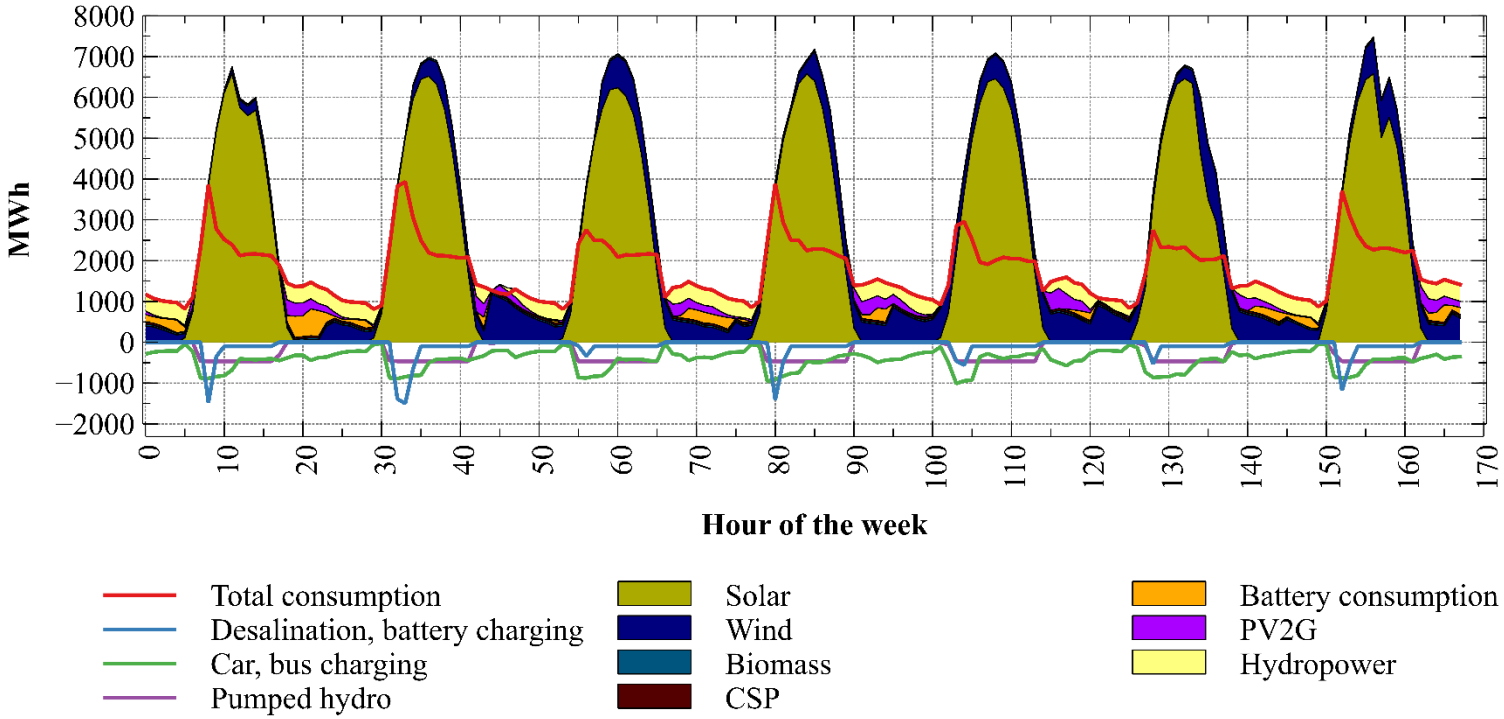

Fig. 4.14. Summer hourly electricity production and consumption for Cyprus, for a typical week, in July 2050, for the Renewables scenario.

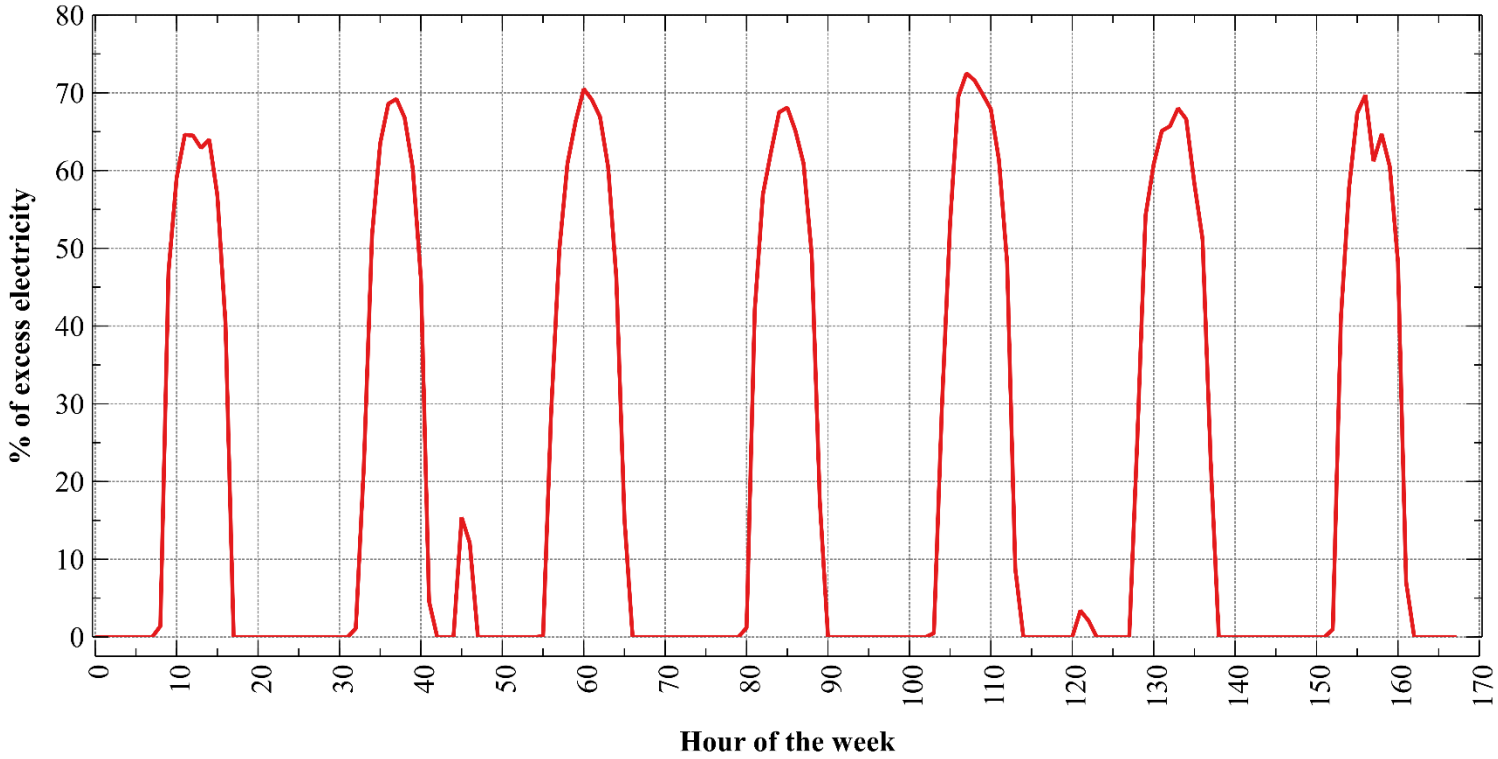

Fig. 4.15. Summer hourly percentage of excess electricity production for Cyprus for a typical week, in July 2050, as generated by the Renewables scenario.

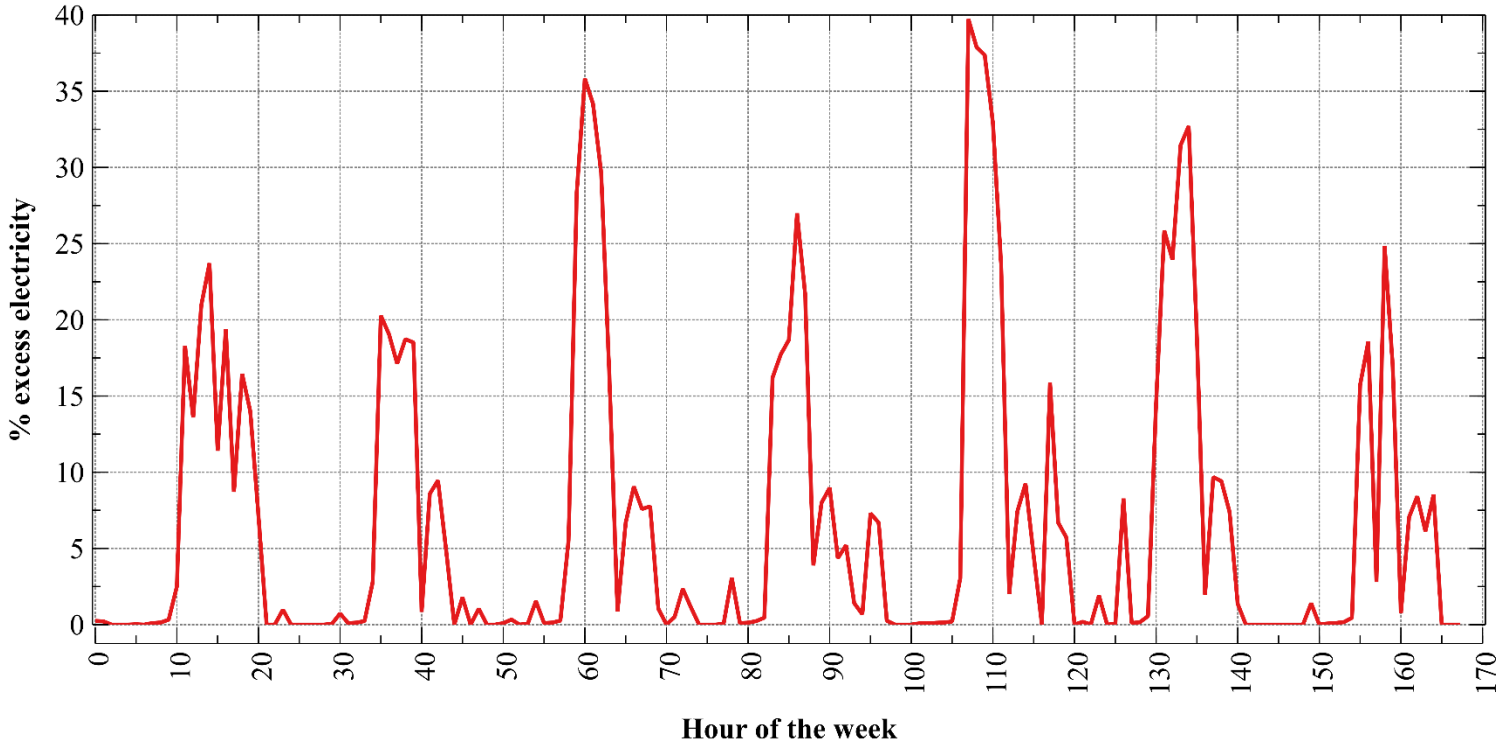

Fig. 4.16. Cypriot summer hourly percentage of excess electricity production for a typical week, in July 2050, for the Carbon Capture and Storage scenario.

4.5 Future capital costs of renewables

This section outlines the details of the learning rate of wind and solar energy based on the methods presented in §3.1.3. The future capital costs of solar energy are revealed in Fig. 4.18 and Fig. 4.17 (Demetriou and Hadjistassou, 2021). As the candidate sites for installing solar photovoltaic parks, near demand, are gradually occupied the capital costs of additional solar power begin to mount mostly due to the remote location of the energy parks (International Energy Agency, 2012; He and Kammen, 2014).

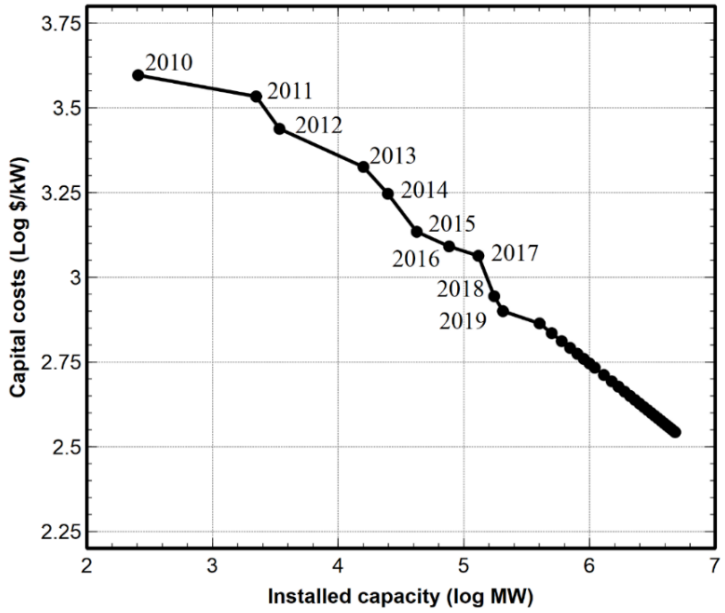

Fig. 4.17. Future capital costs of solar energy ranging between 2020 and 2050 (log-log plot). Real data for years 2010 to 2019 derived from the International Renewable Energy Agency (2019).

In year 2019, onshore wind made-up 98.2% of the total wind power generation capacity of China (China Energy Portal, 2019). It is important to stress that onshore wind capacity can reach 2TW at a height of 50m above the mean sea level and at a wind power density of 300W/m^2, as outlined in Table A2. In an effort to augment overall power generation from wind energy, three different approaches were adopted. More offshore wind capacity is one possible solution. Meanwhile, installing wind generators at lower wind power density areas will presumably become a necessity. Last but not least, opting for taller wind turbines mounted at higher altitudes can boost wind energy yield as pointed out in section A.1. Once a capacity of 2TW of wind turbines is

installed, it was assumed that ¾ (75%) of new wind installations will be located onshore while the remaining ¼ (25%) will be sited offshore (Fig. 4.19 and Fig. 4.20). These figures conform with the wind energy potential of China (International Energy Agency, 2012; Yang *et al.*, 2017).

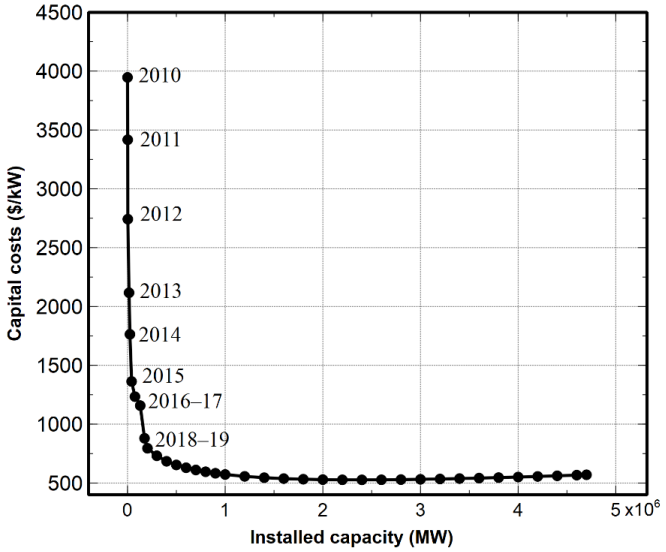

Fig. 4.18. Future capital costs of solar energy spanning between 2020 and 2050. Actual data covering years 2010 to 2019 were obtained from the International Renewable Energy Agency (2019).

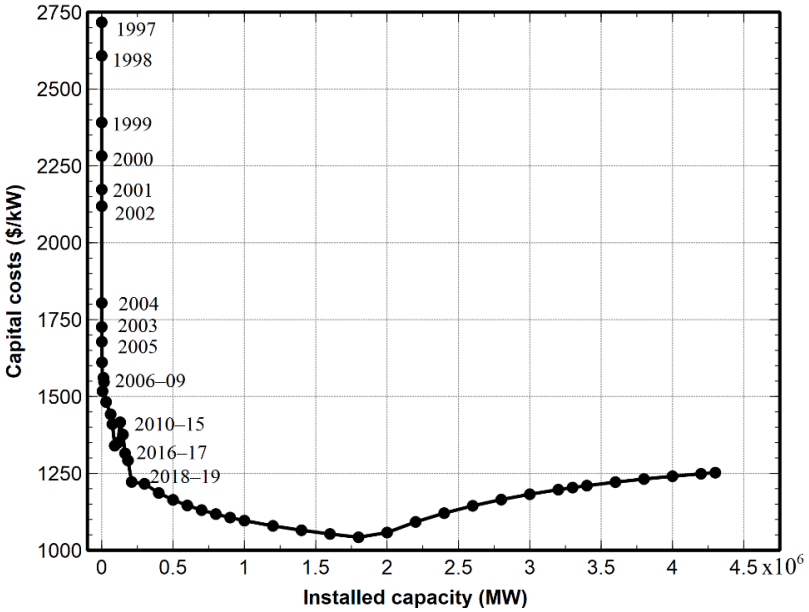

Fig. 4.19. Future capital costs of wind energy between 2020 and 2050. Costs data between 1997 and 2019 were sourced from the International Renewable Energy Agency (2019).

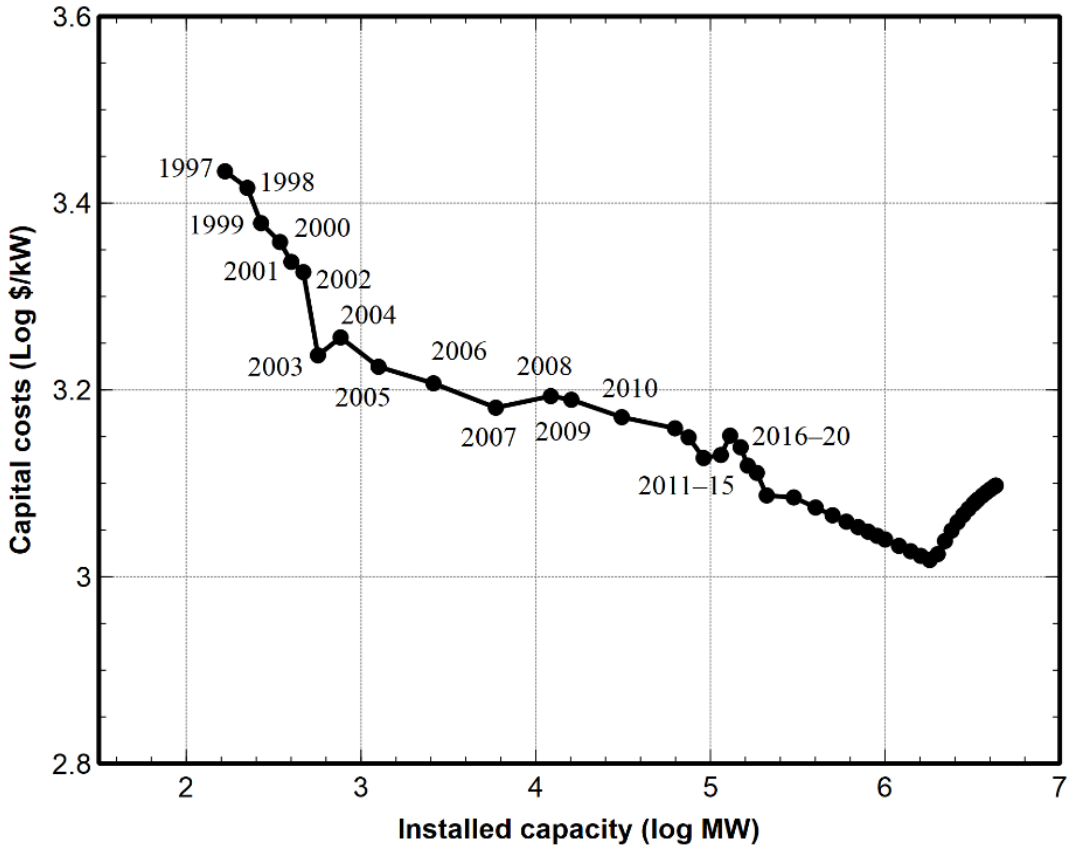

Fig. 4.20. Future capital costs of wind energy for years 2020 to 2050 (log-log plot). Costs data between 1997 and 2019, were obtained from the International Renewable Energy Agency (2019).

4.6 Forecast of fuel prices in China

Another major cost variable that merits attention is the future fuel costs. For the sake of simplicity, it is assumed that the costs of nuclear energy will remain essentially unaltered for the period of interest, that is, until 2050. During the same interval, projections were obtained pertaining to the future price of coal and the costs of piped natural gas. The future coal price was determined from the ARMA method with data sourced from BP (2018). Suffice to say that the ARMA technique discerned a decrease in coal's costs to year 2050, as indicated by most of the recent data alluding to a slight depression in costs (Fig. 4.21). The same method was considered for natural gas which demonstrated a slight increase in the fuel's price (Fig. 4.22). Gas prices originated from the EIA (2017b).

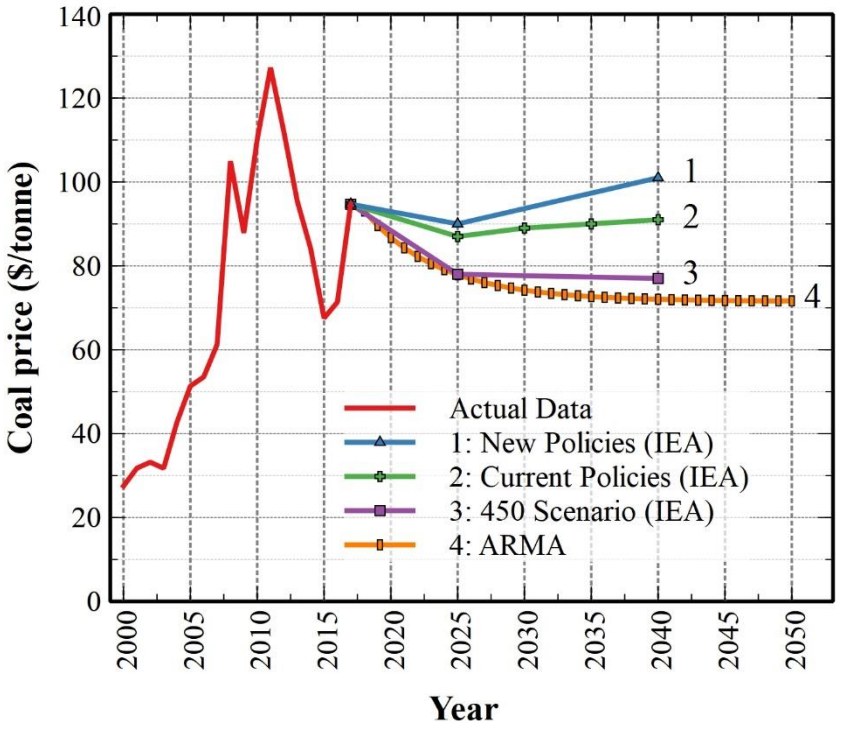

Fig. 4.21. Post-2017 coal fuel price projection obtained from: (1) the Current Policies, (2) the New Policies, (3) the 450 Scenario according to the IEA (2017), and the ARMA technique (this study). Coal price data prior to 2016 were obtained from BP (2018).

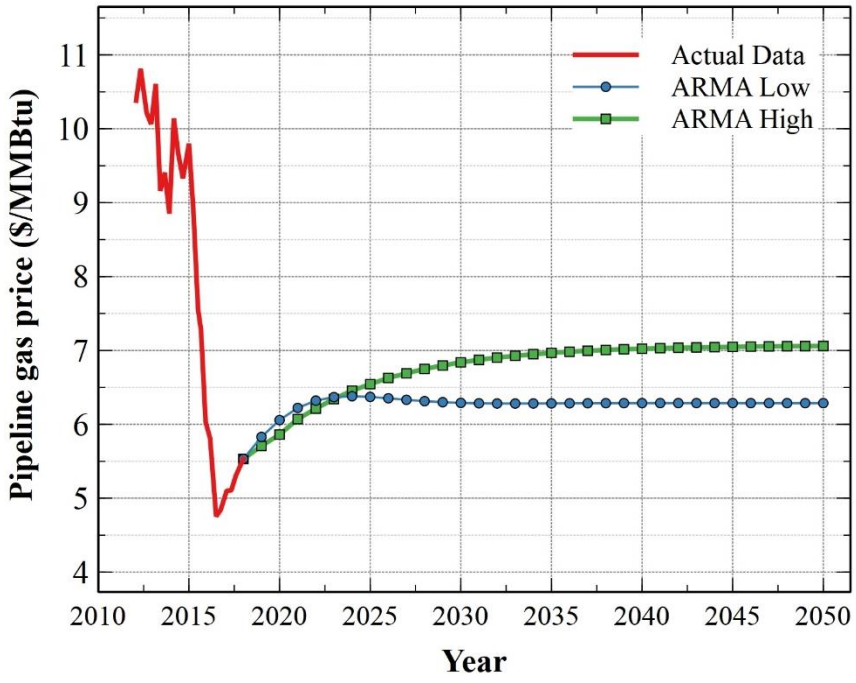

Fig. 4.22. Future price ($/MMBtu) of pipeline natural gas in China stretching between 2018 and 2050. Here actual data were retrieved from the EIA (2017b).

4.7 Future CO_2 emissions and electricity costs

Two of the central calculations of this study refer to the estimation of the electricity costs and carbon dioxide emissions. It is crucial to demonstrate if Cyprus can comfortably meet the goals set by the European Union with regard to maintaining emissions at a level that world temperature will be constrained by 1.5°C or 2.0°C compared to the pre-industrial levels. Estimating the future carbon dioxide emissions along with the carbon sinks in China, deriving from the sector of Land-Use, Land Use Change and Forestry (LULUCF) is a key to investigate if the goal of carbon neutrality by 2050 is possible. In this sub-section, the total CO_2 emissions of each scenario were depicted along with their levelised cost of electricity beginning with China and concluding with Cyprus.

4.7.1 China

4.7.1.1 Future levelised cost of electricity

Invoking the methodology outlined in §3.1.3, the future Levelised Cost of Electricity (LCOE) was calculated for a range of interest rates, that is, 5%, 7% and 10% until the year 2050 which are discussed in detail in the A.2. As a way of comparing the different technologies, the LCOE of nuclear, biomass, and hydro was determined based on a yearly capacity factor. Whatsmore, the costs of coal and natural gas were taken to vary on a yearly basis according to the capacity factor and the fuel price projections, as shown in Fig. 4.21 and Fig. 4.22 (Demetriou and Hadjistassou, 2021). Wind and solar energy costs were considered to change on an annual basis depending on the scenario of interest. Interestingly, hydrogen storage yields the highest LCOE followed by battery storage. An exception occurs in 2050 when coal is utilised only when there is a need to keep an uninterrupted power supply to the grid.

4.7.1.2 Future carbon sinks and CO_2 emissions

It was deemed helpful to examine the potential emission sinks from Land Use, Land-Use Change and Forestry (LULUCF). The LULUCF emissions forecasts were obtained from the Holt-Winters and the logistic methods and compared to the targets defined by the State Forestry Administration of China. The values of these three scenarios, in 2050, vary from −0.98 to −1.06Gt of CO_2 (Fig. 4.23). The predicted

emissions were compared with the goals set by China's State Forestry Administration (2014). Holt-Winters scenario almost matches the State Forestry Administration Goals with a deviation of less than 1%. These calculations are essential for assessing whether the Chinese electricity sector will be able to attain net zero emissions. Likewise, the emissions of the electricity sector are estimated for two different cases.

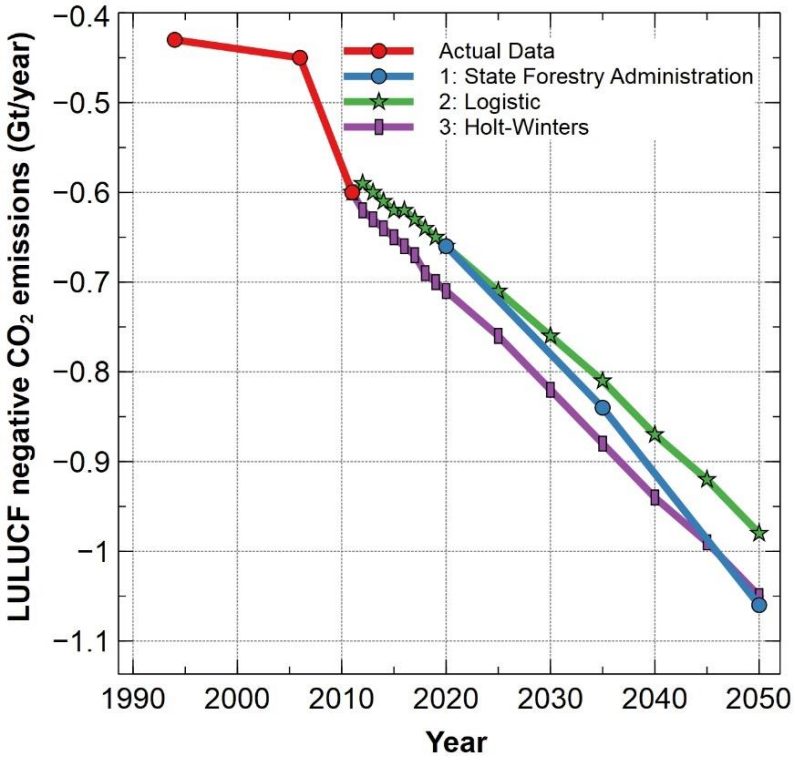

Fig. 4.23: Future Chinese LULUCF negative CO_2 emission projections obtained from the logistic method (this study), the Holt-Winters method (this study) and data from the Chinese State Forestry Administration (State Council the People's Republic of China, 2018).

In the first case, the emissions factors for each power generation technology were considered to remain unaltered for the 33-year time horizon. The second case posits that, by 2040, the average emissions factor of each electricity generation technology will taper to its minimum level compared to 2017 values and then plateau. Surprisingly, the CFr scenario liberates fewer emissions than the RESc. Adjusting the electricity sector emissions, by factoring in the LULUCF emissions sinks, it was possible to obtain the maximum CO_2 levels without LULUCF and the minimum CO_2 footprint with LULUCF, respectively— as discerned in Fig. 4.24.

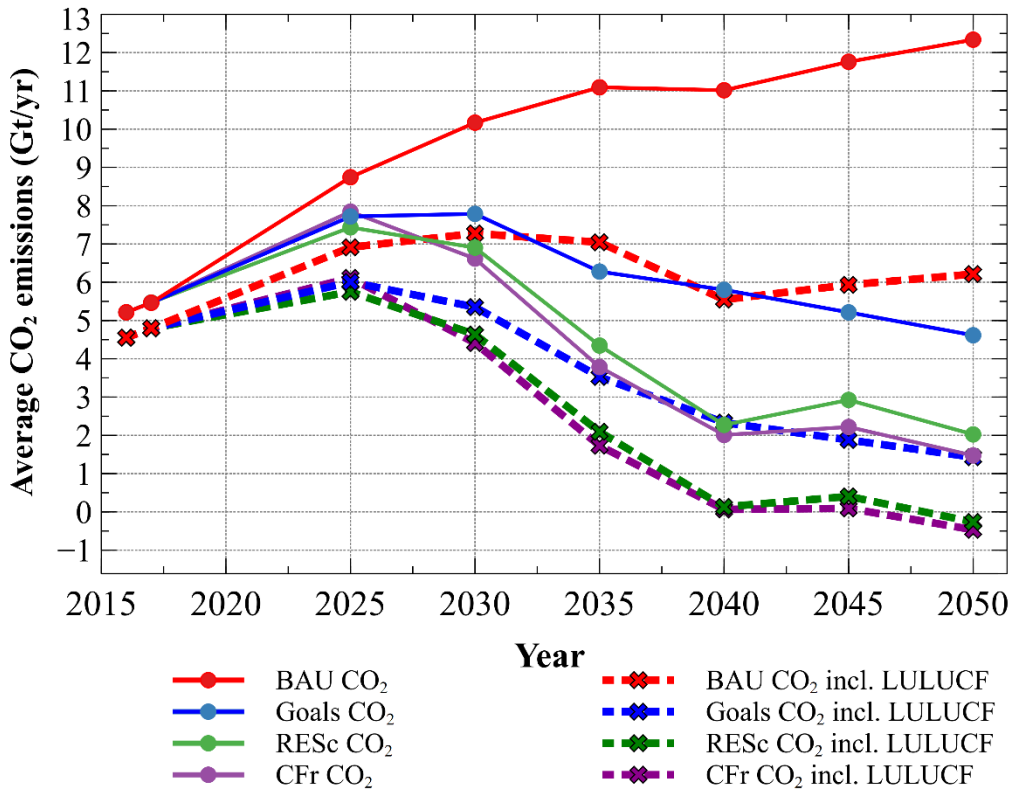

Fig. 4.24. Average and minimum CO_2 levels including LULUCF, between 2016 and 2050, for the BAU, the Goals, the CFr and the RESc scenarios for China.

Furthermore, other estimates considered the impact of CO_2 emissions and the influence on the costs of electricity. That is, the average electricity costs were obtained from an interest rate of 10% while the emissions factor remained constant from 2017 until 2050 without considering LULUCF (Fig. 4.25). China aims to arrest its CO_2 emissions by year 2030. Consulting the four scenarios described earlier, the BAU not only does it fail to contain national emissions during the post-2030 period, but the emissions rise by at least 1.4 times. Emissions generated from the RESc scenario do not plateau until 2030. Carbon dioxide emissions for the CFr and the Goals scenarios appear to flatten by 2030 assuming values between 4.83 to 6.14Gt for the former and 6.17 to 7.79Gt for the latter scenario. Projected emissions from the CFr scenario compare well with predictions by Wu and Peng (2016) who anticipated that Chinese CO_2 emissions will range between 3.95–5.81Gt, by 2030.

Thereafter, progressing to 2050 the RESc emissions shrink by at least a factor of 2 and constitute the second-best case in terms of the least emitted mitted emissions which amount to between 0.78 to 2.03Gt of CO_2. However, the lowest emissions were

obtained from the CFr case with an emissions footprint ranging from 0.58 to 1.47Gt of CO_2 (Demetriou and Hadjistassou, 2021). Relative to the maximum drop in carbon dioxide emissions of 87.2% attained by the CFr scenario, a study published by Liu et al. (2019a) estimated a comparable reduction in CO_2 levels of 67.5%. An earlier report disseminated by Khanna et al. (2016) concluded that Chinese emissions will bottom at 2.61Gt.

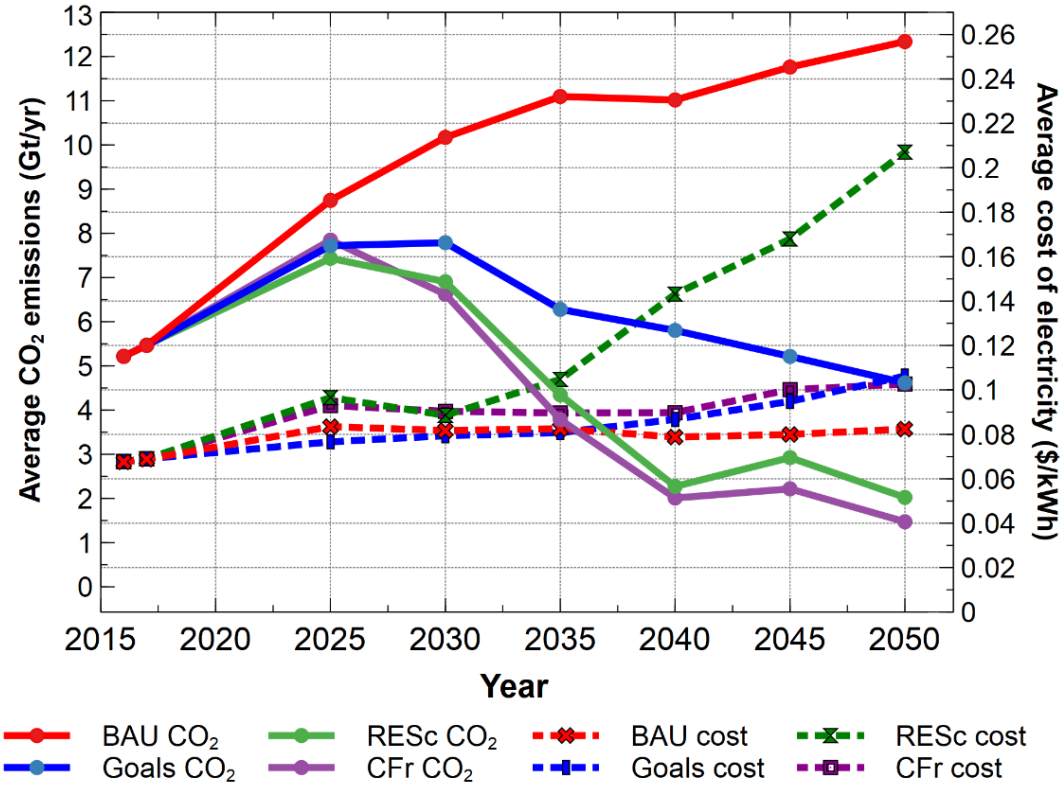

Fig. 4.25. Average electricity costs and CO_2 emissions spanning between 2016 and 2050 for the BAU, the Goals, the CFr and the RESc for an interest rate of 10%, for China.

If the Chinese Government is to honour its proposed targets, as expounded in the Goals scenario, CO_2 emissions in year 2050 will need to plummet between 2.47 to 4.62Gt compared to 5.21Gt in 2016. Shifting attention on the LULUCF, CO_2 emissions sinks are estimated to absorb 1.06Gt by 2050. Evidently, it appears that the CFr scenario is the only one expected to yield a negative total emissions inventory of 0.47Gt in 2050. Concluding, the most economically attractive scenario as pertains to power generation costs is the BAU with 0.082$/kWh followed by the Goals and the CFr scenarios with 0.106$/kWh and 0.103$/kWh, respectively, in 2050. Notwithstanding, the RESc is the most expensive case producing electricity at a cost of 0.207$/kWh.

4.7.2 Cyprus

Due to their importance, the future CO_2 emissions were estimated from electricity production. Originally, natural gas consumption was calculated for each scenario. Furthermore, based on the emissions factors listed in Table 3.5, the future emissions for each scenario were obtained with and in the absence of carbon capture and storage. Overall emissions for each technology were deduced from the product of the electricity production and the pertinent emission factor. Interestingly, each scenario displays a large variability in its emission footprint. In absolute numbers, the Least Cost scenario is expected to release 2,200kt of CO_2 in 2050. Constituting the best proposition, the BAU scenario will liberate 1,785kt of CO_2 during the same year. Surprisingly, the Carbon Capture and Storage scenario produces 191kt of carbon emissions, or 11.5 times less than the LCSc (Fig. 4.26), by 2050. Lastly, the renewables scenario attains zero emissions.

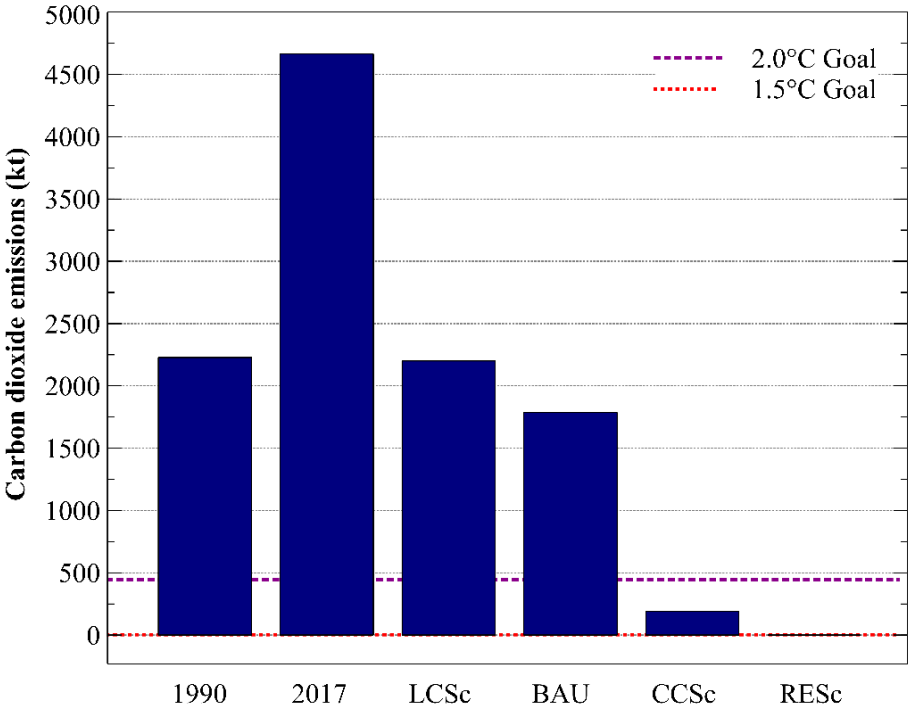

Fig. 4.26. Carbon dioxide emissions of the electricity and the transport sectors, including cars and buses for, year 2050, compared to actual data of 1990 and 2017. BAU refers to the Business As Usual, LCSc to the Least Cost, CCS to Carbon Capture and Storage, and RESc to the Renewables scenarios. The 1.5°C Goal line indicates zero carbon emissions. The 2°C Goal line refers to an 85% reduction in CO_2 emissions compared to 1990 (Demetriou *et al.*, 2021).

For the record, in 1990 the total emissions originating from the electricity sector and vehicles amounted to 2,228kt of CO_2. By 2017, the emissions of the latter sectors doubled to 4,663kt of CO_2 (Mesimeris *et al.*, 2020). The European Union in 2009 had set a goal for all its member states, that in year 2050, to reduce their emissions levels, by at least 80%, compared to 1990 so as to stave off a temperature increase by 2.0°C relative to 1990 (European Commission, 2018). Finally, a more aggressive goal has been set in 2019 by the EU which aims to contain temperature increase by 1.5°C, compared to 1990 (European Commission, 2019). To realise this target, EU emissions must become net-zero as attained by the RESc formulated in this study.

Brussels has set specific targets designed to contain temperature increase to a minimum attainable level. Two of the scenarios, that is, the BAU and the LCSc for Cyprus fail to restrain carbon emissions below the targets mandated by the EU. Assessing the remaining scenarios, the CCSc yields a decrease in emissions well below the threshold of 2.0°C. Meanwhile, the RESc case goes one step further to achieve the goal of constraining the temperature rise by 1.5°C compared to the pre-industrial levels. Besides carbon emissions, the economic dimensions of environmental goals are of paramount importance. Hence, for each technology, including passenger vehicle-to-grid, the levelised cost of electricity were obtained from the data listed in Table 3.2, Table 3.3 and Table 3.5.

As a way of making the investigation more comprehensive, a carbon tax of 50€/t of CO_2 was incorporated in the projections. Even though the preceding carbon levy is deemed high, it helps capture the impact of a carbon tax in the event it rises considerably. In this regard, the LCSc scenario yields electricity at 0.07€/kWh followed by the BAU with 0.076€/kWh. When the same carbon tax was factored in the CCSc and the RESc scenarios that abide by the European Commission's goals, the costs of electricity escalated to 0.094€/kWh and 0.115€/kWh, respectively, as shown in Fig. 4.27. Thus, the RESc is 64% more expensive than the LCSc case and 57% more costly than the BAU and, finally, 22% more pricey than the CCSc scenario. Before concluding, carbon tax rates were incorporated in the LCSc and compared with the RESc and the CCSc cases, as can be observed from Fig. 4.28. Results reveal that with a carbon tax of about 155€/t of CO_2 and 245€/t of CO_2, the LCSc is more costly relative to

the CCSc and the RESc cases. Finally, based on the current value of carbon credits of 25€/t of CO_2, the electricity price for the LCSc amounts to 0.062€/kWh.

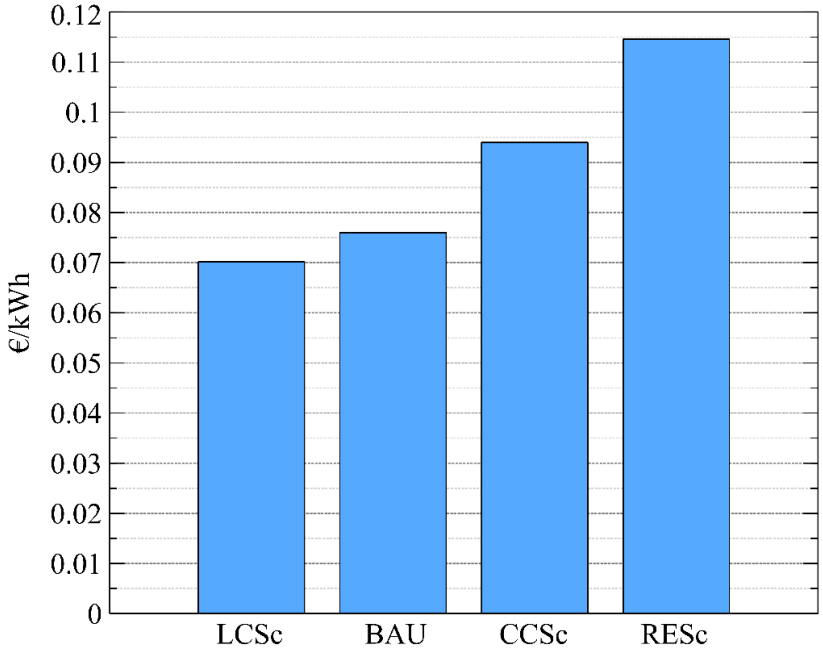

Fig. 4.27. Electricity costs in 2050, for the BAU, the LCSc, the CCSc and the RESc scenarios with a carbon tax of 50€/t of CO_2 for Cyprus.

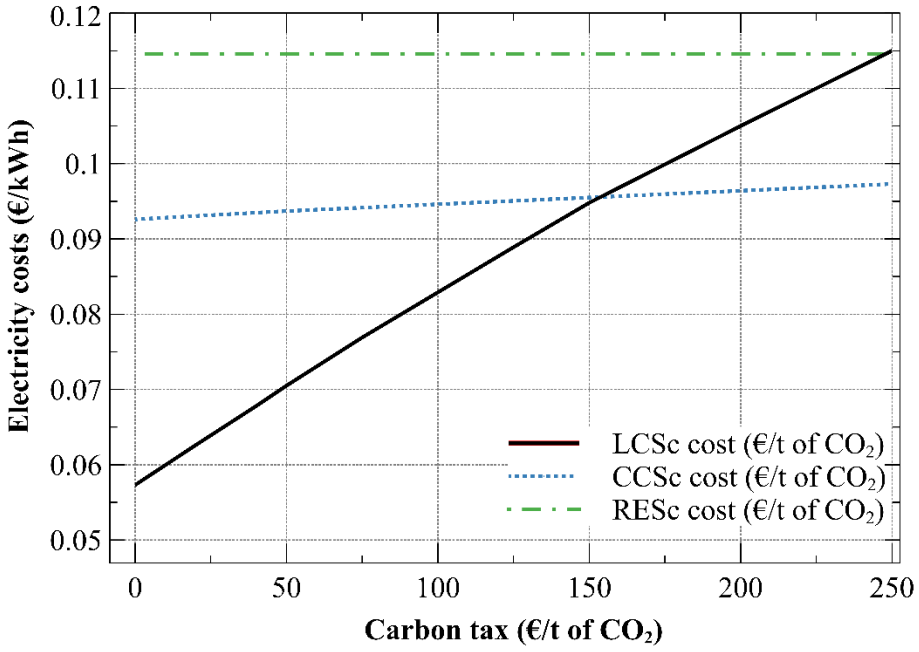

Fig. 4.28. Sensitivity analysis of the electricity costs for Cyprus, in year 2050 based on three scenarios, namely, the LCSc, the CCSc and the RESc while increasing the carbon tax rates ranging from 20 to 250€/t of CO_2.

During the past three decades, the European Commission has instituted ambitious goals towards mitigating the effects of climate change. Our analysis indicates that only two of the proposed scenarios accomplish these goals for Cyprus. Interestingly, the Carbon Capture and Storage scenario complies with the 2°C temperature goal and the renewables case meets the 1.5°C objective (Demetriou *et al.*, 2021). Both of these scenarios could also be applied in the context of the electricity demand of the island.

The methodology presented here besides being applicable to Cyprus, it could be suitable for other geographic regions such as islands or remote locations. Evidently, the methods explained in this thesis can help guide the transition to a 100% renewable energy grid with the synergy of power storage and electric passenger vehicles. In other words, this study may serve as a template to enlighten other jurisdictions of the candidate technologies and energy strategies on a path to a more sustainable future as far as electricity costs and emissions are concerned.

4.8 Road traffic and residential heat dispersion modelling

This section presents the dispersion analysis applied at the centre of Nicosia, the capital of Cyprus concerning vehicle and residential heat pollutants which is performed in GRAL®. At first, the study validated concentration values of four pollutants, namely, CO, NO_x, $PM_{2.5}$ and PM_{10} with hourly measurements from an air quality station situated in Nicosia during a 9-month period from 1/2017 until 9/2017. Afterwards, the statistical performance of the model was evaluated on a daily and an hourly basis for all four pollutants. Subsequently, 9 scenarios and 8 distinct traffic cases for NO_x and $PM_{2.5}$ were simulated. Lastly, based on the concentrations drawn from each scenario/case a health impact assessment was founded by an IER function to estimate the premature risk mortality.

4.8.1 Validation of the dispersion model

Hourly traffic and residential heating-related emissions of CO, $PM_{2.5}$, PM_{10} and NO_x were factored in the dispersion model for a nine-month period, that is, from January 2017 until September 2017. Calibration of the theoretical model findings was performed against real emissions measurements. The daily comparison of all pollutants is displayed in Fig. 4.29.

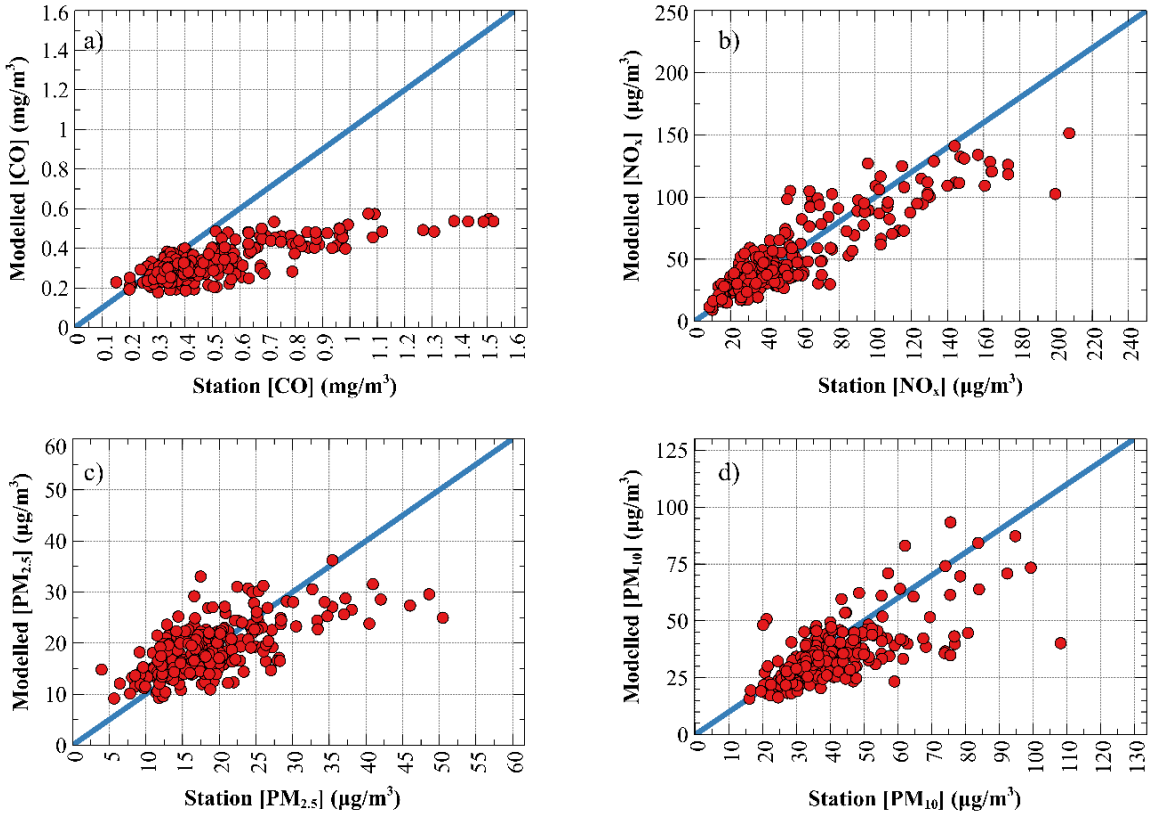

Fig. 4.29: Scatter plots of the average daily modelled vs. average daily station (measured) concentration for: a) Carbon monoxide, b) Nitrogen oxides, c) Particulate matter less than 2.5µm and d) Particulate matter less than 10µm, respectively. Diagonal line denotes $y=x$.

All particles, as reflected by plots a) to d) (Fig. 4.29) demonstrated excellent congruence between the theoretical pollution results and the experimental observations except for carbon monoxide which proved more difficult to replicate. Put differently, the dispersion simulations underestimate the concentration of carbon monoxide compared to road measurements. Nitrogen oxides and particulate matter with a diameter less than or equal to 2.5 µm congregate around the straight line $y = x$. Subject to further scrutiny both the daily and hourly pollution projections were assessed in relation to five statistical parameters, as illustrated in Table 4.2 and Table 4.3, in light of different criteria.

The statistical performance of the model lied within the acceptance threshold for an urban environment (Hanna and Chang, 2012) as they pertain to hourly and daily rates. In excess of 86% of the daily modelled values and 67% of the simulated hourly concentration of pollutants were in accord with the measured levels. Average NO_x and

$PM_{2.5}$ levels differed by less than 3% compared to actual readings. Overall, the model slightly underestimated the daily levels of NO_x and the hourly values of all pollutants in relation to the actual values.

Table 4.2: The statistical performance indicators of the predicted levels of NO_x, $PM_{2.5}$, PM_{10} and CO on a daily basis.

Parameter	Acceptance value	Perfect score	NO_x	$PM_{2.5}$	PM_{10}	CO
FB	<|0.67|	0	–0.03	–0.01	–0.16	–0.43
FAC2	>0.3	1	0.98	0.99	0.97	0.86
NMSE	<6	0	0.09	0.08	0.10	0.40
NAD	<0.5	0	0.13	0.02	0.11	0.22
R		1	0.89	0.67	0.70	0.78

Table 4.3: The statistical performance indicators of the modelled hourly concentrations of NO_x, $PM_{2.5}$, PM_{10} and CO.

Parameter	Acceptance value	Perfect score	NO_x	$PM_{2.5}$	PM_{10}	CO
FB	<|0.67|	0	–0.03	0.01	0.32	–0.43
FAC2	>0.3	1	0.67	0.68	0.85	0.76
NMSE	<6	0	0.59	0.63	0.38	1.28
NAD	<0.5	0	0.29	0.24	0.19	0.28
R		1	0.59	0.21	0.46	0.42

4.8.2 Traffic and vehicle composition scenarios

Having established a reliable dispersion model for Nicosia with regards to NO_x and $PM_{2.5}$, the next step was to implement a total of 9 scenarios as shown in Table 3.11. Traffic connected emissions derived from the emissions factors cited in the Appendix which varied according to the vehicle type, their transit speed, age and type of fuel (Ntziachristos and Samaras, 2019). Each one of the 9 scenarios was carefully crafted to gauge whether the specific policy had a positive or a detrimental impact on the concentration of NO_x and $PM_{2.5}$ (Fig. 4.30 and Fig. 4.31).

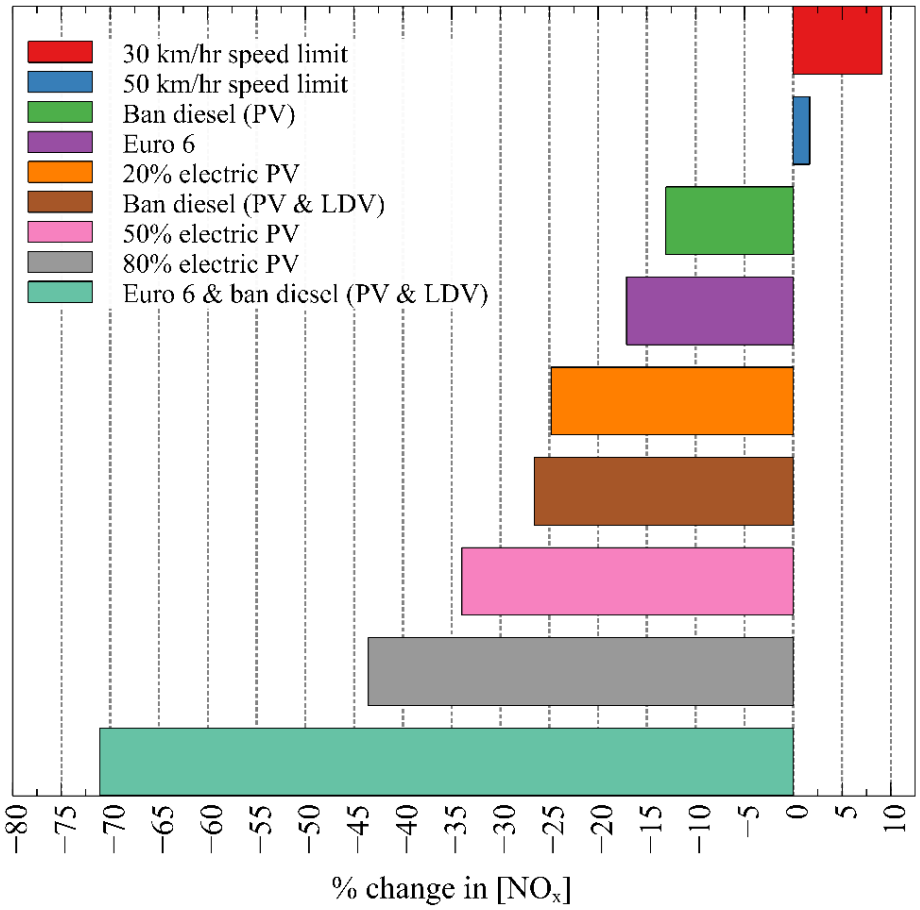

Fig. 4.30: Variations in NO_x concentration, compared to year 2017 levels, for each of the scenarios summarised in Table 3.11 for Nicosia.

Apparently, each policy decision or scenario can result in different levels of emissions in Nicosia. For instance, the imposed speed limit of 30 km/hr or 50 km/hr fosters a surge in pollutants in line with the findings from other studies (Ntziachristos and Samaras, 2019). Banning diesel passenger vehicles from the streets of the capital does not fundamentally affect NO_x, $PM_{2.5}$ and PM_{10} emissions owing to the fact that the proportion of diesel fuelled vehicles in Cyprus is about 16% (European Environment Agency, 2019a). Contrary to public perceptions regarding electric vehicles, even by displacing internal combustion engine cars they are not accompanied by an equally precipitous drop in emissions. This is attributed to two specific reasons. Firstly, being heavier in mass electric automobiles generate more non-exhaust pollution of $PM_{2.5}$ compared to conventional vehicles. And even if electric cars made-up 80% of Cyprus' vehicle fleet there will still be a small fraction of older vehicles that will conform to Euro 1 standards or later ones (Demetriou and Hadjistassou, 2022).

Shifting attention to $PM_{2.5}$ levels, it is evident that the Euro 6 vehicle standard scenario alone could be considered the best policy as it lowered particulate matter average concentration by more than 14%. Similarly, for NO_x if diesel passenger and light duty vehicles were banned while the rest of the vehicles abided to Euro 6 standards, nitrogen oxides sustained a reduction of 71%. Portraying the urban centre of Nicosia, the maps in Fig. 4.32 and Fig. 4.33 depict the levels of NO_x and $PM_{2.5}$ during a nine month period, in 2017, in comparison with the least pollution scenario which assumes Euro 6 standard vehicles and a ban of diesel PVs and LDVs (Demetriou and Hadjistassou, 2022).

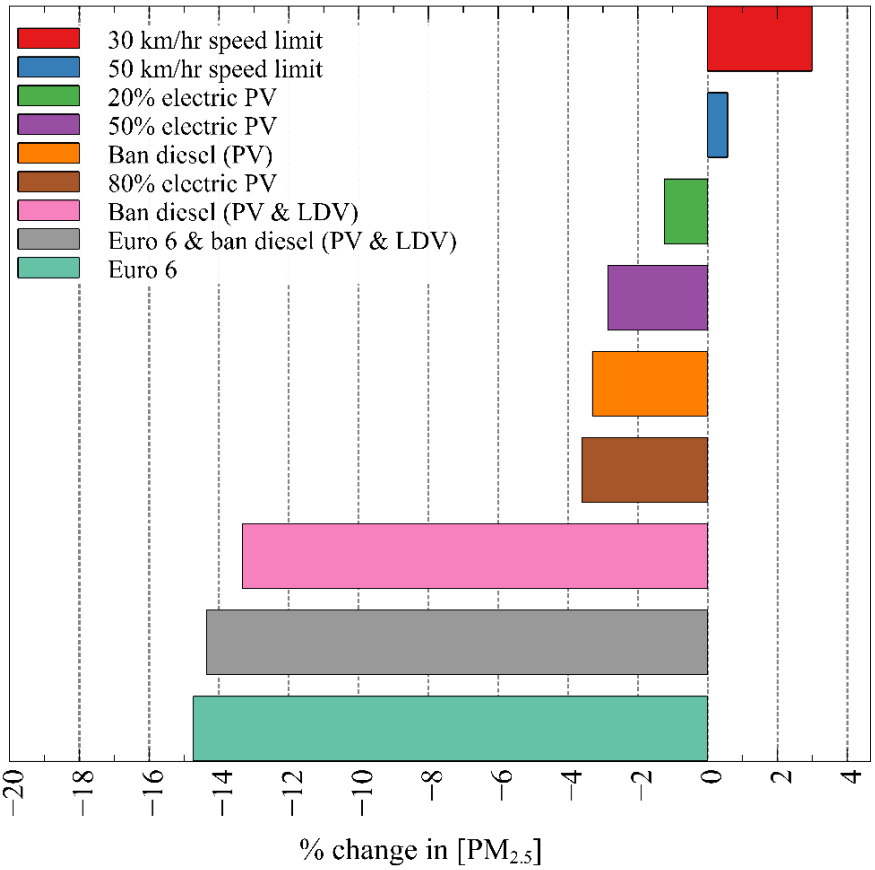

Fig. 4.31. Changes in the concentration of $PM_{2.5}$ regarding different policy decisions as described in Table 3.11 compared to year 2017.

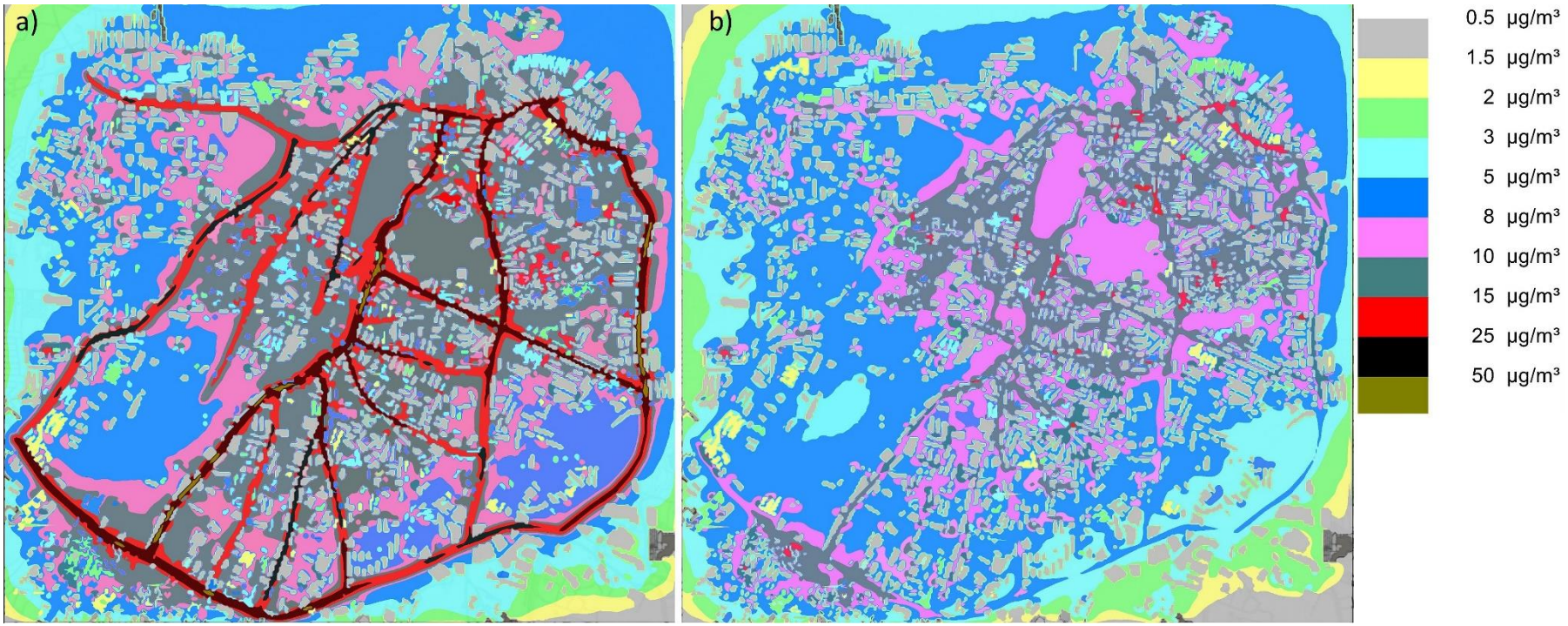

Fig. 4.32: Average concentration of NO_x emissions in Nicosia for a nine month period. Left figure a) displays 2017 simulated values while map b) shows the Euro 6 standard and a potential ban in diesel PVs and LDVs for the same nine-month time frame.

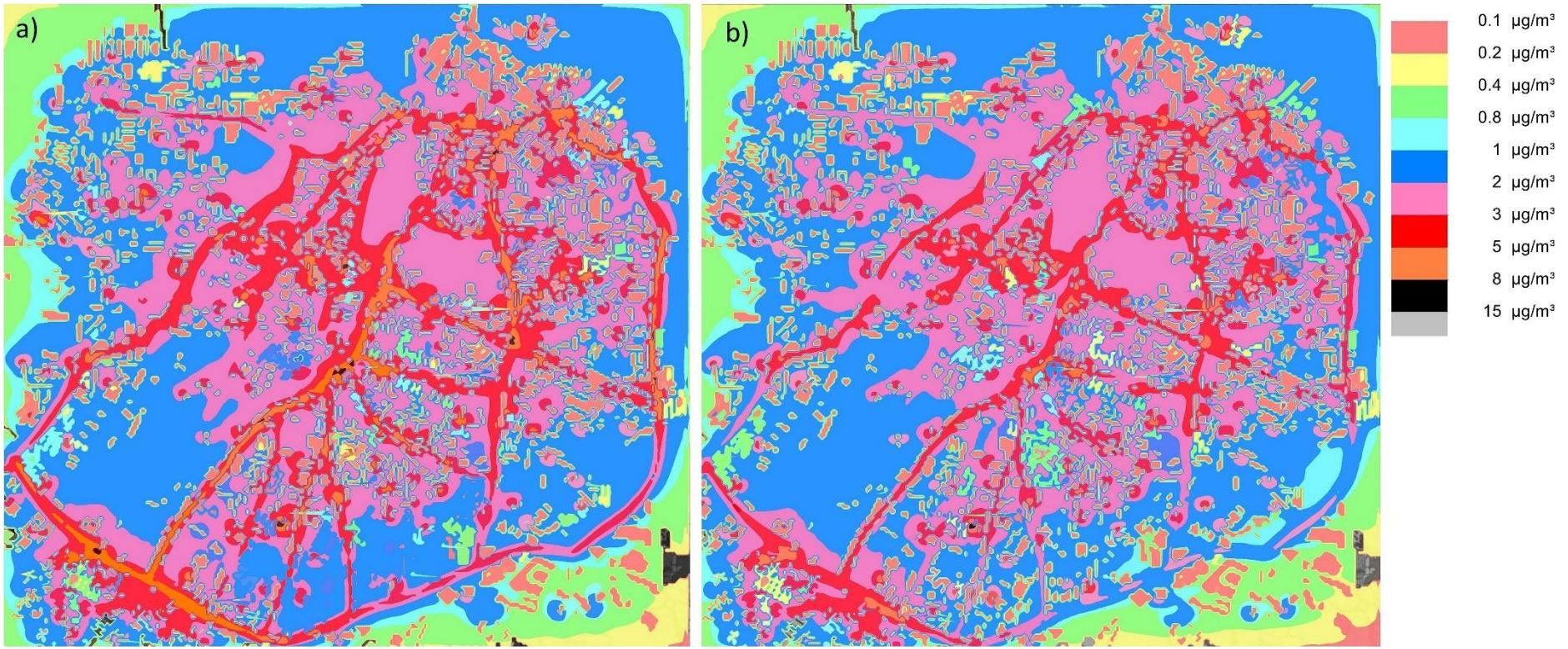

Fig. 4.33. The average concentration of $PM_{2.5}$ in Nicosia for a nine month period. Half left a) illustrates simulation for 2017 whereas map b) depicts $PM_{2.5}$ levels, assuming all vehicles were Euro 6 standard compatible, for the same 9-month duration.

Atmospheric particulate matter pollution could not vary as significantly as the levels of NO_x because a substantial amount of them originates from sea salt or dust storms (Department of Labour Inspection of Cyprus, 2019). Nevertheless, Nicosia's traffic junctions and neighbourhoods bordering the capital's roads experienced a decline in the concentration of both NO_x and $PM_{2.5}$. Nitrogen oxides on the contrary, clearly pointed out to the beneficial impact that the Euro 6 standard together with the phase-out of diesel passenger and light-duty vehicles are expected to have.

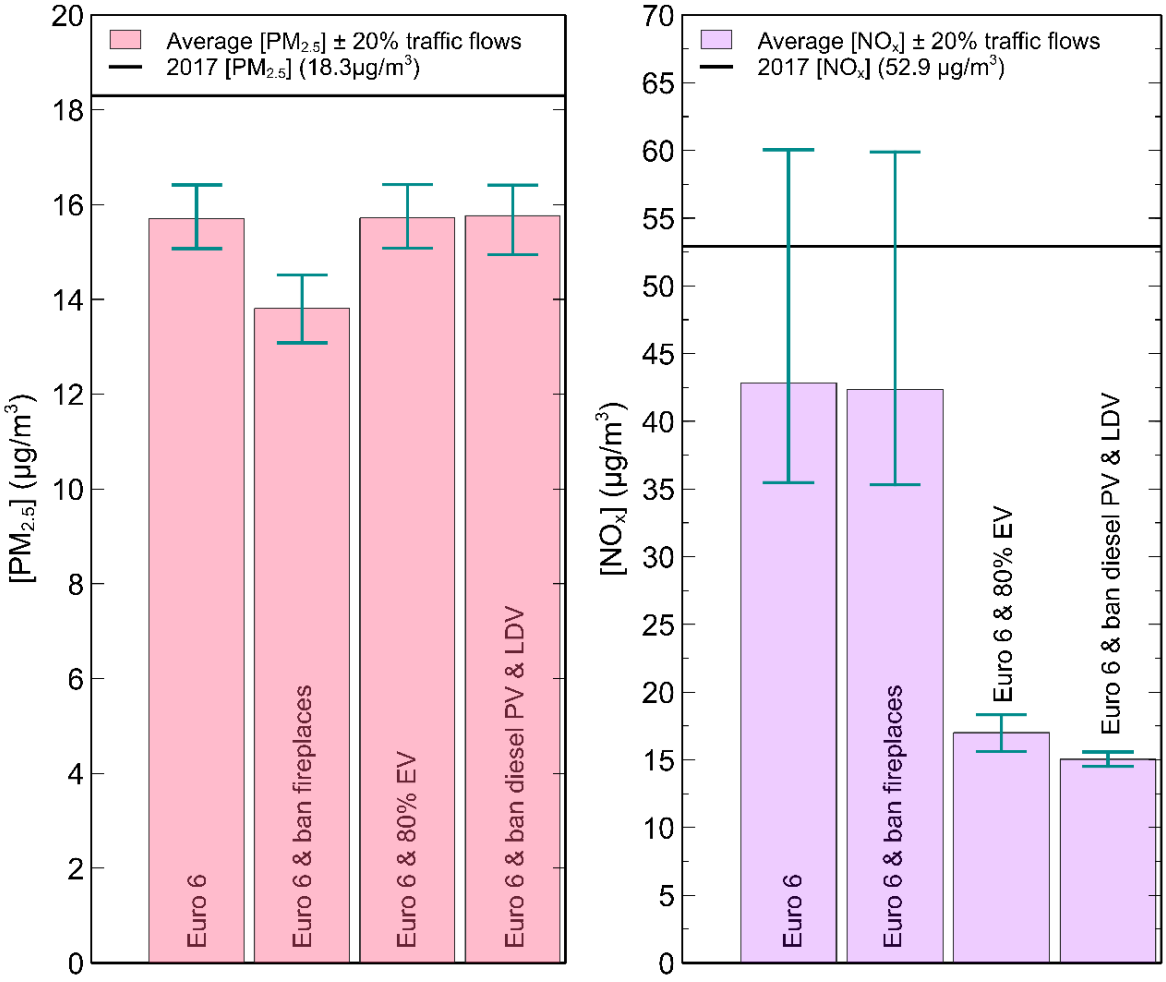

Fig. 4.34: Projected levels of $PM_{2.5}$ and NO_x compared to average 2017 concentrations (black line) for 4 distinct cases, namely, a) Euro 6, b) Euro 6 and ban fireplaces, c) Euro 6 and 80% EV and d) Euro 6 and ban diesel PV and LDV with traffic change of ±20%. Error bars indicate the change in traffic flows while the bar graph shows the change in concentrations in relation to 2017 traffic levels.

Eventually, in 2030, almost all of the vehicles will have to meet Euro 6 standards. In light of this policy change, 4 individual cases were formulated: a) no other

policies are to be implemented b) fireplaces are banned c) diesel LDV and PV will no longer be allowed on the streets and d) 80% of passenger vehicles are electric. Notably, in these 4 policies, traffic flows were adjusted by ±20%. Collectively, the results of all 8 cases are shown in Fig. 4.34.

It is striking to observe that the levels of particulate matter, in 2030, are expected to be well below the 2017 concentrations even with a surge in traffic flows. A vehicle fleet consisting entirely of Euro 6 compliant automobiles realised a 14% reduction in the amount of $PM_{2.5}$. Remarkably, extensive deployment of electric vehicles or a ban of diesel-powered vehicles did not attain a significant effect on atmospheric pollution levels. It is worth mentioning that forbidding fireplaces conjointly with a 20% traffic reduction led to a 30% decline in the concentration of $PM_{2.5}$ (Demetriou and Hadjistassou, 2022).

On the contrary, banning fireplaces did not appear to affect much the amount of nitrogen oxides. This occurs because burning 1 gigajoule of biomass liberates only 50g of NO_x compared to 820g of $PM_{2.5}$ (Kuenen and Trozzi, 2019). Naturally, changes in the traffic flow markedly affected nitrogen oxide emission. A 20% surge in traffic flows is accompanied by a dramatic elevation in NO_x emissions which will surpass the 2017 levels. On the other hand, a drop in traffic is poised to lower NO_x emissions by 20% compared to 2017 nitrogen oxides atmospheric levels. Ultimately, in the last two cases, Euro 6 and banning diesel PV and LDV constituted the most promising solution for containing environmental NO_x emissions (Demetriou and Hadjistassou, 2022).

4.8.3 Health impacts

Atmospheric pollutants have been implicated in increased mortality rates. In this research, various parameters from several sources were utilised to probe the health impacts of the scenarios and cases presented in subsection 3.2.4. Results pertaining to the total and cardiovascular related mortality rates tied to NO_x emissions and respiratory associated mortality rates for $PM_{2.5}$ are shown in Table 4.4 and Table 4.5.

Total mortality rates exhibited a wide variability based on the inputs from various studies (Cao *et al.*, 2011b; Atkinson *et al.*, 2014; Stockfelt *et al.*, 2015; European Environment Agency, 2020a) as it will be explained in the sequel. Nitrogen oxides triggered mortality rates were deduced from the simulated concentrations of NO_x, the population of Nicosia, the total mortality and the risk coefficient (β_i) Stockfelt

et al. (2015) and predicted an average of 238 premature deaths per year. Concurrently, Cao *et al.* (2011b) risk coefficient projected 124 more premature life losses compared to Stockfelt *et al.* (2015). Banning both non-Euro 6 vehicles and diesel-powered PV and LDV (scenario 9) could save up to 165 lives or 70% of premature deaths partially caused by NO_x emissions. Concerning the cardiovascular mortality risk, for NO_x, scenario 9 is poised to spare 45 human lives. Even though lowering the road speed limit to 30 km/hr could potentially reduce traffic accidents, still is expected to contribute to 8% more premature deaths compared to 2017 statistics (Demetriou and Hadjistassou, 2022).

Table 4.4: Overall and average cardiovascular causes of mortality, in Nicosia, from NO_x emissions compiled from a number of scenarios with a 95% confidence interval.

	Total Mortality [95% CI]	Total Mortality [95% CI]	Cardiovascular Mortality [95% CI]
Risk coefficient (β) from	(Stockfelt *et al.*, 2015)	(Cao *et al.*, 2011b)	(Cao *et al.*, 2011b)
2017	238 [83, 377]	124 [34, 201]	64 [17, 108]
Scenario			
1	258 [91, 407]	134 [37, 218]	69 [19, 117]
2	242 [85, 383]	126 [34, 204]	65 [18, 110]
3	209 [73, 333]	108 [29, 176]	56 [15, 96]
4	178 [62, 287]	92 [25, 150]	47 [13, 82]
5	200 [69, 320]	103 [28, 168]	53 [14, 91]
6	182 [63, 293]	94 [26, 153]	49 [13, 84]
7	161 [56, 260]	83 [22, 135]	43 [12, 74]
8	139 [48, 225]	71 [19, 117]	37 [10, 64]
9	73 [25, 119]	37 [10, 61]	19 [5, 34]

Meanwhile for particulate matter again, Atkinson *et al.* (2014) and the European Environment Agency (2020a) offer diverging estimates regarding premature mortalities, but when the preceding risk coefficient was incorporated in the dispersion model coupled with Euro 6 standards (scenario 5), 15% more lives could have been saved. Cardiovascular and respiratory mortality rates were incrementally affected by all measures such as banning diesel or allowing only Euro 6 vehicles. Henceforth, the premature mortalities obtained from 4 different cases, in 2030, will be compared with 2017 mortality statistics. Considering the uncertainties that surround Nicosia's future population changes, to the year 2030, and whatsmore, to enable the comparison with 2017 pollution levels, all mortality risks were averaged per 100,000 inhabitants, as

displayed in Table 4.6 and Table 4.7. Subsequently, the most and the least pollution-related scenarios for both $PM_{2.5}$ and NO_x are revealed in Fig. 4.35 and Fig. 4.36.

Table 4.5: Total and cardiovascular associated average mortality rates, for Nicosia, obtained from $PM_{2.5}$ levels with a 95% confidence interval.

	Total Mortality (95% CI)	Total Mortality (95% CI)	Cardiovascular Mortality (95% CI)	Cardiovascular Mortality (95% CI)	Respiratory Mortality (95% CI)
Risk coefficient (β) from	(European Environment Agency, 2020a)	(Atkinson *et al.*, 2014)	(Atkinson *et al.*, 2014)	(Cao *et al.*, 2011a)	(Atkinson *et al.*, 2014)
2017	180 [118, 237]	37 [14, 77]	23 [13, 34]	29 [9, 46]	11 [2, 21]
Scenario					
1	185 [122, 243]	39 [14, 79]	24 [13, 35]	30 [10, 48]	12 [2, 22]
2	181 [119, 238]	37 [14,77]	23 [13, 34]	29 [9, 47]	12 [2, 21]
3	175 [115, 229]	36 [13, 74]	23 [12, 33]	28 [9, 45]	11 [2, 20]
4	157 [103, 207]	32 [12, 67]	20 [11, 29]	25 [8, 40]	10 [1, 18]
5	155 [102, 204]	32 [12, 66]	20 [11, 29]	25 [8, 40]	10 [1, 18]
6	178 [117, 234]	37 [14, 76]	23 [13, 33]	28 [9, 46]	11 [2, 21]
7	175 [115, 230]	36 [13, 75]	23 [12, 33]	28 [9, 45]	11 [2, 21]
8	174 [114, 229]	36[13, 74]	22 [12, 32]	28 [9, 45]	11 [2, 20]
9	156 [102, 205]	32 [12, 66]	20 [11, 29]	25 [8, 40]	10 [1, 18]

Table 4.6: Aggregate and cardiovascular related mortality, in Nicosia, for NO_x cases per 100,000 inhabitants with a 95% confidence interval.

	Total Mortality (95% CI)	Total Mortality (95% CI)	Cardiovascular Mortality (95% CI)
Risk coefficient (β) from	(Stockfelt *et al.*, 2015)	(Cao *et al.*, 2011b)	(Cao *et al.*, 2011b)
2017	155 [55, 247]	81 [22, 131]	42 [11, 71]
Case			
1	180 [64, 283]	94 [26, 152]	48 [13, 82]
2	179 [63, 282]	94 [26, 152]	48 [13, 81]
3	58 [20, 95]	30 [8, 49]	15 [4, 27]
4	50 [17, 82]	25 [7, 42]	13[3, 23]
5	110 [38, 177]	56 [15, 92]	29 [8, 51]
6	109 [38, 175]	56 [15, 91]	29 [8, 50]
7	50 [17, 82]	25 [7, 42]	13 [3, 23]
8	46 [16, 76]	23 [6, 39]	12 [3, 21]

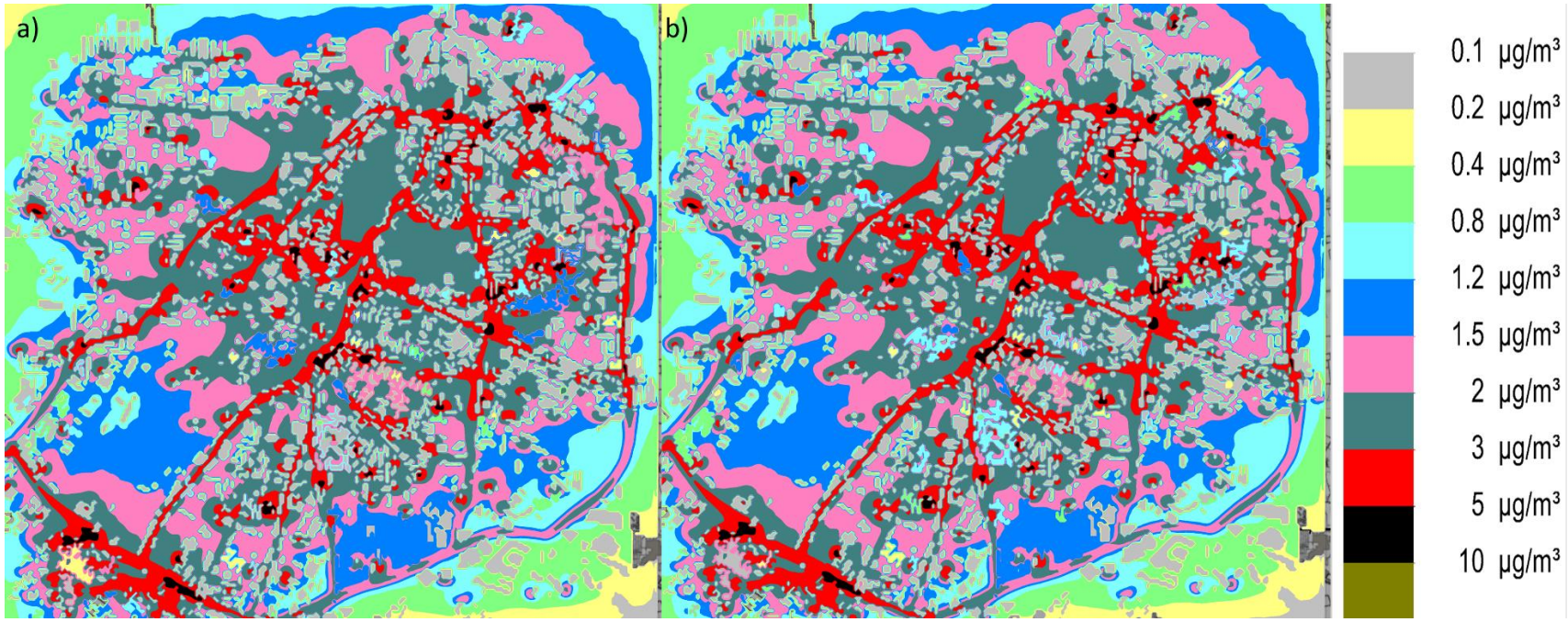

Fig. 4.35: The average concentration of $PM_{2.5}$ in Nicosia for a nine-month period. Half left map displays a) case 1, Euro 6 and 20% increase in traffic flows whereas map b) depicts case 6 $PM_{2.5}$ levels, assuming fireplaces and non-Euro 6 vehicles are banned and a 20% reduction in traffic flows, for the same 9-month time duration.

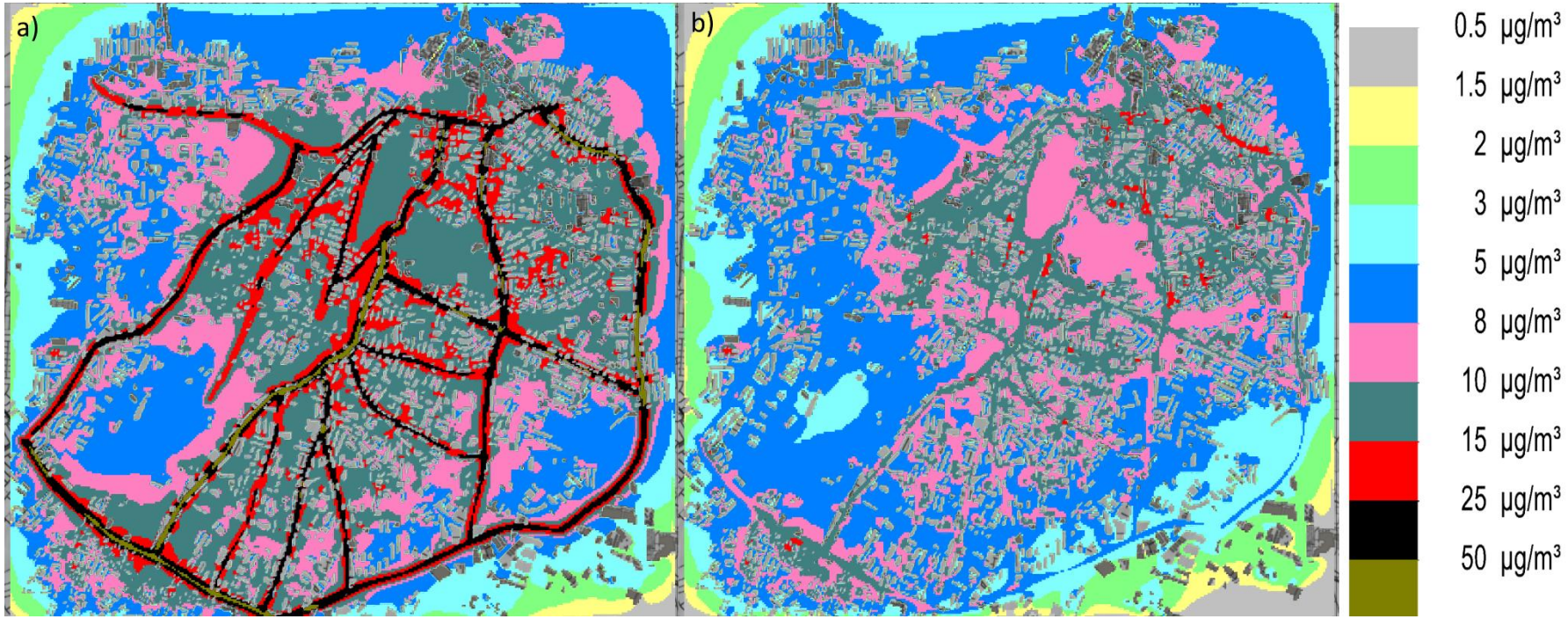

Fig. 4.36: The average concentration of NO_x in Nicosia for a nine-month time span. Half left map a) case 1, Euro 6 and a 20% increase in traffic flows whereas map b) shows case 6 NO_x levels, assuming diesel PV&LDV, as well as non-Euro 6 vehicles, are banned and a 20% reduction in traffic flows, for the same 9-month time window.

Table 4.7: Total and cardiovascular mortality, in Nicosia, for various $PM_{2.5}$ levels per 100,000 people for a 95% confidence interval.

	Total Mortality (95% CI)	Total Mortality (95% CI)	Cardiovascular Mortality (95% CI)	Cardiovascular Mortality (95% CI)	Respiratory Mortality (95% CI)
Risk coefficient (β) from	(European Environment Agency, 2020a)	(Atkinson *et al.*, 2014)	(Atkinson *et al.*, 2014)	(Cao *et al.*, 2011b)	(Atkinson *et al.*, 2014)
2017	118 [77, 155]	24 [9, 50]	15 [8, 22]	19 [6, 30]	7.5 [1.1, 13.8]
Case					
1	106 [69, 139]	22 [8, 45]	14 [7, 20]	17 [6, 27]	6.7 [1.1, 12.3]
2	94 [61, 124]	19 [7, 40]	12 [7, 17]	15 [5, 24]	6.0 [0.9, 11.0]
3	106 [69, 139]	22 [8, 45]	14 [7, 20]	17 [6, 27]	6.7 [1.1, 12.3]
4	106 [69, 139]	22 [8, 45]	14 [7, 20]	17 [6, 27]	6.7 [1.1, 12.3]
5	97 [38, 128]	20 [7, 41]	14 [7, 20]	15 [5, 25]	6.2 [0.9, 11.4]
6	85 [56, 112]	17 [6, 36]	11 [6, 16]	13 [4, 22]	5.4 [0.8, 9.9]
7	97 [64, 128]	20 [7, 41]	13 [7, 18]	15 [5, 25]	6.2 [0.9, 11.4]
8	97 [63, 127]	20 [7, 41]	12 [7, 18]	15 [5, 25]	6.2 [0.9, 11.4]

A possible road vehicle traffic increase of 20% could elicit a rise in mortality risk of up to 16% by 2030. Had fireplaces been banned, they would not have been expected to exert an appreciable influence on the NO_x associated mortality rates. Policies such as outlawing diesel passenger vehicles or an 80% electric passenger vehicle penetration, even accompanied by a boost in traffic flow, have the potential to cut NO_x attributable mortality by nearly 3 times compared to 2017 levels. Additionally, as expected, a 20% reduction in traffic flows compared to 2017 can contain total and cardiovascular mortality rates by 40%! Counter-intuitively, changes in traffic flows do not appreciably affect nitrogen oxides concentrations when diesel PV and LDV were prohibited (cases 3 and 7) or when electric passenger vehicles were rolled out ubiquitously (cases 4 and 8). Finally, even when the movement of vehicles at the main arteries was to intensify, banning diesel PV and LDV still constituted the best strategy for curbing traffic-related health mortality risks (Demetriou and Hadjistassou, 2022).

Euro 6 standards alone, even with a boost of 20% in traffic flows, could arrest particulate matter related mortality by at least 10% compared to 2017 records. If traffic

flow were to shrink by 20%, at least 17% of particulate matter tied deaths could have been avoided. Impressively, of all the policies banning fireplaces was the most promising solution for lowering overall mortality related risks by 28%. Lastly, based on the results presented herein, banning fireplaces had a more pronounced effect than mitigating traffic flows on particulate matter levels.

5 Concluding remarks

During the past decade, China motivated by the need to lower its reliance on coal as well as to mitigate the detrimental environmental effects on air quality from coal-burning has embraced renewable energy technologies. To test the assertion as to what degree can China diversify and decarbonise its electricity mix, four distinct energy scenarios were formulated. Two criteria proved instrumental to our analysis: (1) the lower the average electricity costs the better and (2) there is a drive to contain carbon emissions as much as possible in due course to 2050. Subsequently, we summarise and discuss the major findings:

- Even if China opts to exploit all of its renewable energy potential, it will be insufficient to meet the country's entire power generation needs during winter on renewables alone.
- The BAU power generation scenario is the most cost effective, at a maximum electricity burden of 0.082$/kWh. Interestingly, the Goals and the CFr scenarios with electricity costs at 0.106$/kWh and 0.102$/kWh, respectively, are 1.5 times as costly compared to the BAU case. Remarkably, the renewable energy scenario yields the most expensive electricity at 0.207$/kWh.
- Projections concerning the LULUCF negative emissions reveal that they will amount to 1.06Gt of CO_2 by 2050. Of all scenarios, only the CFr was found to yield net zero emissions. Specifically, the total electricity related CO_2 emissions are expected to drop by 0.46Gt in 2050.

Supported by the results from this investigation, the CFr scenario stands out as it utilises nuclear energy to meet baseload demand complemented by natural gas which fulfils peak shaving needs.

Cyprus as an isolated island from the grid connectivity perspective depicts a different picture compared to the Chinese electricity sector. Next, the major research contributions related to Cyprus are summarised and discussed:

- EU and national temperature goals. Cyprus can meet the obligation to help restrain temperature increase to 1.5℃ above the pre-industrial level. In order to accomplish this target, Cyprus will need to scale renewables to 11,920MW. If the mandatory goals

implemented by the EC were to restrain temperature increase to 2°C compared to the pre-industrial era, the Carbon Capture and Storage scenario is the preferred one. The Business As Usual and the Least Emission scenarios fail to lower the total emissions by at least 80% compared to 1990.

- Carbon tax. To match the electricity costs of the CCSc, the carbon tax price will need to surge to 155€/t of CO_2. If the carbon tax figure soars to 245€/t of CO_2, Cyprus will be better off at drawing all of its electricity from the fully renewable scenario (RESc).
- Carbon dioxide emissions were one of the focal points of this investigation. As mentioned, the renewables scenario attains zero emissions. Referring to the Carbon Capture and Storage scenario, it realises an exceptional reduction in emissions with the final footprint settling to 191kt of CO_2. This figure makes-up a 90% drop in emissions compared to 1990 which was the benchmark year.

Even though natural gas coupled with carbon capture and storage costs are extremely high compared to the costs in the absence of carbon capture, that technology helps minimise emissions at relatively moderate electricity costs.

In this study, the concentration of four pollutants, that is, CO, NO_x, $PM_{2.5}$ and PM_{10} were successfully estimated in the city centre of Nicosia, the capital of Cyprus, through GRAL, a dispersion model. Subsequently, for NO_x and $PM_{2.5}$, 9 different scenarios have been examined to mitigate their atmospheric levels. Furthermore, 8 cases were formulated in an effort to evaluate the impacts changes in traffic patterns could have under four distinct policies in 2030 where all of the vehicles will abide to Euro 6 standards. Lastly, for all the scenarios and cases individually, we reckoned the premature total mortality, cardiovascular and respiratory risks. In summary, the main findings and the major contributions of this research are summarised below:

- Validation of pollutant levels. The GRAL dispersion model was used to estimate all four pollutants for a period of 9 months from January 2017 until September 2017 where all pollutants were within the accepted limits for an hourly and daily rate.
- Formulation of scenarios and cases. Out of the nine policies, setting a speed limit of 30km/hr escalated both NO_x and $PM_{2.5}$ concentration by 9% and 3%, respectively. The

most effective scenario with a 71% reduction rate for NO_x was to ban both diesel PV and LDV while all vehicles abide with Euro 6 standards. Clearly, the Euro 6 standards scenario was the best policy for $PM_{2.5}$ as it diminished its average concentration by 14%. Comparing all 8 cases, prohibiting fireplace usage was the most effective policy with a 28% reduction for $PM_{2.5}$. Changes in traffic affect slightly $PM_{2.5}$. In contrast, NO_x concentration demonstrated a substantial variability of up to 25μg/m^3 for a traffic change of ±20% for both Euro 6 and ban fireplaces scenario. Banning diesel PV and LDV is the most promising strategy as it lessens NO_x concentration by 72%.

- Premature mortality risks in Nicosia. Depending on the input of each case for NO_x, it was estimated that during 2017 mortality was at 238 [83, 377] based on Stockfelt *et al.* (2015) and 124 [34, 201] with Cao *et al.* (2011b) coefficients. Cardiovascular mortality was found to be 64 [17, 108]. If Cyprus was to follow the scenario with the best reduction of NO_x, a total of 165 Nicosia's residents would not have died prematurely. The total particulate matter, the cardiovascular and the respiratory mortality were also calculated. In aggregate, 180 [118, 237], 29 [9, 46] and 11 [2, 21] deaths could be allocated to the total premature death toll, cardiovascular and respiratory mortality during 2017. Last but not least, the most promising policy along with Euro 6 only vehicles would be to ban fireplaces as it could result into a 30% reduction in mortality.

Finally, even though many policies could be introduced to minimise emissions, if only one policy was possible it would be to motivate citizens to buy new vehicles following the Euro 6 standards and withdraw their older vehicles. Perhaps government subsidies could catalyse the early adoption of Euro 6 vehicles.

6 Future research directions

Even though there are multiple ways to further develop the current research, two topics appear promising. First, evaluate the impacts of carbon monoxide on human health under different traffic scenarios. Second, examine various locations of China where environmental pollution has increased during the past years and examine its impact on both morbidity and mortality rates. Third, determine the effect of traffic reduction in Cyprus will have on hospital admission and mortality during the first and second phases of Covid-19 restrictions in the years 2020 and 2021, respectively. The period between March to May 2020 in Cyprus, merits high attention since travel restrictions were applied on the island due to COVID-19 measures.

Carbon monoxide is considered one of the most dangerous pollutants and under certain conditions, it can result in death. In this thesis, a validation of CO emissions using a dispersion model was made. Although the model's values were within the statistical limit of the parameters, the simulation underestimated the measured values. To realise further progress, it will be helpful to determine the origins of emissions which in turn is key to examining other possible emission pathways besides the transportation and heat residential sources.

Secondly, China during the past decade has increased dramatically its carbon footprint. In this thesis, it was only determined whether it is possible to have a carbon-neutral electricity sector along with LULUCF. It would be helpful to examine the impact on morbidity and mortality in areas where pollution has increased dramatically due to the utilisation of recently constructed coal powerplants, traffic increase or other causes.

Finally, the third line of investigation relates to the impact of the two different quarantine periods imposed in Cyprus from March until April 2020 and between December 2020 and February 2021. During these lock-down periods, the number of vehicles travelling through the major road arteries dropped precipitously. Based on the concentration of both nitrogen oxides and particulate matter that can be acquired from the Department of Labour Inspection coupled with traffic data which could be provided by the Department of Civil Works of Cyprus it is possible to estimate the impact vehicles had on

different levels of pollutants at that time. Moreover, based on the premature mortality rate determined by the Statistical Service of Cyprus the COVID restriction period can be compared with previous years and correlations can be drawn between traffic flows and the state of people's health. Understandably, lower transport emissions can benefit urban dwellers.

Appendix

A. China

A.1 Solar and wind potential

An estimate of China's wind and solar potential as well as the capacity factor for each province is shown in Table A1 and Table A2.

Table A1: Power generation potential of renewables for each Chinese province.

Province	Solar potential (MW)[a]	Wind Potential (MW)[b, c, d]	Wind capacity factor (%)[d, e]	Solar capacity factor (%)[e, f, g]
Anhui	12,500	9,030	21.41	13.66
Beijing	7,700	1,590	17.67	13.63
Chongqing	7,600	5,700	22.42	11.66
Fujian	32,000	40,250	24.40	10.64
Gansu	287,000	205,200	16.22	17.11
Guangdong	163,000	70,760	19.14	17.11
Guangxi	199,000	62,990	19.21	10.02
Guizhou	45,000	26,280	17.58	11.86
Hainan	91,000	15,400	19.54	11.08
Hebei	63,000	103,420	20.94	13.49
Heilongjiang	187,000	85,810	19.21	12.94
Henan	17,000	7,000	16.74	12.78
Hubei	15,000	15.710	19.70	10.61
Hunan	5,000	27,930	18.69	12.65
Inner Mongolia	1,398,000	1,305,300	21.51	18.29
Jiangsu	16,800	121,100	20.60	10.91
Jiangxi	57,800	22,480	18.90	10.47
Jilin	255,700	1,115,400	18.80	12.50
Liaoning	65,700	77,370	20.21	13.82
Ningxia	59,000	14,070	18.24	13.49
Qinghai	30,300	80,410	15.95	19.68
Shaanxi	93,300	35,060	17.56	16.20
Shandong	123,000	85,340	19.18	12.72
Shanghai	3,600	25,010	23.59	13.54
Shanxi	53,600	13,570	19.78	12.62
Sichuan	3,000	12,980	20.13	13.50
Tianjin	5,100	5,730	17.38	12.48
Tibet	1,300	830	12.47	22.31
Xinjiang	1,363,000	567,600	16.02	14.33
Yunnan	67,000	33,590	25.60	13.15
Zhejiang	20,000	63,280	20.56	10.95

Data sources: a: He and Kammen (2016), b: International Energy Agency (2012), c: Yang *et al.* (2017), d: He and Kammen (2014), e: National Energy Administration (2019b), f: National Energy Administration (2019a), g: (National Renewable Energy Laboratory, 2019).

Table A2: China's onshore wind potential. Source: International Energy Agency (2012).

Height above ground (m)	Wind power density ≥ 400W/m^2 (GW)	Wind power density ≥ 300W/m^2 (GW)	Wind power density ≥ 200W/m^2 (GW)
50	800	2,000	2,900
70	1,000	2,600	3,600
100	1,500	3,400	4,000

A.2 Levelised cost of electricity

The levelised cost of electricity for each scenario, spanning between 2017 to 2050, is subsequently outlined in the Business As Usual scenario.

The Business As Usual scenario

The calculation of the Levelised Cost of Electricity (LCOE) begins with the Business As Usual scenario. That is, Table A3, Table A4 and Table A5 show the magnitude of the LCOE for the interest rates of 5%, 7% and 10%, respectively. Tables are sorted in descending order based on the LCOE in 2050, with solar costs ($/kWh) appearing first.

Table A3: BAU LCOE for an interest rate of 5% ($/kWh).

Technology	Solar	Natural gas	Biomass	Coal	Wind	Nuclear	Hydro
Year				($/kWh)			
2017	0.136	0.064	0.073	0.055	0.066	0.053	0.040
2025	0.097	0.074	0.076	0.075	0.069	0.052	0.044
2030	0.091	0.076	0.077	0.073	0.069	0.052	0.039
2035	0.090	0.076	0.072	0.073	0.070	0.052	0.046
2040	0.089	0.077	0.072	0.072	0.070	0.052	0.041
2045	0.091	0.077	0.073	0.072	0.069	0.052	0.039
2050	0.088	0.077	0.075	0.072	0.069	0.052	0.039

Table A4: BAU LCOE for an interest rate of 7% ($/kWh).

Technology	Solar	Wind	Biomass	Natural gas	Coal	Nuclear	Hydro
Year				($/kWh)			
2017	0.146	0.077	0.077	0.068	0.059	0.060	0.049
2025	0.111	0.080	0.080	0.076	0.078	0.059	0.054
2030	0.104	0.080	0.082	0.078	0.077	0.059	0.048
2035	0.102	0.080	0.076	0.078	0.076	0.059	0.056
2040	0.102	0.080	0.076	0.078	0.076	0.059	0.050
2045	0.104	0.080	0.077	0.079	0.075	0.059	0.048
2050	0.101	0.080	0.079	0.079	0.075	0.059	0.047

Table A5: BAU LCOE for an interest rate of 10% ($/kWh).

Technology	Solar	Wind	Biomass	Natural gas	Coal	Nuclear	Hydro
Year				($/kWh)			
2017	0.165	0.095	0.084	0.074	0.065	0.072	0.063
2025	0.135	0.097	0.088	0.079	0.083	0.071	0.069
2030	0.125	0.098	0.091	0.081	0.082	0.071	0.062
2035	0.123	0.098	0.083	0.081	0.081	0.071	0.072
2040	0.122	0.008	0.082	0.081	0.081	0.071	0.065
2045	0.124	0.097	0.083	0.082	0.080	0.071	0.062
2050	0.120	0.097	0.086	0.082	0.080	0.071	0.061

Electricity prices from renewables surge with increasing interest rate. This rise in costs is attributed to the capital expenditures of renewables which are significant compared to fossil fuels and hydro. Thus, long distances between the RES production sites and the consumption areas coupled with relatively low capacity factors (Mills *et al.*, 2012; Lacerda and van den Bergh, 2016; Lin and Wu, 2017; Chen *et al.*, 2019) yield pronounced RES power costs. Natural gas and coal prices are expected to lie between 0.07 and 0.09 $/kWh, by the year 2050, or 1.3 times more competitive than solar power.

The goals scenario

Drawing on the Business As Usual scenario, the same calculations were also performed for the Goals scenario again for different interest rates (Table A6, Table A7 and Table A8).

Table A6: Goals LCOE for an interest rate of 5% ($/kWh).

Technology	Solar	Wind	Natural gas	Biomass	Coal	Nuclear	Hydro
Year				($/kWh)			
2017	0.136	0.066	0.064	0.073	0.055	0.053	0.040
2025	0.087	0.069	0.075	0.076	0.069	0.053	0.039
2030	0.085	0.070	0.075	0.077	0.068	0.053	0.039
2035	0.081	0.072	0.078	0.072	0.073	0.053	0.039
2040	0.086	0.074	0.079	0.072	0.074	0.053	0.038
2045	0.090	0.077	0.079	0.073	0.078	0.053	0.038
2050	0.095	0.080	0.089	0.075	0.084	0.053	0.038

Table A7: Goals LCOE for an interest rate of 7% ($/kWh).

Technology	Solar	Natural gas	Wind	Biomass	Coal	Nuclear	Hydro
Year				($/kWh)			
2017	0.146	0.068	0.077	0.077	0.059	0.060	0.049
2025	0.099	0.077	0.080	0.080	0.071	0.060	0.048
2030	0.096	0.077	0.080	0.082	0.070	0.060	0.048
2035	0.090	0.080	0.081	0.076	0.077	0.060	0.048
2040	0.095	0.081	0.083	0.076	0.077	0.060	0.047
2045	0.099	0.081	0.085	0.077	0.082	0.060	0.047
2050	0.104	0.093	0.089	0.079	0.089	0.060	0.047

Table A8: Goals LCOE for an interest rate of 10% ($/kWh).

Technology	Solar	Wind	Natural gas	Coal	Biomass	Nuclear	Hydro
Year				($/kWh)			
2017	0.165	0.095	0.074	0.065	0.084	0.072	0.063
2025	0.118	0.097	0.081	0.075	0.088	0.071	0.062
2030	0.114	0.096	0.080	0.075	0.091	0.071	0.062
2035	0.106	0.097	0.084	0.082	0.083	0.071	0.062
2040	0.110	0.098	0.084	0.083	0.082	0.071	0.060
2045	0.114	0.100	0.084	0.089	0.083	0.071	0.060
2050	0.119	0.104	0.099	0.097	0.086	0.071	0.060

Similarly, the Goals and the Business As Usual scenarios feature comparable LCOE values for most power generation technologies.

The coal free scenario

Like the Business As Usual and the Goals scenarios, the LCOE was obtained for the coal free scenario for the interest rates of 5%, 7% and 10%. The outcome of these calculations appears in Table A9, Table A10 and Table A11.

Table A9: CFr LCOE for an interest rate of 5% ($/kWh).

Technology	Natural gas	Solar	Wind	Biomass	Coal	Nuclear	Hydro
Year				($/kWh)			
2017	0.064	0.136	0.066	0.073	0.055	0.053	0.040
2025	0.098	0.087	0.069	0.076	0.075	0.052	0.039
2030	0.100	0.085	0.070	0.077	0.073	0.053	0.039
2035	0.101	0.081	0.072	0.072	0.080	0.052	0.039
2040	0.121	0.086	0.074	0.072	0.085	0.052	0.038
2045	0.108	0.090	0.077	0.073	0.085	0.054	0.038
2050	0.107	0.095	0.080	0.075	0.085	0.053	0.038

Table A10: CFr LCOE for an interest rate of 7% ($/kWh).

Technology	Natural gas	Solar	Wind	Biomass	Coal	Nuclear	Hydro
Year			($/kWh)				
2017	0.068	0.146	0.077	0.077	0.059	0.060	0.049
2025	0.103	0.099	0.080	0.080	0.079	0.059	0.048
2030	0.105	0.096	0.080	0.082	0.076	0.060	0.048
2035	0.107	0.090	0.081	0.076	0.084	0.059	0.048
2040	0.130	0.095	0.083	0.076	0.090	0.059	0.047
2045	0.114	0.099	0.085	0.077	0.090	0.062	0.047
2050	0.114	0.104	0.089	0.079	0.090	0.060	0.047

Table A11: CFr LCOE for an interest rate of 10% ($/kWh).

Technology	Natural gas	Solar	Wind	Coal	Biomass	Nuclear	Hydro
Year			($/kWh)				
2017	0.074	0.165	0.095	0.065	0.084	0.072	0.063
2025	0.112	0.118	0.097	0.084	0.088	0.071	0.062
2030	0.114	0.114	0.096	0.082	0.091	0.072	0.062
2035	0.116	0.106	0.097	0.091	0.083	0.071	0.062
2040	0.144	0.110	0.098	0.099	0.082	0.071	0.060
2045	0.125	0.114	0.100	0.099	0.083	0.074	0.060
2050	0.124	0.119	0.104	0.099	0.086	0.072	0.060

Two main distinctions exist between the Goals and CFr scenarios. The first one is that the LCOE of natural gas rises. This happens because natural gas power generation is used only for peak shaving purposes. The second difference is that coal's LCOE rises as time goes by compared to the Goals scenario. Apparently, this is attributed to the diminished utilisation of coal on a per year-to-year basis.

The renewables energy scenario

Finally, the LCOE results of the RESc scenario are listed next. Again, the same methodology of LCOE was used as in the case of the BAU, the Goals and the CFr scenarios. Table A12, Table A13 and Table A14 list all values in descending order based on the LCOE in 2050.

Table A12: RESc LCOE for an interest rate of 5% ($/kWh).

Technology	Coal	Hydrogen	Batteries	Solar	Wind	Natural gas	Biomass	Nuclear	Hydro
Year					($/kWh)				
2017	0.055	0.152	0.132	0.136	0.066	0.064	0.073	0.053	0.040
2025	0.072	0.152	0.132	0.074	0.070	0.075	0.076	0.060	0.039
2030	0.070	0.156	0.124	0.075	0.072	0.077	0.077	0.060	0.039
2035	0.086	0.161	0.131	0.084	0.080	0.077	0.072	0.058	0.042
2040	0.126	0.181	0.144	0.100	0.098	0.088	0.072	0.049	0.039
2045	0.103	0.197	0.148	0.111	0.105	0.086	0.073	0.058	0.039
2050	0.228	0.202	0.165	0.122	0.115	0.106	0.075	0.066	0.039

Table A13: RESc LCOE for an interest rate of 7% ($/kWh).

Technology	Coal	Hydrogen	Batteries	Solar	Wind	Natural gas	Biomass	Nuclear	Hydro
Year					($/kWh)				
2017	0.059	0.182	0.151	0.146	0.077	0.068	0.077	0.060	0.049
2025	0.075	0.182	0.151	0.082	0.080	0.077	0.080	0.069	0.048
2030	0.073	0.187	0.141	0.083	0.082	0.079	0.082	0.069	0.048
2035	0.091	0.191	0.148	0.091	0.089	0.079	0.076	0.067	0.052
2040	0.138	0.212	0.161	0.107	0.108	0.091	0.076	0.056	0.048
2045	0.111	0.231	0.164	0.119	0.115	0.089	0.077	0.066	0.048
2050	0.255	0.235	0.172	0.130	0.125	0.112	0.079	0.077	0.048

Table A14: RESc LCOE for an interest rate of 10% ($/kWh).

Technology	Coal	Hydrogen	Batteries	Solar	Wind	Natural gas	Nuclear	Biomass	Hydro
Year					($/kWh)				
2017	0.065	0.233	0.183	0.165	0.095	0.074	0.072	0.084	0.063
2025	0.079	0.233	0.183	0.096	0.096	0.095	0.084	0.088	0.062
2030	0.078	0.239	0.170	0.096	0.097	0.094	0.084	0.091	0.062
2035	0.100	0.240	0.175	0.104	0.103	0.096	0.081	0.083	0.062
2040	0.156	0.263	0.188	0.119	0.125	0.130	0.066	0.082	0.062
2045	0.124	0.285	0.190	0.131	0.131	0.106	0.080	0.083	0.062
2050	0.299	0.288	0.197	0.143	0.142	0.105	0.094	0.086	0.062

The renewables scenario differs significantly from other cases. Wind and solar energy reach the astronomical LCOE value of 0.14 $/kWh. The same happens with coal which will be used only a few hours per year and hence it reaches an LCOE of 0.292 $/kWh.

A.3 Future capital cost of storage

Table A15 summarises the assumed future capital costs of batteries Cole and Frazier (2019) and hydrogen (Schmidt *et al.*, 2019) storage. These hypothetical values indicate that, by 2050, the capital costs of hydrogen will shrink by 3 times compared to 2018. Thus, battery storage costs will drop by 59% (Table A15).

Table A15: Normalised cost reduction of battery and hydrogen storage.

Year	Battery normalised cost reduction	Hydrogen normalised cost reduction
2018	1	1
2025	0.65	0.66
2030	0.55	0.53
2035	0.51	0.44
2040	0.48	0.39
2045	0.44	0.36
2050	0.41	0.33
Source	Cole and Frazier (2019)	(Schmidt *et al.*, 2019)

B. Cyprus

B.1 Electricity sector assumptions

Table B1 and Table B2 display some population parameters and the predicted GDP growth rate, correspondingly. Moreover, the projection for tourist arrivals as well as the swine and cattle population are shown in Fig. B1 and Fig. B2, respectively. Lastly, Table B3 lists the values of the symbols that appear in equation (1), found in subsection 3.1.1. The preceding values were used to calculate the future vehicle fleet of Cyprus.

Table B1: Population related parameters until 2050.

Period (years)	Immigration rate (%)	Birth-death rate (%)
2019–2024	0.8	0.40
2025–2026	0.8	0.35
2027–2030	0.7	0.35
2031–2034	0.6	0.30
2035–2037	0.6	0.20
2038–2040	0.6	0.10
2041–2045	0.3	−0.10
2046–2050	0.3	−0.20

Table B2: Projected GDP growth rate of Cyprus between 2019 and 2050.

Period (years)	Growth rate (%)
2019–2030	2.5
2031–2039	2.0
2040–2050	1.0

Table B3: Parameters for estimating the future vehicle fleet size.

Symbol	Value
F	884,719
α_o	0.0711
α_1	−2.5986
MAPE	4.4%

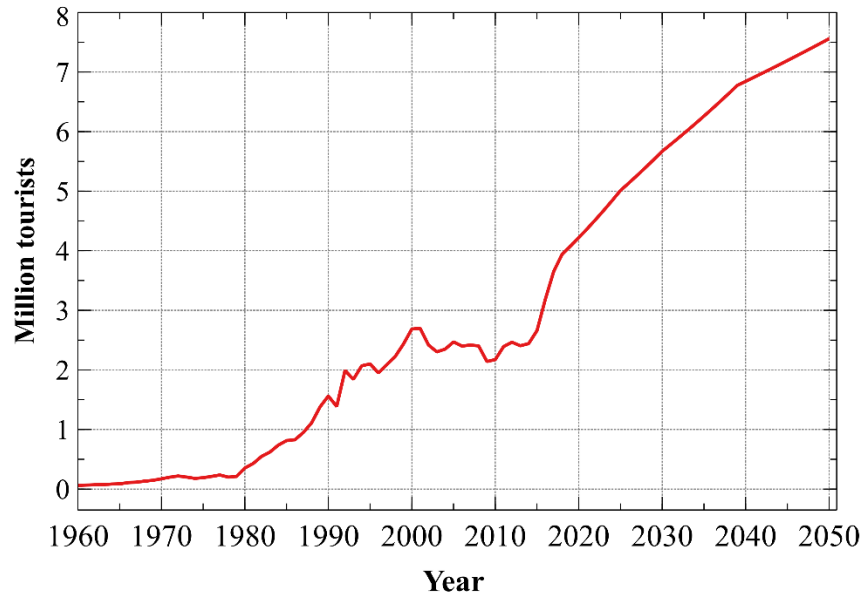

Fig. B1. Projection of the number of tourists from 2018 until 2050. Arrival flows until 2017 derive from the Cyprus Tourism Strategy (2017).

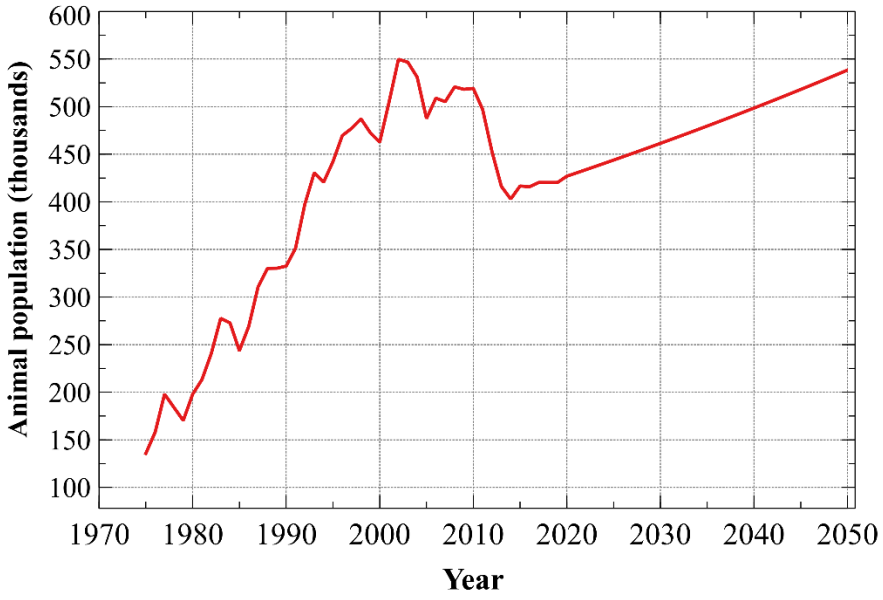

Fig. B2. Projection of the swine and cattle population as generated from the Holt-Winters method, from 2019–2050, based on data from CYSTAT (2019a).

B.2 Vehicle fleet age

Table B4 and Table B5 display the characteristics of the Cypriot vehicle fleet.

Table B4: Vehicle fleet fuel characteristics in Cyprus, during 2017 (CYSTAT, 2020b).

Type of vehicle	Total (number)	Petrol (%)	Diesel (%)	Electric	Other
Passenger	526.917	83.2	15.9	<0.1	0.9
Light Duty	95.705	0.3	99.7	<0.1	<0.1
Heavy Duty	12.040	0.1	99.9	–	–
Mopeds	12.156	99.3	–	0.7	–
Motorcycles	27.242	99.1	–	0.9	–
Buses	2.991	0.3	99.7	–	–
Others	20.787	2.5	97.5	<0.1	–

Table B5: Vehicle fleet age characteristics in Cyprus, during 2017 (CYSTAT, 2020b).

Vehicle age	<1 (%)	1–3 (%)	3–5 (%)	5–10 (%)	10–15 (%)	15–20 (%)	20–25 (%)	>25 (%)
Passenger	2.4	4.4	5.3	23.7	31.9	19.0	9.5	3.8
Light Duty	1.8	2.5	1.9	15.5	22.8	22.4	16.1	17.0
Heavy Duty	0.8	0.9	0.7	11.4	29.9	35.0	10.0	11.3
Mopeds	2.0	2.3	2.6	11.8	12.9	19.1	11.1	38.2
Motorcycles	7.1	10.9	9.3	30.2	18.2	10.2	5.7	8.4
Buses	1.6	3.5	1.1	19.3	26.2	24.9	12.1	11.3
Others	1.2	1.7	0.8	19.2	30.0	17.9	9.7	19.5
SUM	2.4	4.1	4.8	22.0	29.1	19.0	10.3	8.3

B.3 Vehicle and residential heat emissions equations

The equations used for estimating both exhaust and non-exhaust emissions are shown below:

$$ExhEf = \frac{a \times V^2 + \beta \times V + \gamma + \delta / V}{\varepsilon \times V^2 + \zeta \times V + \eta} \times (1 - RF) \quad (42)$$

$$nExhTyBr = \sum_j N_j \times EF_{TSP,j} \times fs_i \times S_S(V) \quad (43)$$

$$nExhRsw = \sum_{j} N_j \times EF_{TSP,\,j} \times fs_i \quad (44)$$

where $\alpha, \beta, \gamma, \delta, \varepsilon, \zeta,$ *and* η are parameters that relate to the type and age of vehicles, V is the vehicular velocity, RF is the reduction factor and $ExhEf$ the exhaust emission factor. Abbreviations $nExhTyBr$ and $nExhRsw$ correspond to the non-exhaust tyre, brake emissions and road surface wear emissions. Term N_j is the total number of vehicles from each category, fs_i corresponds to the mass fraction of the total suspended particles whose size is denoted by i. Parameters $EF_{TSP,\,j}$ and $S_s(V)$ are the mass emission factor and the correction factor of the mean vehicle speed. The values of each parameter listed above are detailed in Ntziachristos and Samaras (2019) for exhaust and for non-exhaust emissions (Ntziachristos and Samaras (2019)). Heat emission factors for both fireplaces and oil boilers are shown in Table B6.

Table B6: Heat emission factors (Kuenen and Trozzi, 2019).

Pollutant	Fireplace (g/GJ)	Oil boilers (g/kg fuel)
Carbon monoxide	4000	3.7
Nitrogen oxides	50	69
Particulate matter 2.5μm	820	1.5
Particulate matter 10μm	840	1.5

Hourly percentage usage of fireplaces and oil boilers are based on the ambient temperature profiles, as shown in Table B7.

Table B7: Hourly heat emission percentage factor (Bundesverband der deutschen Gas- und Wasserwirtschaft, 2006).

	Temperature								
Hour	T≤−5°C (%)	−15°C<T ≤−10 °C (%)	−10°C<T ≤−5°C (%)	−5°C<T ≤0°C (%)	0°C<T ≤5°C (%)	5°C<T ≤10°C (%)	10°C<T ≤15°C (%)	15°C<T ≤ 20°C (%)	20°C<T ≤25°C (%)
0	2.92	2.87	2.77	2.27	1.94	1.46	0.99	0.40	0.40
1	2.92	2.87	2.77	2.32	2.04	1.53	1.02	0.43	0.43
2	3.00	2.95	2.86	2.40	2.14	1.63	1.10	0.39	0.39
3	3.05	3.01	2.92	2.59	2.46	1.95	1.58	0.76	0.76
4	3.21	3.17	3.09	3.17	3.33	3.05	3.00	1.92	1.92
5	3.83	3.81	3.78	4.57	4.92	5.51	6.78	6.10	6.10
6	5.60	5.70	6.02	5.75	6.23	6.98	8.56	9.92	9.92
7	5.25	5.29	5.36	5.40	5.77	6.64	7.39	7.80	7.80
8	5.03	5.06	5.12	5.15	5.26	5.74	6.03	6.11	6.11
9	4.80	4.82	4.86	4.90	4.85	5.22	5.99	5.77	5.77
10	4.68	4.70	4.73	4.64	4.49	4.68	4.94	5.02	5.02
11	4.38	4.39	4.39	4.48	4.32	4.32	4.79	5.62	5.62
12	4.26	4.25	4.25	4.39	4.25	4.16	4.42	5.30	5.30
13	4.24	4.24	4.24	4.41	4.25	4.00	3.90	4.13	4.13
14	4.23	4.22	4.22	4.49	4.38	3.98	3.70	3.96	3.96
15	4.45	4.45	4.46	4.64	4.60	4.17	3.55	3.55	3.55
16	4.71	4.73	4.77	4.83	4.82	4.44	3.94	4.13	4.13
17	4.82	4.84	4.88	5.02	5.12	4.85	4.22	5.08	5.08
18	4.73	4.74	4.78	5.07	5.25	5.26	4.66	4.93	4.93
19	4.70	4.72	4.75	5.05	5.26	5.57	5.20	5.17	5.17
20	4.61	4.63	4.65	4.81	5.00	5.37	5.25	5.29	5.29
21	4.23	4.22	4.23	4.25	4.30	4.69	4.43	4.60	4.60
22	3.43	3.40	3.33	3.00	2.88	2.99	3.01	2.53	2.53
23	2.93	2.89	2.78	2.40	2.16	1.79	1.54	1.08	1.08

References

[1] Achilleos, S., Evans, J.S., Yiallouros, P.K., Kleanthous, S., Schwartz, J., Koutrakis, P., 2014. PM_{10} concentration levels at an urban and background site in Cyprus: the impact of urban sources and dust storms. Journal of the Air & Waste Management Association 64, 1352–1360, 10.1080/10962247.2014.923061.

[2] Aghahosseini, A., Bogdanov, D., Breyer, C., 2020. Towards sustainable development in the MENA region: Analysing the feasibility of a 100% renewable electricity system in 2030. Energy Strategy Reviews 28, 100466, https://doi.org/10.1016/j.esr.2020.100466.

[3] Alexopoulos, S., Hoffschmidt, B., 2010. Solar tower power plant in Germany and future perspectives of the development of the technology in Greece and Cyprus. Renewable Energy 35, 1352-1356, https://doi.org/10.1016/j.renene.2009.11.003.

[4] Almbauer, R.A., Oettl, D., Bacher, M., Sturm, P.J., 2000. Simulation of the air quality during a field study for the city of Graz. Atmospheric Environment 34, 4581–4594, https://doi.org/10.1016/S1352-2310(00)00264-8.

[5] Atkinson, R.W., Kang, S., Anderson, H.R., Mills, I.C., Walton, H.A., 2014. Epidemiological time series studies of $PM_{2.5}$ and daily mortality and hospital admissions: a systematic review and meta-analysis. Thorax 69, 660–5, 10.1136/thoraxjnl-2013-204492.

[6] Beddows, D.C.S., Harrison, R.M., 2021. PM_{10} and $PM_{2.5}$ emission factors for non-exhaust particles from road vehicles: Dependence upon vehicle mass and implications for battery electric vehicles. Atmospheric Environment
244, 117886, https://doi.org/10.1016/j.atmosenv.2020.117886.

[7] Berchet, A., Zink, K., Oettl, D., Brunner, J., Emmenegger, L., Brunner, D., 2017. Evaluation of high-resolution GRAMM–GRAL (v15.12/v14.8) NOx simulations over the city of Zürich, Switzerland. Geoscience Model Deviation 10, 3441–3459, 10.5194/gmd-10-3441-2017.

[8] Bloomberg New Energy Finance, 2019. New Energy Outlook 2019. https://about.bnef.com/new-energy-outlook/ (accessed January 22, 2020).

[9] Bodger P. S. , Tay, H.S., 1986. Trend extrapolation in long-term forecasting: An investigation using New Zealand electricity consumption data. Technological Forecasting and Social Change 30, 167–188, https://doi.org/10.1016/0040-1625(86)90018-1.

[10] Bodger, P.S., Tay, H.S., 1987. Logistic and energy substitution models for electricity forecasting: A comparison using New Zealand consumption data. Technological Forecasting and Social Change 31, 27–48, https://doi.org/10.1016/0040-1625(87)90021-7.

[11] Bogdanov, D., Breyer, C., 2016. North-East Asian Super Grid for 100% renewable energy supply: Optimal mix of energy technologies for electricity, gas and heat supply options. Energy Conversion and Management 112, 176–190, https://doi.org/10.1016/j.enconman.2016.01.019.

[12] Boningari, T., Smirniotis, P.G., 2016. Impact of nitrogen oxides on the environment and human health: Mn-based materials for the NOx abatement. Current Opinion in Chemical Engineering 13, 133-141, https://doi.org/10.1016/j.coche.2016.09.004.

[13] Boretti, A., Al Zubaidy, S., 2021. Reducing CO_2 emissions to a sustainable level in the Bahamas islands. Current Research in Environmental Sustainability 3, 100046, https://doi.org/10.1016/j.crsust.2021.100046.

[14] BP, 2018. BP Statistical Review of World Energy. https://www.bp.com/content/dam/bp/en/corporate/pdf/energy-economics/statistical-review/bp-stats-review-2018-full-report.pdf (accessed June 22, 2019).

[15] BP, 2019. Natural gas. https://on.bp.com/2lH89Od (accessed July 29, 2019).

[16] Budinis, S., Krevor, S., Dowell, N.M., Brandon, N., Hawkes, A., 2018. An assessment of CCS costs, barriers and potential. Energy Strategy Reviews 22, 61–81, https://doi.org/10.1016/j.esr.2018.08.003.

[17] Bukhary, S., Ahmad, S., Batista, J., 2018. Analyzing land and water requirements for solar deployment in the Southwestern United States. Renewable and Sustainable Energy Reviews 82, 3288–3305, https://doi.org/10.1016/j.rser.2017.10.016.

[18] Bundesverband der deutschen Gas- und Wasserwirtschaft, 2006. Praxisinformation P 2006/8 Gastransport/Betriebswirtschaft. Abwicklung von

Standardlastprofilen zur Belieferung nicht-leistungsgemessener Kunden. Technical Report. Berlin.
[19] Burnett, R.T., Pope, C.A., 3rd, Ezzati, M., Olives, C., Lim, S.S., Mehta, S., *et al.*, 2014. An integrated risk function for estimating the global burden of disease attributable to ambient fine particulate matter exposure. Environmental health perspectives 122, 397-403, 10.1289/ehp.1307049.
[20] Cao, J., Yang, C., Li, J., Chen, R., Chen, B., Gu, D., *et al.*, 2011a. Association between long-term exposure to outdoor air pollution and mortality in China: A cohort study. J. of Hazard. Mater. 186, 1594–1600, https://doi.org/10.1016/j.jhazmat.2010.12.036.
[21] Cao, J., Yang, C., Li, J., Chen, R., Chen, B., Gu, D., *et al.*, 2011b. Association between long-term exposure to outdoor air pollution and mortality in China: A cohort study. Journal of Hazardous Material 186, 1594–1600, https://doi.org/10.1016/j.jhazmat.2010.12.036.
[22] Carlsson, J., Fortes, M., de Marco, G., Giuntoli, J., Jakubcionis, M., Jäger-Waldau, A., *et al.*, 2014. ETRI 2014-Energy technology Reference Indicator Projections for 2010–2050; European Commission, Joint Research Centre. Publications Office of the European Union, http://publications.jrc.ec.europa.eu/repository/handle/JRC92496.
[23] Chen, A.A., Stephens, A.J., Koon Koon, R., Ashtine, M., Mohammed-Koon Koon, K., 2020. Pathways to climate change mitigation and stable energy by 100% renewable for a small island: Jamaica as an example. Renewable and Sustainable Energy Reviews 121, 109671, https://doi.org/10.1016/j.rser.2019.109671.
[24] Chen, W., Yang, M., Zhang, S., Andrews-Speed, P., Li, W., 2019. What accounts for the China-US difference in solar PV electricity output? An LMDI analysis. Journal of Cleaner Production 231, 161–170, https://doi.org/10.1016/j.jclepro.2019.05.207.
[25] Cheng, Y., Zhang, N., Kirschen, D.S., Huang, W., Kang, C., 2020. Planning multiple energy systems for low-carbon districts with high penetration of renewable energy: An empirical study in China. Applied Energy 261, 114390, https://doi.org/10.1016/j.apenergy.2019.114390.
[26] China, 2015. Enhanced Actions on Climate Change: China's Intended Nationally Determined Contributions. http://bit.ly/2KJKgjt (accessed June 2, 2019).
[27] China Energy Portal, 2018. Electricity & other energy statistics. http://bit.ly/2ZbfgN3 (accessed June 6, 2019).
[28] China Energy Portal, 2019. 2019 wind power installations and production by province. https://chinaenergyportal.org/en/2019-wind-power-installations-and-production-by-province/ (accessed July 11, 2020).
[29] China Energy Storage Alliance, 2019. CNESA's 2018 Year in Energy Storage. http://en.cnesa.org/latest-news/2019/2/23/cnesas-2018-year-in-energy-storage (accessed November 15, 2019).
[30] China Energy Storage Alliance, 2020. CNESA's 2020 Year in Energy Storage. https://static1.squarespace.com/static/55826ab6e4b0a6d2b0f53e3d/t/5f07d55aca644a4180546cd8/1594348898913/CNESA+White+Paper+2020+%28Summary%29.pdf (accessed February 12, 2021).
[31] China National Renewable Energy Centre, 2018. China Renewable Energy Outlook 2018. http://boostre.cnrec.org.cn/wp-content/uploads/2018/11/China-Renewable-Energy-Outlook-2018-Folder_ENG.pdf (accessed November 13, 2019).
[32] Chiodi, A., Gargiulo, M., Rogan, F., Deane, J.P., Lavigne, D., Rout, U.K., *et al.*, 2013. Modelling the impacts of challenging 2050 European climate mitigation targets on Ireland's energy system. Energy Policy 53, 169–189, https://doi.org/10.1016/j.enpol.2012.10.045.
[33] Chowdhury, S., Dey, S., 2016. Cause-specific premature death from ambient $PM_{2.5}$ exposure in India: Estimate adjusted for baseline mortality. Environment International 91, 283-90, 10.1016/j.envint.2016.03.004.
[34] Clack, C.T.M., Qvist, S.A., Apt, J., Bazilian, M., Brandt, A.R., Caldeira, K., *et al.*, 2017. Evaluation of a proposal for reliable low-cost grid power with 100% wind, water, and solar. Proceedings of the National Academy of Sciences 114, 6722–6727, https://doi.org/10.1073/pnas.1610381114.

[35] Cloete, S., Hirth, L., 2020. Flexible power and hydrogen production: Finding synergy between CCS and variable renewables. Energy 192, 116671, https://doi.org/10.1016/j.energy.2019.116671.
[36] CNPC Economics and Technology Research Institute, 2018. China Energy Outlook 2050. https://eneken.ieej.or.jp/data/8192.pdf (accessed July 21, 2019).
[37] Cohen, A.J., Brauer, M., Burnett, R., Anderson, H.R., Frostad, J., Estep, K., *et al.*, 2017. Estimates and 25-year trends of the global burden of disease attributable to ambient air pollution: an analysis of data from the Global Burden of Diseases Study 2015. The Lancet 389, 1907-1918, https://doi.org/10.1016/S0140-6736(17)30505-6.
[38] Cole, W.J., Frazier, A., 2019. Cost projections for utility-scale battery storage. https://www.nrel.gov/docs/fy19osti/73222.pdf (accessed July 12, 2020).
[39] Cyprus Department of Environment, 2018. Seventh National Communication & Third Biennial Report. https://unfccc.int/documents/64731 (accessed June 22, 2020).
[40] Cyprus Department of Environment, 2019. National Greenhouse Gas Inventory 2019. https://di.unfccc.int/ghg_profile_annex1 (accessed July 31, 2020).
[41] Cyprus Tourism Strategy, 2017. Cyprus Tourism Strategy. Prepared by THR: Innovative Tourism Advisors, Barcelona, March 2017. https://rb.gy/u5uiq6
[42] Cyprus Transmission System Operator, 2018. Archive total daily wind and solar farm generation. https://tsoc.org.cy/archive-total-daily-wind-and-solar-farm-generation/?startdt=-6days&enddt=today (accessed August 28, 2020).
[43] Cyprus Transmission System Operator, 2019a. Long term forecast. https://tsoc.org.cy/electrical-energy-generation/long-term-forecast/ (accessed August 2, 2020).
[44] Cyprus Transmission System Operator, 2019b. Penetration of renewable energy sources into the Cyprus electrical system. https://tsoc.org.cy/files/electrical-system/energy-generation-records/renewable/RES_PENETRATION_2017-2018_EN.pdf (accessed August 25, 2020).
[45] CYSTAT, 2011. Final energy consumption in households, 2009. shorturl.at/dwANU (accessed December 29, 2020).
[46] CYSTAT, 2013. Population Cencus. shorturl.at/ahDMQ (accessed December 30, 2020).
[47] CYSTAT, 2018. Statistical Abstract, Energy and Environment, Nicosia, Cyprus.
[48] CYSTAT, 2019a. Agriculture Statistics. https://www.mof.gov.cy/mof/cystat/statistics.nsf/agriculture_51main_en/agriculture_51main_en?OpenForm&sub=1&sel=1 (accessed November 20, 2020).
[49] CYSTAT, 2019b. Health and Hospital statistics, 2017. shorturl.at/dCGV8 (accessed January 2, 2021).
[50] CYSTAT, 2019c. Transport Statistics. https://www.mof.gov.cy/mof/cystat/statistics.nsf/services_72main_en/services_72main_en?OpenForm&sub=2&sel=2 (accessed August 10, 2020).
[51] CYSTAT, 2020a. Population summary data. shorturl.at/eCEM9 (accessed January 12, 2021).
[52] CYSTAT, 2020b. Road Transport 2017. shorturl.at/fsM58 (accessed December 30, 2020).
[53] Daggash, H.A., Heuberger, C.F., Mac Dowell, N., 2019. The role and value of negative emissions technologies in decarbonising the UK energy system. International Journal of Greenhouse Gas Control 81, 181-198, https://doi.org/10.1016/j.ijggc.2018.12.019.
[54] Davidson, M.R., Zhang, D., Xiong, W., Zhang, X., Karplus, V.J., 2016. Modelling the potential for wind energy integration on China's coal-heavy electricity grid. Nature Energy 1, 16086, https://doi.org/10.1038/nenergy.2016.86.
[55] de Oliveira, E.M., Cyrino Oliveira, F.L., 2018. Forecasting mid-long term electric energy consumption through bagging ARIMA and exponential smoothing methods. Energy 144, 776–788, https://doi.org/10.1016/j.energy.2017.12.049.
[56] Deivanayagam, R., 2017. Vehicle-to-grid Technology: Concept, Status, and Challenges. The Journal of Undergraduate Research at the University of Illinois at Chicago 10, 10.5210/jur.v10i1.8013.
[57] Demetriou, E., Hadjistassou, C., 2021. Can China decarbonize its electricity sector? Energy Policy 148, 111917, https://doi.org/10.1016/j.enpol.2020.111917.

[58] Demetriou, E., Hadjistassou, C., 2022. Lowering mortality risks in urban areas by containing atmospheric pollution. Environmental Research 211, 113096, https://doi.org/10.1016/j.envres.2022.113096.
[59] Demetriou, E., Mallouppas, G., Hadjistassou, C., 2021. Embracing carbon neutral electricity and transportation sectors in Cyprus. Energy 229, 120625, https://doi.org/10.1016/j.energy.2021.120625.
[60] Department of Labour Inspection of Cyprus, 2019. Annual Air Quality Technical Report 2017 Nicosia, Cyprus.
[61] Department of Labour Inspection of Cyprus, 2021. Air Quality in Cyprus. https://www.airquality.dli.mlsi.gov.cy/ (accessed February 7, 2021).
[62] Department of Public Works, 2018. Traffic Information. http://www.traffic4cyprus.org.cy/trafficapp/?wp=index-en (accessed July 22, 2020).
[63] Dilaver, Z., Hunt, L.C., 2011. Turkish aggregate electricity demand: An outlook to 2020. Energy 36, 6686–6696, https://doi.org/10.1016/j.energy.2011.07.043.
[64] Ding, S., Zhang, M., Song, Y., 2019. Exploring China's carbon emissions peak for different carbon tax scenarios. Energy Policy 129, 1245–1252, https://doi.org/10.1016/j.enpol.2019.03.037.
[65] Diyoke, C., 2019. A new approximate capacity factor method for matching wind turbines to a site: case study of Humber region, UK. International Journal of Energy and Environmental Engineering 10, 451–462, 10.1007/s40095-019-00320-5.
[66] Du, Y., Xu, X., Chu, M., Guo, Y., Wang, J., 2016. Air particulate matter and cardiovascular disease: the epidemiological, biomedical and clinical evidence. Journal of thoracic disease 8, E8-E19, 10.3978/j.issn.2072-1439.2015.11.37.
[67] EASE and Delta-EE, 2020. European market monitor on energy storage. https://ease-storage.eu/category/publications/emmes/ (accessed December 19, 2020).
[68] Ebisu, K., Malig, B., Hasheminassab, S., Sioutas, C., 2019. Age-specific seasonal associations between acute exposure to PM2.5 sources and cardiorespiratory hospital admissions in California. Atmospheric Environment 218, 117029, https://doi.org/10.1016/j.atmosenv.2019.117029.
[69] Egbo, M., 2017. Utility-scale energy storage systems for electricity: Pumped hydro energy storage (PHES). 10.13140/RG.2.2.13208.60169.
[70] Electricity Authority of Cyprus, 2020. Electricity sales by category. https://www.eac.com.cy/EN/EAC/FinancialInformation/Pages/StatisticalFigures.aspx (accessed November 24, 2020).
[71] Elyakova, I.D., Khristoforov, A., Elyakov, A.L., Danilova, L.I., Karataeva, T.A., Danilova, E.V., 2017. Forecast scenarios of world prices for natural gas. European Research Studies Journal 20, 284–297, https://doi.org/10.35808/ersj/835.
[72] Energy Information Administration, 2017a. International Energy Outlook 2017.
[73] Energy Information Administration, 2017b. Natural Gas Weekly Update. http://bit.ly/2KJxJws (accessed May 24, 2019).
[74] ENTSO-E transparency platform, 2019. Actual generation per production type. http://bit.ly/2P0Q7VB (accessed July 30, 2020).
[75] Ercan, F., Yenen, M., Fahrioglu, M., 2013. Method and Case Study for Wind Power Assessment in Cyprus. Renewable Energy Resources Symposium, 10.13140/2.1.2139.8400.
[76] EU Science Hub, 2018. Photovoltaic geographical information system. https://ec.europa.eu/jrc/en/pvgis (accessed October 21, 2020).
[77] European Commission, 2018. A clean planet for all. A European strategic long-term vision for a prosperous, modern, competitive and climate neutral economy. https://eur-lex.europa.eu/legal-content/EN/TXT/?uri=CELEX:52018DC0773 (accessed July 22, 2020).
[78] European Commission, 2019. The European Green Deal COM/2019/640 Final. https://eur-lex.europa.eu/legal-content/EN/TXT/?qid=1596443911913&uri=CELEX:52019DC0640#document2 (accessed October 29, 2020).
[79] European Commission, 2020. Commission Proposal for a Regulation: European Climate Law. European Commission Brussels, Belgium.

[80] European Commission, 2021. Delivering the European Green Deal. https://ec.europa.eu/clima/eu-action/european-green-deal/delivering-european-green-deal_en (accessed October 29, 2021).
[81] European Environment Agency, 2016. Average age of road vehicles per country. https://www.eea.europa.eu/data-and-maps/daviz/average-age-of-road-vehicles-6#tab-chart_1_filters=%7B%22rowFilters%22%3A%7B%7D%3B%22columnFilters%22%3A%7B%7D%3B%22sortFilter%22%3A%5B%22passenger_cars%22%5D%7D (accessed January 10, 2021).
[82] European Environment Agency, 2019a. Dieselisation (share of diesel cars in the total passenger car fleet) in Europe. shorturl.at/kR567 (accessed January 9, 2021).
[83] European Environment Agency, 2019b. EMEP/EEA Air Pollutant Emission Inventory Guidebook 2019. Section 1.A.3.b.I-iv Road Transport - Update Sep. 2020, EEA – European Environmental Agency, Copenhagen, Denmark (2016).
[84] European Environment Agency, 2020a. Air quality in Europe — 2020 report. https://www.eea.europa.eu/publications/air-quality-in-europe-2020-report (accessed 14 January, 2021).
[85] European Environment Agency, 2020b. National emissions reported to the Convention on Long-range Transboundary Air Pollution (LRTAP Convention). https://www.eea.europa.eu/data-and-maps/daviz/share-of-eea-33-emissions-5#tab-chart_1
[86] European Parliament, 2007. Regulation (EC) No 715/2007 of the European Parliament and of the Council of 20 June 2007 on type approval of motor vehicles with respect to emissions from light passenger and commercial vehicles (Euro 5 and Euro 6) and on access to vehicle repair and maintenance information. http://data.europa.eu/eli/reg/2007/715/oj (accessed November 22, 2021).
[87] Eurostat, 2020. Cooling and heating degree days by country. https://appsso.eurostat.ec.europa.eu/nui/show.do?dataset=nrg_chdd_a&lang=en (accessed November 21, 2020).
[88] Fabbi, S., Asaro, S., Bigi, A., Teggi, S., Ghermandi, G., 2019. Impact of vehicular emissions in an urban area of the Po valley by microscale simulation with the GRAL dispersion model. IOP Conference Series: Earth and Environmental Science 296, 012006, 10.1088/1755-1315/296/1/012006.
[89] Fallah-Shorshani, M., Shekarrizfard, M., Hatzopoulou, M., 2017. Evaluation of regional and local atmospheric dispersion models for the analysis of traffic-related air pollution in urban areas. Atmospheric Environment 167, 270–282, https://doi.org/10.1016/j.atmosenv.2017.08.025.
[90] Fan, J.-L., Wei, S., Yang, L., Wang, H., Zhong, P., Zhang, X., 2019. Comparison of the LCOE between coal-fired power plants with CCS and main low-carbon generation technologies: Evidence from China. Energy 176, 143–155, https://doi.org/10.1016/j.energy.2019.04.003.
[91] Fauré, E., Finnveden, G., Gunnarsson-Östling, U., 2019. Four low-carbon futures for a Swedish society beyond GDP growth. Journal of Cleaner Production 236, 117595, https://doi.org/10.1016/j.jclepro.2019.07.070.
[92] Ferbar Tratar, L., Mojškerc, B., Toman, A., 2016. Demand forecasting with four-parameter exponential smoothing. International Journal of Production Economics 181, 162–173, https://doi.org/10.1016/j.ijpe.2016.08.004.
[93] Fisher, J.C., Pry, R.H., 1971. A simple substitution model of technological change. Technological Forecasting and Social Change 3, 75–88, https://doi.org//10.1016/S0040-1625(71)80005-7.
[94] Forsell, N., Turkovska, O., Gusti, M., Obersteiner, M., Elzen, M., Havlik, P., 2016. Assessing the INDCs' land use, land-use change, and forest emission projections. Carbon Balance and Management 11, 26, https://doi.org/10.1186/s13021-016-0068-3.
[95] Fragkos, P., Tasios, N., Paroussos, L., Capros, P., Tsani, S., 2017. Energy system impacts and policy implications of the European Intended Nationally Determined Contribution and low-carbon pathway to 2050. Energy Policy 100, 216–226, https://doi.org/10.1016/j.enpol.2016.10.023.

[96] Friedlingstein, P., O'Sullivan, M., Jones, M.W., Andrew, R.M., Hauck, J., Olsen, A., *et al.*, 2020. Global Carbon Budget 2020. Earth System Science Data 12, 3269-3340, 10.5194/essd-12-3269-2020.
[97] Fu, X., Xiang, S., Liu, Y., Liu, J., Yu, J., Mauzerall, D.L., *et al.*, 2020. High-resolution simulation of local traffic-related NOx dispersion and distribution in a complex urban terrain. Environmental Pollution 263, 114390, https://doi.org/10.1016/j.envpol.2020.114390.
[98] García-Martos, C., Rodríguez, J., Sánchez, M.J., 2013. Modelling and forecasting fossil fuels, CO_2 and electricity prices and their volatilities. Applied Energy 101, 363–375, https://doi.org/10.1016/j.apenergy.2012.03.046.
[99] Global Modeling Assimilation Office, 2015. MERRA-2 tavg1_2d_slv_Nx: 2d, 1-Hourly, Time-Averaged, Single-Level, Assimilation, Single-Level Diagnostics V5. 12.4, Greenbelt, MD, USA, Goddard Earth Sciences Data and Information Services Center (GES DISC). (accessed July 10, 2020).
[100] Glynn, J., Gargiulo, M., Chiodi, A., Deane, P., Rogan, F., Ó Gallachóir, B., 2019. Zero carbon energy system pathways for Ireland consistent with the Paris Agreement. Climate Policy 19, 30–42, https://doi.org/10.1080/14693062.2018.1464893.
[101] Golden, R., Paulos, B., 2015. Curtailment of Renewable Energy in California and Beyond. The Electricity Journal 28, 36-50, https://doi.org/10.1016/j.tej.2015.06.008.
[102] Gorman, W., Mills, A., Wiser, R., 2019. Improving estimates of transmission capital costs for utility-scale wind and solar projects to inform renewable energy policy. Energy Policy 135, 110994, https://doi.org/10.1016/j.enpol.2019.110994.
[103] Gorre, J., Ortloff, F., van Leeuwen, C., 2019. Production costs for synthetic methane in 2030 and 2050 of an optimized Power-to-Gas plant with intermediate hydrogen storage. Applied Energy 253, 113594, https://doi.org/10.1016/j.apenergy.2019.113594.
[104] Green, C., 2000. Potential scale-related problems in estimating the costs of CO_2 mitigation policies. Climatic Change 44, 331–349, https://doi.org/10.1023/a:1005597112439.
[105] Grennfelt, P., Engleryd, A., Forsius, M., Hov, Ø., Rodhe, H., Cowling, E., 2020. Acid rain and air pollution: 50 years of progress in environmental science and policy. Ambio 49, 849-864, 10.1007/s13280-019-01244-4.
[106] Griliches, Z., 1957. Hybrid corn: An exploration in the economics of technological change. Econometrica 25, 501–522, https://doi.org/10.2307/1905380.
[107] Grineski, S.E., Herrera, J.M., Bulathsinhala, P., Staniswalis, J.G., 2015. Is there a Hispanic Health Paradox in sensitivity to air pollution? Hospital admissions for asthma, chronic obstructive pulmonary disease and congestive heart failure associated with NO_2 and $PM_{2.5}$ in El Paso, TX, 2005–2010. Atmospheric Environment 119, 314-321, https://doi.org/10.1016/j.atmosenv.2015.08.027.
[108] Handl, G., 2012. Declaration of the United Nations conference on the human environment (Stockholm Declaration), 1972 and the Rio Declaration on Environment and Development, 1992. United Nations Audiovisual Library of International Law 11, https://legal.un.org/avl/ha/dunche/dunche.html.
[109] Hanna, S., Chang, J., 2012. Acceptance criteria for urban dispersion model evaluation. Meteorology and Atmospheric Physics 116, 10.1007/s00703-011-0177-1.
[110] He, G., Avrin, A.-P., Nelson, J.H., Johnston, J., Mileva, A., Tian, J., *et al.*, 2016. SWITCH-China: A Systems Approach to Decarbonizing China's Power System. Environmental Science & Technology 50, 5467–5473, 10.1021/acs.est.6b01345.
[111] He, G., Kammen, D.M., 2014. Where, when and how much wind is available? A provincial-scale wind resource assessment for China. Energy Policy 74, 116–122, https://doi.org/10.1016/j.enpol.2014.07.003.
[112] He, G., Kammen, D.M., 2016. Where, when and how much solar is available? A provincial-scale solar resource assessment for China. Renewable Energy 85, 74–82, https://doi.org/10.1016/j.renene.2015.06.027.
[113] He, L., Zhang, S., Chen, Y., Ren, L., Li, J., 2018. Techno-economic potential of a renewable energy-based microgrid system for a sustainable large-scale residential community in Beijing, China. Renewable and Sustainable Energy Reviews 93, 631-641, https://doi.org/10.1016/j.rser.2018.05.053.

[114] Heidt, C., Jamet, M., Lambrecht, U., Bergk, F., Allekotte, M., 2017. Penetration of alternative fuels in Cyprus road and maritime sectors, ifeu – Institut für Energie- und Umweltforschung, Heidelberg.
[115] Helden, G.J.V., Muysken, J., 1983. Diseconomies of scale for plant utilisation in electricity generation. Economics Letters 11, 285–289, https://doi.org/10.1016/0165-1765(83)90149-0.
[116] Hernandez, R.R., Hoffacker, M.K., Murphy-Mariscal, M.L., Wu, G.C., Allen, M.F., 2015. Solar energy development impacts on land cover change and protected areas. Proceedings of the National Academy of Sciences 112, 13579, 10.1073/pnas.1517656112.
[117] Hooftman, N., Messagie, M., Coosemans, T., 2018. Analysis of the potential for electric buses, European Copper Institute, Brussel.
[118] Host, S., Honoré, C., Joly, F., Saunal, A., Le Tertre, A., Medina, S., 2020. Implementation of various hypothetical low emission zone scenarios in Greater Paris: Assessment of fine-scale reduction in exposure and expected health benefits. Environmental Research 185, 109405, https://doi.org/10.1016/j.envres.2020.109405.
[119] Huang, X., Zhang, H., Zhang, X., 2019a. Decarbonising electricity systems in major cities through renewable cooperation – A case study of Beijing and Zhangjiakou. Energy, https://doi.org/10.1016/j.energy.2019.116444.
[120] Huang, Y.W., Kittner, N., Kammen, D.M., 2019b. ASEAN grid flexibility: Preparedness for grid integration of renewable energy. Energy Policy 128, 711–726, https://doi.org/10.1016/j.enpol.2019.01.025.
[121] Iacovides, I., 2007. National Report on Monitoring progress and promotion of water demand management policies in Cyprus, Nicosia, Cyprus.
[122] International Energy Agency, 2011. World Energy Outlook 2011. https://doi.org/10.1787/weo-2011-en.
[123] International Energy Agency, 2012. China Wind Energy Development Roadmap 2050. https://doi.org/10.1787/9789264166752-en.
[124] International Energy Agency, 2017. World Energy Outlook 2017. https://doi.org/https://doi.org/10.1787/weo-2017-en.
[125] International Energy Agency, 2018. Energy storage tracking clean energy progress. http://bit.ly/2m230kb (accessed September 13, 2019).
[126] International Law Commission, 1956. Articles concerning the law of the sea with commentaries, Yearbook of the International Law Commission, p. 273.
[127] International Renewable Energy Agency, 2019. Renewable power generation costs in 2019. Report. https://www.irena.org/publications/2020/Jun/Renewable-Power-Costs-in-2019
[128] IRENA, 2012. Biomass for power generation. http://bit.ly/34sk8Qq (accessed June 21, 2019).
[129] IRENA, 2017. Electricity storage and renewables: costs and markets to 2030. http://bit.ly/2sw95sv (accessed July 31, 2019).
[130] Jacobson, M.Z., Delucchi, M.A., Cameron, M.A., Frew, B.A., 2015. Low-cost solution to the grid reliability problem with 100% penetration of intermittent wind, water, and solar for all purposes. Proceedings of the National Academy of Sciences 112, 15060–15065, https://doi.org/10.1073/pnas.1510028112.
[131] Ježek, I., Blond, N., Skupinski, G., Močnik, G., 2018. The traffic emission-dispersion model for a Central-European city agrees with measured black carbon apportioned to traffic. Atmospheric Environment 184, 177–190, https://doi.org/10.1016/j.atmosenv.2018.04.028.
[132] Joan, H., Omid, J., Hanan, A., Karin, H., David, W., 2015. Learning curve analysis of concentrated photovoltaic systems. Progress in Photovoltaics: Research and Applications 23, 1678–1686, https://doi.org/10.1002/pip.2567.
[133] Junginger M., Faaij A., Turkenburg W. C., 2005. Global experience curves for wind farms. Energy Policy 33, 133–150, https://doi.org/10.1016/S0301-4215(03)00205-2.
[134] Kahrl, F., Williams, J., Jianhua, D., Junfeng, H., 2011. Challenges to China's transition to a low carbon electricity system. Energy Policy 39, 4032–4041, https://doi.org/10.1016/j.enpol.2011.01.031.

[135] Kang, M., 2007. Generation cost assessment of an isolated power system with a fuzzy wind power generation model. IEEE Transactions on Energy Conversion 22, 397–404, https://doi.org/10.1109/TEC.2005.853786.
[136] Keeling, R.F., Keeling, C.D., 2021. Atmospheric Monthly In Situ CO_2 Data - Mauna Loa Observatory, Hawaii. In Scripps CO2 Program Data. UC San Diego Library Digital Collections. https://doi.org/10.6075/J08W3BHW (accessed February 22, 2021).
[137] Ketzel, M., Omstedt, G., Johansson, C., Düring, I., Aarnio, M., Oettl, D., *et al.*, 2007. Estimation and validation of $PM_{2.5}$/PM_{10} exhaust and non-exhaust emission factors for practical street pollution modelling. Atmospheric Environment 41, 9370-9385, 10.1016/j.atmosenv.2007.09.005.
[138] Khanna, N.Z., Zhou, N., Fridley, D., Ke, J., 2016. Quantifying the potential impacts of China's power-sector policies on coal input and CO2 emissions through 2050: A bottom-up perspective. Utilities Policy 41, 128–138, https://doi.org/10.1016/j.jup.2016.07.001.
[139] Kim, S., Koo, J., Lee, C.J., Yoon, E.S., 2012. Optimization of Korean energy planning for sustainability considering uncertainties in learning rates and external factors. Energy 44, 126–134, https://doi.org/10.1016/j.energy.2012.02.062.
[140] Klinge Jacobsen, H., Schröder, S.T., 2012. Curtailment of renewable generation: Economic optimality and incentives. Energy Policy 49, 663-675, https://doi.org/10.1016/j.enpol.2012.07.004.
[141] Kong, Z., Lu, X., Jiang, Q., Dong, X., Liu, G., Elbot, N., *et al.*, 2019. Assessment of import risks for natural gas and its implication for optimal importing strategies: A case study of China. Energy Policy 127, 11–18, https://doi.org/10.1016/j.enpol.2018.11.041.
[142] Koroneos, C., Fokaidis, P., Moussiopoulos, N., 2005. Cyprus energy system and the use of renewable energy sources. Energy 30, 1889-1901, https://doi.org/10.1016/j.energy.2004.11.011.
[143] Krausmann, E., 2017. Chapter 7 - Natech Risk and Its Assessment, in: Krausmann, E., Cruz, A.M., Salzano, E. (Eds.), Natech Risk Assessment and Management. Elsevier, pp. 105-118. https://doi.org/10.1016/B978-0-12-803807-9.00007-3.
[144] Krey, V., Masera, O., Bruckner, T., Cooke, R., Vanden, K., Haberl, H., *et al.*, 2014. Climate Change 2014: Mitigation. Annex II: Methodology and Metrics. In: Fifth Assessment Report of the Intergovernmental Panel on Climate Change.
[145] Kuenen, J., Trozzi, C., 2019. EMEP/EEA Emission Inventory Guidebook. Small combustion. https://www.eea.europa.eu/publications/emep-eea-guidebook-2019/part-b-sectoral-guidance-chapters/1-energy/1-a-combustion/1-a-4-small-combustion/view (accessed December 31, 2020).
[146] Kurz, C., Orthofer, R., Sturm, P., Kaiser, A., Uhrner, U., Reifeltshammer, R., *et al.*, 2014. Projection of the air quality in Vienna between 2005 and 2020 for NO_2 and PM_{10}. Urban Climate 10, 703–719, https://doi.org/10.1016/j.uclim.2014.03.008.
[147] Kythreotou, N., Mesimeris, T., 2020. Cyprus. National Inventory Report (NIR), Nicosia, May 2020.
[148] Kythreotou, N., Tassou, S.A., Florides, G., 2012. An assessment of the biomass potential of Cyprus for energy production. Energy 47, 253–261, https://doi.org/10.1016/j.energy.2012.09.023.
[149] Lacerda, J.S., van den Bergh, J.C.J.M., 2016. Mismatch of wind power capacity and generation: causing factors, GHG emissions and potential policy responses. Journal of Cleaner Production 128, 178–189, https://doi.org/10.1016/j.jclepro.2015.08.005.
[150] Langsdorf, S., 2011. EU Energy Policy: from the ECSC to the Energy Roadmap 2050, Brussels: Green European Foundation.
[151] Lazard, 2017. Lazard's Levelized cost of storage analysis— version 3.0. https://www.lazard.com/media/450338/lazard-levelized-cost-of-storage-version-30.pdf (accessed November 2, 2020).
[152] Li, C., Shi, H., Cao, Y., Wang, J., Kuang, Y., Tan, Y., *et al.*, 2015. Comprehensive review of renewable energy curtailment and avoidance: A specific example in China. Renewable and Sustainable Energy Reviews 41, 1067-1079, https://doi.org/10.1016/j.rser.2014.09.009.

[153] Li, X.-X., Liu, C.-H., Leung, D.Y.C., Lam, K.M., 2006. Recent progress in CFD modelling of wind field and pollutant transport in street canyons. Atmospheric Environment 40, 5640-5658, https://doi.org/10.1016/j.atmosenv.2006.04.055.
[154] Li, X., Tan, Y., Liu, X., Liao, Q., Sun, B., Cao, G., *et al.*, 2020. A cost-benefit analysis of V2G electric vehicles supporting peak shaving in Shanghai. Electric Power Systems Research 179, 106058, https://doi.org/10.1016/j.epsr.2019.106058.
[155] Li, X., Yao, X., 2020. Can energy supply-side and demand-side policies for energy saving and emission reduction be synergistic?--- A simulated study on China's coal capacity cut and carbon tax. Energy Policy 138, 111232, https://doi.org/10.1016/j.enpol.2019.111232.
[156] Liang, Z., Chen, H., Chen, S., Lin, Z., Kang, C., 2019. Probability-driven transmission expansion planning with high-penetration renewable power generation: A case study in northwestern China. Applied Energy 255, 113610, https://doi.org/10.1016/j.apenergy.2019.113610.
[157] Liang, Z., Chen, H., Wang, X., Chen, S., Zhang, C., 2020. Risk-Based Uncertainty Set Optimization Method for Energy Management of Hybrid AC/DC Microgrids With Uncertain Renewable Generation. IEEE Transactions on Smart Grid 11, 1526–1542, 10.1109/TSG.2019.2939817.
[158] Lilliestam, J., Pitz-Paal, R., 2018. Concentrating solar power for less than USD 0.07 per kWh: finally the breakthrough? Renewable Energy Focus 26, 17–21, https://doi.org/10.1016/j.ref.2018.06.002.
[159] Lin, B., Wu, W., 2017. Cost of long distance electricity transmission in China. Energy Policy 109, 132–140, https://doi.org/10.1016/j.enpol.2017.06.055.
[160] Ling, H., Candice Lung, S.-C., Uhrner, U., 2020. Micro-scale particle simulation and traffic-related particle exposure assessment in an Asian residential community. Environmental Pollution 266, 115046, https://doi.org/10.1016/j.envpol.2020.115046.
[161] Liu, H., Brown, T., Andresen, G.B., Schlachtberger, D.P., Greiner, M., 2019a. The role of hydro power, storage and transmission in the decarbonization of the Chinese power system. Applied Energy 239, 1308–1321, https://doi.org/10.1016/j.apenergy.2019.02.009.
[162] Liu, J., Kiesewetter, G., Klimont, Z., Cofala, J., Heyes, C., Schöpp, W., *et al.*, 2019b. Mitigation pathways of air pollution from residential emissions in the Beijing-Tianjin-Hebei region in China. Environment International 125, 236-244, https://doi.org/10.1016/j.envint.2018.09.059.
[163] Liu, S., Bie, Z., Lin, J., Wang, X., 2018. Curtailment of renewable energy in Northwest China and market-based solutions. Energy Policy 123, 494-502, https://doi.org/10.1016/j.enpol.2018.09.007.
[164] Liu, Z., Guan, D., Crawford-Brown, D., Zhang, Q., He, K., Liu, J., 2013. Energy policy: A low-carbon road map for China. Nature 500, 143–145, https://doi.org/10.1038/500143a.
[165] Machado, M.M., de Sousa, M.C.S., Hewings, G., 2016. Economies of scale and technological progress in electric power production: The case of Brazilian utilities. Energy Economics 59, 290–299, https://doi.org/10.1016/j.eneco.2016.06.017.
[166] Maesano, C.N., Morel, G., Matynia, A., Ratsombath, N., Bonnety, J., Legros, G., *et al.*, 2020. Impacts on human mortality due to reductions in PM_{10} concentrations through different traffic scenarios in Paris, France. Science of The Total Environment 698, 134257, https://doi.org/10.1016/j.scitotenv.2019.134257.
[167] Mahmood, F.H., Resen, A.K., Khamees, A.B., 2020. Wind characteristic analysis based on Weibull distribution of Al-Salman site, Iraq. Energy Reports 6, 79–87, https://doi.org/10.1016/j.egyr.2019.10.021.
[168] Mathews, J.A., Tan, H., 2013. The transformation of the electric power sector in China. Energy Policy 52, 170–180, https://doi.org/10.1016/j.enpol.2012.10.010.
[169] Mbelambela, E.P., Hirota, R., Eitoku, M., Muchanga, S.M.J., Kiyosawa, H., Yasumitsu-Lovell, K., *et al.*, 2017. Occupation exposed to road-traffic emissions and respiratory health among Congolese transit workers, particularly bus conductors, in Kinshasa: a cross-sectional study. Environmental Health and Prevention Medicine 22, 11, 10.1186/s12199-017-0608-9.
[170] Mechleri, E., Fennell, P.S., Dowell, N.M., 2017. Optimisation and evaluation of flexible operation strategies for coal- and gas-CCS power stations with a multi-period design approach.

International Journal of Greenhouse Gas Control 59, 24-39, https://doi.org/10.1016/j.ijggc.2016.09.018.
[171] Menz, F.C., Seip, H.M., 2004. Acid rain in Europe and the United States: an update. Environmental Science & Policy 7, 253-265, https://doi.org/10.1016/j.envsci.2004.05.005.
[172] Mesimeris, T., Kythreotou, N., Partasides, G., Piripitsi, K., Karapitta-Zachariadou, K., Hadjinikolaou, N., *et al.*, 2020. Cyprus draft integrated national energy and climate plan for the period 2021–2030. https://ec.europa.eu/energy/sites/ener/files/documents/cyprus_draftnecp.pdf. (accessed June 01, 2020).
[173] Middleton, N., Yiallouros, P., Kleanthous, S., Kolokotroni, O., Schwartz, J., Dockery, D.W., *et al.*, 2008. A 10-year time-series analysis of respiratory and cardiovascular morbidity in Nicosia, Cyprus: the effect of short-term changes in air pollution and dust storms. Environmental Health 7, 39, 10.1186/1476-069X-7-39.
[174] Milando, C.W., Batterman, S.A., 2018. Operational evaluation of the RLINE dispersion model for studies of traffic-related air pollutants. Atmospheric Environment 182, 213–224, https://doi.org/10.1016/j.atmosenv.2018.03.030.
[175] Mills, A., Phadke, A., Wiser, R., 2011. Exploration of resource and transmission expansion decisions in the Western Renewable Energy Zone initiative. Energy Policy 39, 1732–1745, https://doi.org/10.1016/j.enpol.2011.01.002.
[176] Mills, A., Wiser, R., Porter, K., 2012. The cost of transmission for wind energy: A review of transmission planning studies. Renewable and Sustainable Energy Reviews 16, https://doi.org/10.1016/j.rser.2011.07.131.
[177] Ministry of Foreign Affairs of the People's Republic of China, 2020. Statement by H.E. Xi Jinping President of the People's Republic of China At the General Debate of the 75th Session of The United Nations General Assembly. https://www.fmprc.gov.cn/mfa_eng/zxxx_662805/t1817098.shtml (accessed February 05, 2021).
[178] Mohamed, Z., Bodger, P., 2005. A variable asymptote logistic (VAL) model to forecast electricity consumption. https://doi.org/10.1504/IJCAT.2005.006937.
[179] Mohammad, N., Mohamad Ishak, W.W., Mustapa, S.I., Ayodele, B.V., 2021. Natural Gas as a Key Alternative Energy Source in Sustainable Renewable Energy Transition: A Mini Review. 9, 10.3389/fenrg.2021.625023.
[180] Mohsin, M., Rao, K.V.S., 2018. Estimation of Weibull Distribution Parameters and Wind Power Density for Wind Farm Site at Akal at Jaisalmer in Rajasthan, 2018 3rd International Innovative Applications of Computational Intelligence on Power, Energy and Controls with their Impact on Humanity (CIPECH), pp. 1-6. 10.1109/CIPECH.2018.8724170.
[181] Mongird, K., Viswanathan, V.V., Balducci, P.J., Alam, M.J.E., Fotedar, V., Koritarov, V.S., *et al.*, 2019. Energy Storage Technology and Cost Characterization Report. Pacific Northwest National Lab. (PNNL), Richland, WA (United States).
[182] Morabito, A., Hendrick, P., 2019. Pump as turbine applied to micro energy storage and smart water grids: A case study. Applied Energy 241, 567-579, https://doi.org/10.1016/j.apenergy.2019.03.018.
[183] Murray, P., Orehounig, K., Grosspietsch, D., Carmeliet, J., 2018. A comparison of storage systems in neighbourhood decentralized energy system applications from 2015 to 2050. Applied Energy 231, 1285–1306, https://doi.org/10.1016/j.apenergy.2018.08.106.
[184] NASA's Goddard Institute for Space Studies, 2018. Global Temperature. https://climate.nasa.gov/vital-signs/global-temperature/ (accessed 29.12.2017).
[185] National Bureau of Statistics of China, 2018. China Statistical Yearbook 2018. http://bit.ly/2k2YjpH (accessed July 23, 2019).
[186] National Bureau of Statistics of China, 2019. National data. http://data.stats.gov.cn/english/easyquery.htm?cn=A01 (accessed July 21, 2019).
[187] National Energy Administration, 2019a. Photovoltaic power generation statistics for 2018. http://www.nea.gov.cn/2019-03/19/c_137907428.htm (accessed June 10, 2019).
[188] National Energy Administration, 2019b. Wind power grid connection operation in 2018 http://www.nea.gov.cn/2019-01/28/c_137780779.htm (accessed 10 August 2019).

[189] National Renewable Energy Laboratory, 2019. Solar Resource Data. https://pvwatts.nrel.gov/pvwatts.php (accessed October 30, 2020).
[190] Nicholas, M., 2019. Estimating electric vehicle charging infrastructure costs across major US metropolitan areas. International Council on Clean Transportation, https://theicct.org/publications/charging-cost-US
[191] Ntziachristos, L., Samaras, Z., 2019. EMEP/EEA Emission Inventory Guidebook. 1.A.3.b.i-iv Road transport 2019. https://www.eea.europa.eu/publications/emep-eea-guidebook-2019/part-b-sectoral-guidance-chapters/1-energy/1-a-combustion/road-transport-appendix-4-emission/view (accessed December 26, 2020).
[192] Nuclear Energy Agency, International Energy Agency, OECD, 2015. Projected costs of generating electricity 2015. OECD Publishing, Paris. http://bit.ly/2Z3Uhk1.
[193] Oettl, D., 2014. High Resolution maps of Nitrogen dioxide for the province of Styria, Austria. International Journal of Environment and Pollution 54, 137–146, 10.1504/IJEP.2014.065114.
[194] Oettl, D., 2015. Quality assurance of the prognostic, microscale wind-field model GRAL 14.8 using wind-tunnel data provided by the German VDI guideline 3783-9. Journal of Wind Engineering and Industrial Aerodynamics 142, 104–110, https://doi.org/10.1016/j.jweia.2015.03.014.
[195] Oettl, D., 2020. Documentation of the Lagrangian Particle Model GRAL - Version 20.01.
[196] Oettl, D., Almbauer, R.A., Sturm, P.J., Pretterhofer, G., 2003. Dispersion modelling of air pollution caused by road traffic using a Markov Chain–Monte Carlo model. Stochastic Environmental Research and Risk Assessment 17, 58–75, 10.1007/s00477-002-0120-6.
[197] Oettl, D., Kropsch, M., Mandl, M., 2018. Odour assessment in the vicinity of a pig-fatting farm using field inspections (EN 16841-1) and dispersion modelling. Atmospheric Environment 181, 54–60, https://doi.org/10.1016/j.atmosenv.2018.03.029.
[198] Oettl, D., Kukkonen, J., Almbauer, R.A., Sturm, P.J., Pohjola, M., Härkönen, J., 2001. Evaluation of a Gaussian and a Lagrangian model against a roadside data set, with emphasis on low wind speed conditions. Atmospheric Environment 35, 2123–2132, https://doi.org/10.1016/S1352-2310(00)00492-1.
[199] Oettl, D., Uhrner, U., 2011. Development and evaluation of GRAL-C dispersion model, a hybrid Eulerian–Lagrangian approach capturing NO–NO_2–O_3 chemistry. Atmospheric Environment 45, 839–847, https://doi.org/10.1016/j.atmosenv.2010.11.028.
[200] Oyewo, A.S., Aghahosseini, A., Ram, M., Lohrmann, A., Breyer, C., 2019. Pathway towards achieving 100% renewable electricity by 2050 for South Africa. Solar Energy 191, 549–565, https://doi.org/10.1016/j.solener.2019.09.039.
[201] Pasquill, F., 1961. The Estimation of The Dispersion of Windborne Material. Meteorology Magazine 90, 33, https://ci.nii.ac.jp/naid/10016363794/en/
[202] Penev, M., Hunter, C., Eichman, J.D., 2019. Energy Storage: Days of Service Sensitivity Analysis. https://www.nrel.gov/docs/fy19osti/73520.pdf (accessed 30 June, 2020).
[203] Penman, J., Gytarsky, M., Hiraishi, T., Krug, T., Kruger, D., Pipatti, R., *et al.*, 2003. Good practice guidance for land use, land-use change and forestry. Institute for Global Environmental Strategies, Kanagawa Prefecture.
[204] Pérez Sánchez, J., Aguillón Martínez, J.E., Mazur Czerwiec, Z., Zavala Guzmán, A.M., 2019. Theoretical assessment of integration of CCS in the Mexican electrical sector. Energy 167, 828-840, https://doi.org/10.1016/j.energy.2018.11.043.
[205] Petsas, C., Stylianou, M., Zorpas, A., Agapiou, A., 2020. Measurements of Local Sources of Particulates with a Portable Monitor along the Coast of an Insular City. Sustainability 13, 261, https://doi.org/10.3390/su13010261.
[206] Poullikkas, A., 2013. Optimization analysis for pumped energy storage systems in small isolated power systems. Journal of Power Technologies 93, 78–89, http://papers.itc.pw.edu.pl/index.php/JPT/article/view/382.
[207] Prentice, I.C., Farquhar, G., Fasham, M., Goulden, M., Heimann, M., Jaramillo, V., *et al.*, 2001. The carbon cycle and atmospheric carbon dioxide. Cambridge University Press.

[208] Psyllides, G., 2021. Electricity from natural gas projected from 2023. https://cyprus-mail.com/2021/11/09/electricity-from-natural-gas-projected-from-2023/ (accessed January 09, 2022).
[209] Pukkila, T., Koreisha, S., Kallinen, A., 1990. The identification of ARMA models. Biometrika 77, 537–548, https://doi.org/10.1093/biomet/77.3.537.
[210] Qi, T., Zhang, X., Karplus, V.J., 2014. The energy and CO_2 emissions impact of renewable energy development in China. Energy Policy 68, 60–69, https://doi.org/10.1016/j.enpol.2013.12.035.
[211] Rafiei, M., Sturm, P.J., 2018. Modeling of carbon monoxide dispersion around the urban tunnel portals. Global Journal of Environmental Science and Management 4, 359–372, 10.22034/GJESM.2018.03.009.
[212] Raub, J.A., Mathieu-Nolf, M., Hampson, N.B., Thom, S.R., 2000. Carbon monoxide poisoning — a public health perspective. Toxicology 145, 1-14, https://doi.org/10.1016/S0300-483X(99)00217-6.
[213] Rehman, S., Al-Hadhrami, L.M., Alam, M.M., 2015. Pumped hydro energy storage system: A technological review. Renewable and Sustainable Energy Reviews 44, 586-598, https://doi.org/10.1016/j.rser.2014.12.040.
[214] Ritchie, H., 2020. Sector by sector: where do global greenhouse gas emissions come from? https://ourworldindata.org/ghg-emissions-by-sector (accessed February 22, 2021).
[215] Ritchie, H., Roser, M., 2020a. CO_2 and greenhouse gas emissions. https://ourworldindata.org/co2/country/cyprus#citation (accessed June 22, 2021).
[216] Ritchie, H., Roser, M., 2020b. Emissions by sector. https://ourworldindata.org/emissions-by-sector (accessed February 22, 2021).
[217] Rodrigues Teixeira, A.C., Borges, R.R., Machado, P.G., Mouette, D., Dutra Ribeiro, F.N., 2020. PM emissions from heavy-duty trucks and their impacts on human health. Atmospheric Environment 241, 117814, https://doi.org/10.1016/j.atmosenv.2020.117814.
[218] Rubin, E.S., Davison, J.E., Herzog, H.J., 2015. The cost of CO_2 capture and storage. International Journal of Greenhouse Gas Control 40, 378–400, https://doi.org/10.1016/j.ijggc.2015.05.018.
[219] Sahu, S.K., Sharma, S., Zhang, H., Chejarla, V., Guo, H., Hu, J., *et al.*, 2020. Estimating ground level PM2.5 concentrations and associated health risk in India using satellite based AOD and WRF predicted meteorological parameters. Chemosphere 255, 126969, https://doi.org/10.1016/j.chemosphere.2020.126969.
[220] Saidi, M.S., Rismanian, M., Monjezi, M., Zendehbad, M., Fatehiboroujeni, S., 2014. Comparison between Lagrangian and Eulerian approaches in predicting motion of micron-sized particles in laminar flows. Atmospheric Environment 89, 199-206, https://doi.org/10.1016/j.atmosenv.2014.01.069.
[221] Santiago, J.L., Sanchez, B., Quaassdorff, C., de la Paz, D., Martilli, A., Martín, F., *et al.*, 2020. Performance evaluation of a multiscale modelling system applied to particulate matter dispersion in a real traffic hot spot in Madrid (Spain). Atmospheric Pollution Research 11, 141-155, https://doi.org/10.1016/j.apr.2019.10.001.
[222] Santos, M.J., Ferreira, P., Araújo, M., 2016. A methodology to incorporate risk and uncertainty in electricity power planning. Energy 115, 1400–1411, https://doi.org/10.1016/j.energy.2016.03.080.
[223] Sarasketa-Zabala, E., Gandiaga, I., Martinez-Laserna, E., Rodriguez-Martinez, L.M., Villarreal, I., 2015. Cycle ageing analysis of a $LiFePO_4$/graphite cell with dynamic model validations: Towards realistic lifetime predictions. Journal of Power Sources 275, 573–587, https://doi.org/10.1016/j.jpowsour.2014.10.153.
[224] Sarigiannis, D.A., Karakitsios, S.P., Kermenidou, M.V., 2015. Health impact and monetary cost of exposure to particulate matter emitted from biomass burning in large cities. Science of The Total Environment 524-525, 319–330, https://doi.org/10.1016/j.scitotenv.2015.02.108.
[225] Schenkeveld, M.M., Morris, R., Budding, B., Helmer, J., Innanen, S., 2004. Seawater and brackish water desalination in the Middle East, North Africa and Central Asia, Annex 6, Cyprus, World Bank.

[226] Schlömer S, Bruckner, T., Fulton, L., Hertwich E., McKinnon A., Perczyk D., *et al.*, 2014. Climate Change 2014: Mitigation of Climate Change: Working Group III Contribution to the IPCC Fifth Assessment Report.
[227] Schmidt, O., Melchior, S., Hawkes, A., Staffell, I., 2019. Projecting the Future Levelized Cost of Electricity Storage Technologies. Joule 3, 81–100, https://doi.org/10.1016/j.joule.2018.12.008.
[228] Sferra, F., Krapp, M., Roming, N., Schaeffer, M., Malik, A., Hare, B., *et al.*, 2019. Towards optimal 1.5° and 2 °C emission pathways for individual countries: A Finland case study. Energy Policy 133, 110705, https://doi.org/10.1016/j.enpol.2019.04.020.
[229] Shu, Y., Zhu, L., Yuan, F., Kong, X., Huang, T., Cai, Y.D., 2016. Analysis of the relationship between PM2.5 and lung cancer based on protein-protein interactions. Combinatorial Chemistry & High Throughput Screening 19, 100-8, 10.2174/1386207319666151110123345.
[230] Soltani, S.M., Fennell, P.S., Mac Dowell, N., 2017. A parametric study of CO_2 capture from gas-fired power plants using monoethanolamine (MEA). International Journal of Greenhouse Gas Control 63, 321-328, https://doi.org/10.1016/j.ijggc.2017.06.001.
[231] Sousa Santos, G., Sundvor, I., Vogt, M., Grythe, H., Haug, T.W., Høiskar, B.A., *et al.*, 2020. Evaluation of traffic control measures in Oslo region and its effect on current air quality policies in Norway. Transport Policy 99, 251–261, https://doi.org/10.1016/j.tranpol.2020.08.025.
[232] State Council the People's Republic of China, 2018. China sets forestry development goals for 2050. http://bit.ly/33JFN7H (accessed July 10, 2019).
[233] State Forestry Administration of China, 2014. Forestry in China, Bejing, China.
[234] Stockfelt, L., Andersson, E.M., Molnár, P., Rosengren, A., Wilhelmsen, L., Sallsten, G., *et al.*, 2015. Long term effects of residential NOx exposure on total and cause-specific mortality and incidence of myocardial infarction in a Swedish cohort. Environmental Research 142, 197–206, https://doi.org/10.1016/j.envres.2015.06.045.
[235] Sturm, P., Kurz, C., Vogelsang, S., Oettl, D., Hafner, W., 2007. Effects of PM_{10} emission abatement strategies on air quality in urban and rural areas, Book Effects of PM_{10} emission abatement strategies on air quality in urban and rural areas.
[236] Taliotis, C., Rogner, H., Ressl, S., Howells, M., Gardumi, F., 2017. Natural gas in Cyprus: The need for consolidated planning. Energy Policy 107, 197–209, https://doi.org/10.1016/j.enpol.2017.04.047.
[237] Tang, J., McNabola, A., Misstear, B., 2020. The potential impacts of different traffic management strategies on air pollution and public health for a more sustainable city: A modelling case study from Dublin, Ireland. Sustainable Cities and Society 60, 102229, https://doi.org/10.1016/j.scs.2020.102229.
[238] Tarlock, D., 2009. History of Environmental Law, Environmental Laws Their Enforcement, pp. 42-64.
[239] Tezel-Oguz, M.N., Sari, D., Ozkurt, N., Keskin, S.S., 2020. Application of reduction scenarios on traffic-related NOx emissions in Trabzon, Turkey. Atmospheric Pollution Research 11, 2379–2389, https://doi.org/10.1016/j.apr.2020.06.014.
[240] The Wind Power, 2020. National report China. https://www.thewindpower.net/store_market_en.php?id_crep=9 (accessed July 11,2020).
[241] The World Bank, 2019. Solar resource maps of Cyprus. https://solargis.com/maps-and-gis-data/download/cyprus (accessed February 6, 2021).
[242] Timmers, V.R.J.H., Achten, P.A.J., 2016. Non-exhaust PM emissions from electric vehicles. Atmospheric Environment 134, 10–17, https://doi.org/10.1016/j.atmosenv.2016.03.017.
[243] Tischer, V., Fountas, G., Polette, M., Rye, T., 2019. Environmental and economic assessment of traffic-related air pollution using aggregate spatial information: A case study of Balneário Camboriú, Brazil. Journal of Transport & Health 14, 100592, https://doi.org/10.1016/j.jth.2019.100592.
[244] Tobollik, M., Keuken, M., Sabel, C., Cowie, H., Tuomisto, J., Sarigiannis, D., *et al.*, 2016. Health impact assessment of transport policies in Rotterdam: Decrease of total traffic and

increase of electric car use. Environmental Research 146, 350–358, https://doi.org/10.1016/j.envres.2016.01.014.
[245] Tsangari, H., Paschalidou, A.K., Kassomenos, A.P., Vardoulakis, S., Heaviside, C., Georgiou, K.E., *et al.*, 2016. Extreme weather and air pollution effects on cardiovascular and respiratory hospital admissions in Cyprus. Science of The Total Environment 542, 247–253, https://doi.org/10.1016/j.scitotenv.2015.10.106.
[246] Tsoukalas, I., Efstratiadis, A., Makropoulos, C., 2018. Stochastic Periodic Autoregressive to Anything (SPARTA): modeling and simulation of cyclostationary processes with arbitrary marginal distributions. Water Resources Research 54, 161–185, https://doi.org/10.1002/2017WR021394.
[247] Tu, Q., Betz, R., Mo, J., Fan, Y., Liu, Y., 2019. Achieving grid parity of wind power in China – Present levelized cost of electricity and future evolution. Applied Energy 250, 1053–1064, https://doi.org/10.1016/j.apenergy.2019.05.039.
[248] United Nations Climate Change, 2020. National Inventory Submissions. https://unfccc.int/ghg-inventories-annex-i-parties/2020 (accessed January 21, 2021).
[249] United Nations Framework Convention on Climate Change, 2015. Intended Nationally Determined Contributions as communicated by Parties. http://bit.ly/31Vd3at (accessed June 12, 2019).
[250] United Nations Framework Convention on Climate Change, 2021. What is the Kyoto Protocol? https://unfccc.int/kyoto_protocol (accessed February 22, 2021).
[251] United Nations Treaty Series, 2015. Paris Agreement. https://treaties.un.org/pages/ViewDetails.aspx?src=TREATY&mtdsg_no=XXVII-7-d&chapter=27&clang=_en (accessed January 30, 2021).
[252] Veratti, G., Fabbi, S., Bigi, A., Lupascu, A., Tinarelli, G., Teggi, S., *et al.*, 2020. Towards the coupling of a chemical transport model with a micro-scale Lagrangian modelling system for evaluation of urban NOx levels in a European hotspot. Atmospheric Environment 223, 117285, https://doi.org/10.1016/j.atmosenv.2020.117285.
[253] Vetter, M., Lux, S., 2016. Chapter 11 - Rechargeable Batteries with Special Reference to Lithium-Ion Batteries, in: Letcher, T.M. (Ed.), Storing Energy. Elsevier, Oxford, pp. 205-225. https://doi.org/10.1016/B978-0-12-803440-8.00011-7.
[254] Viana, M., Rizza, V., Tobías, A., Carr, E., Corbett, J., Sofiev, M., *et al.*, 2020. Estimated health impacts from maritime transport in the Mediterranean region and benefits from the use of cleaner fuels. Environment International 138, 105670, https://doi.org/10.1016/j.envint.2020.105670.
[255] Vogel, R.W., McMartin, D.E., 1991. Probability plot goodness-of-fit and skewness estimation procedures for the Pearson type 3 distribution. Water Resources Research 27, 3149–3158, https://doi.org/10.1029/91wr02116.
[256] Vougiouklakis, Y., Struss, B., Zachariadis, T., Michopoulos, A., 2017. A draft energy efficiency strategy for Cyprus up to 2020, 2030 and 2050, Deliverable 1.1. Deutsche Gesellschaft für Internationale Zusammenarbeit (GIZ) GmbH.
[257] Walford, L.A., 1946. A new graphic method of describing the growth of animals. The Biological Bulletin 90, 141–147, https://doi.org/10.2307/1538217.
[258] Wang, F., Qiu, X., Cao, J., Peng, L., Zhang, N., Yan, Y., *et al.*, 2021. Policy-driven changes in the health risk of $PM_{2.5}$ and O_3 exposure in China during 2013–2018. Science of The Total Environment 757, 143775, https://doi.org/10.1016/j.scitotenv.2020.143775.
[259] Wang, Q., Wang, J., He, M.Z., Kinney, P.L., Li, T., 2018. A county-level estimate of PM2.5 related chronic mortality risk in China based on multi-model exposure data. Environment International 110, 105-112, https://doi.org/10.1016/j.envint.2017.10.015.
[260] Wang, Y., Zhang, D., Ji, Q., Shi, X., 2020. Regional renewable energy development in China: A multidimensional assessment. Renewable and Sustainable Energy Reviews 124, 109797, https://doi.org/10.1016/j.rser.2020.109797.
[261] Water Development Department of Cyprus, 2019. Desalination Plants. http://www.moa.gov.cy/moa/wdd/wdd.nsf/page23_en/page23_en?opendocument (accessed November 29, 2020).

[262] World Commission on Dams, 2000. Dams and development: a new framework for decision-making. The report of the World Commission on dams. Earthscan Publications Ltd, London.
[263] World Energy Council 2016. World Energy Resources http://bit.ly/2KHaMd3 (accessed July 15, 2019).
[264] World Health Organization, 2000. Air quality guidelines for Europe, 2nd ed. Copenhagen : WHO Regional Office for Europe. https://apps.who.int/iris/handle/10665/107335
[265] World Nuclear Association, 2019. Economics of nuclear power. http://bit.ly/33JGu0N (accessed May 19, 2019).
[266] Wu, C., Zhang, X.-P., 2018. Economic analysis of energy interconnection between Europe and China with 100% renewable energy generation. Global Energy Interconnection 1, 528-536, https://doi.org/10.14171/j.2096-5117.gei.2018.05.001.
[267] Wu, J., Albrecht, J., Fan, Y., Xia, Y., 2016. The design of renewable support schemes and CO_2 emissions in China. Energy Policy 99, 4–11, https://doi.org/10.1016/j.enpol.2016.09.045.
[268] Wu, L., Gao, X., Xiao, Y., Yang, Y., Chen, X., 2018. Using a novel multi-variable grey model to forecast the electricity consumption of Shandong Province in China. Energy 157, 327–335, https://doi.org/10.1016/j.energy.2018.05.147.
[269] Wu, Q., Peng, C., 2016. Scenario Analysis of Carbon Emissions of China's Electric Power Industry Up to 2030. Energies 9, 988, 10.3390/en9120988.
[270] Xia, T., Nitschke, M., Zhang, Y., Shah, P., Crabb, S., Hansen, A., 2015. Traffic-related air pollution and health co-benefits of alternative transport in Adelaide, South Australia. Environment International 74, 281–290, https://doi.org/10.1016/j.envint.2014.10.004.
[271] Xiao, X.-J., Jiang, K.-J., 2018. China's nuclear power under the global 1.5 °C target: Preliminary feasibility study and prospects. Advances in Climate Change Research 9, 138–143, https://doi.org/10.1016/j.accre.2018.05.002.
[272] Yang, J., Liu, Q., Li, X., Cui, X., 2017. Overview of wind power in China: status and future. Sustainability 9, 1454, https://doi.org/10.3390/su9081454.
[273] Yu, S., Yarlagadda, B., Siegel, J.E., Zhou, S., Kim, S., 2020. The role of nuclear in China's energy future: Insights from integrated assessment. Energy Policy 139, 111344, https://doi.org/10.1016/j.enpol.2020.111344.
[274] Zachariadis, T., 2010. Forecast of electricity consumption in Cyprus up to the year 2030: The potential impact of climate change. Energy Policy 38, 744–750, https://doi.org/10.1016/j.enpol.2009.10.019.
[275] Zachariadis, T., Poullikkas, A., 2012. The costs of power outages: A case study from Cyprus. Energy Policy 51, 630-641, https://doi.org/10.1016/j.enpol.2012.09.015.
[276] Zachariadis, T., Taibi, E., 2015. Exploring drivers of energy demand in Cyprus – Scenarios and policy options. Energy Policy 86, 166–175, https://doi.org/10.1016/j.enpol.2015.07.003.
[277] Zaghib, K., Mauger, A., Julien, C.M., 2015. 12 - Rechargeable lithium batteries for energy storage in smart grids, in: Franco, A.A. (Ed.), Rechargeable Lithium Batteries. Woodhead Publishing, pp. 319-351. https://doi.org/10.1016/B978-1-78242-090-3.00012-2.
[278] Zakeri, B., Syri, S., 2015. Electrical energy storage systems: A comparative life cycle cost analysis. Renewable and Sustainable Energy Reviews 42, 569–596, https://doi.org/10.1016/j.rser.2014.10.011.
[279] Zappa, W., Junginger, M., van den Broek, M., 2019. Is a 100% renewable European power system feasible by 2050? Applied Energy 233–234, 1027–1050, https://doi.org/10.1016/j.apenergy.2018.08.109.
[280] Zeng, W., Tomppo, E., Healey, S.P., Gadow, K.V., 2015. The national forest inventory in China: History — Results — International context. Forest Ecosystems 2, 23, 10.1186/s40663-015-0047-2.
[281] Zhang, S., Andrews-Speed, P., Li, S., 2018. To what extent will China's ongoing electricity market reforms assist the integration of renewable energy? Energy Policy 114, 165–172, https://doi.org/10.1016/j.enpol.2017.12.002.

[282] Zhang, X., Ji, Z., Yue, Y., Liu, H., Wang, J., 2020a. Infection Risk Assessment of COVID-19 through Aerosol Transmission: a Case Study of South China Seafood Market. Environmental Science & Technology, acs.est.0c02895, 10.1021/acs.est.0c02895.
[283] Zhang, Y., Campana, P.E., Lundblad, A., Yan, J., 2017. Comparative study of hydrogen storage and battery storage in grid connected photovoltaic system: Storage sizing and rule-based operation. Applied Energy 201, 397-411, https://doi.org/10.1016/j.apenergy.2017.03.123.
[284] Zhang, Y., Ding, Z., Xiang, Q., Wang, W., Huang, L., Mao, F., 2020b. Short-term effects of ambient PM1 and PM2.5 air pollution on hospital admission for respiratory diseases: Case-crossover evidence from Shenzhen, China. International Journal of Hygiene and Environmental Health 224, 113418, https://doi.org/10.1016/j.ijheh.2019.11.001.
[285] Zhao, B., Zhang, X., Chen, J., 2012. Integrated Microgrid Laboratory System. IEEE Transactions on Power Systems 27, 2175–2185, 10.1109/TPWRS.2012.2192140.
[286] Zhao, G., Guerrero, J.M., Jiang, K., Chen, S., 2017a. Energy modelling towards low carbon development of Beijing in 2030. Energy 121, 107–113, https://doi.org/10.1016/j.energy.2017.01.019.
[287] Zhao, X., Cai, Q., Zhang, S., Luo, K., 2017b. The substitution of wind power for coal-fired power to realize China's CO_2 emissions reduction targets in 2020 and 2030. Energy 120, 164–178, https://doi.org/10.1016/j.energy.2016.12.109.
[288] Zhao, X., Yao, J., Sun, C., Pan, W., 2019. Impacts of carbon tax and tradable permits on wind power investment in China. Renewable Energy 135, 1386–1399, https://doi.org/10.1016/j.renene.2018.09.068.
[289] Zhibin, L., Xiaoning, L., 2016. Analysis of the investment cost of typical biomass power generation projects in China. International Conference on Education, Management Science and Economics, https://doi.org/10.2991/icemse-16.2016.63.
[290] Zhou, W., Yang, H., Fang, Z., 2006. Wind power potential and characteristic analysis of the Pearl River Delta region, China. Renewable Energy 31, 739–753, https://doi.org/10.1016/j.renene.2005.05.006.